Title

Investigating the Impacts of Meteorology and Soil NOx Emissions on Air Quality in the Salton Sea Air Basin: A Community-Engaged Approach

Author

Lieb, Heather Casey

Publication Date

2024

Peer reviewed|Thesis/dissertation

Investigating the Impacts of Meteorology and Soil NO_x Emissions on Air Quality in the Salton Sea Air Basin: A Community-Engaged Approach

By

HEATHER CASEY LIEB

DISSERTATION

Submitted in partial satisfaction of the requirements for the degree of

DOCTOR OF PHILOSOPHY

in

Agricultural and Environmental Chemistry

in the

OFFICE OF GRADUATE STUDIES

at the

UNIVERSITY OF CALIFORNIA

DAVIS

Approved:

_____

Ian Faloona, Chair

_____

Cort Anastasio

_____

Wendell Walters

_____

Jonathan K London

Committee in Charge

2024

Table of Contents

Acknowledgements

This work would not have been possible without the tremendous support from Ian Faloona, my mentor and friend. From the beginning, Ian encouraged me to formulate a project that I was passionate about, allowing me to incorporate my non-scientific interests into the foundation of the study. Without this creative freedom, I doubt that this experience would have been as fun, loving, or rewarding. I appreciate his sense of humor, his deep well of patience, and his vulnerability when sharing his experiences. In addition, I have much gratitude for Jonathan London, a co-mentor, and his expertise in community engagement and environmental activism. Jonathan created a warm and welcoming space that provided me the connection with other researchers interested in social justice. Through his mentorship and participation with his group, I have gained more compassion and emotional resilience. Also, I would like to thank Cort Anastasio and Wendell Walters for serving on my dissertation committee, allowing me to borrow instrumentation for analysis and improving the quality of my research projects.

I would also like to thank my community partners at Comité Cívico del Valle for their dedication and commitment to environmental justice in the Salton Sea Air Basin. This project would not have been possible without community engagement. A special thank you to Christian Torres, Matthew Maldonado, and Edgar Ruiz for executing the field sampling in our campaign and aiding with scientific dissemination. Moreover, I would like to thank my friends at Western Service Workers Association. Elena Sanchez and Derek Brunner have been monumental in the development of my leadership and community engagement skills. Elena's patience and openness is unmatched and am so grateful to have her as a mentor throughout this project. I

am especially grateful that I was able to utilize my strengths and resources to contribute towards food sovereignty in Sacramento.

Lastly, I would not have been able to do this without support from all my friends and family. A special thanks goes to Bridget Weimer; you are my best friend, and I have so much gratitude for your presence in my life. Thank you for encouraging me to keep going.

Ian and Heather painting together at the Southside Park Community Garden (Credit: Elena Peters).

Abstract

Air quality management has prioritized reducing anthropogenic nitrogen oxide (NO_x = NO + NO_2) sources to mitigate ozone and particulate matter pollution. This imperative, however, faces challenges in rural agricultural regions like the Salton Sea Air Basin (SSAB) in Southern California, which remains noncompliant with ozone (O_3), particulate matter ≤ 2.5 μg/m^3 ($PM_{2.5}$), and particulate matter ≤ 10 (PM_{10}) National Ambient Air Quality Standards (NAAQS). In-depth investigations, including seasonal, annual, and diurnal climatologies, were conducted to scrutinize meteorological and air pollutant trends in the SSAB. While interregional transport has influence on air quality in cities nearby the Mexican border and the LA basin, both ozone and $PM_{2.5}$ exceedances in the Imperial Valley predominantly arise from local emissions during periods with low advection in the more urban regions of the basin, while the drying of the Salton Sea is more influential at sites closer in proximity to the sea. PM_{10} exceedances were shown to depend largely on elevated wind speeds.

Notably, the research hypothesizes that soil NO_x emissions, exacerbated by year-round agricultural production with over $2 billion in annual sales, contribute significantly to local air quality problems. The nitrogen stable isotope composition ($\delta^{15}N$) is proposed as a valuable tool for NO_x source apportionment due to differences in mean $\delta^{15}N$-NO_x values between anthropogenic and biogenic emission sources. For this reason, nitrogen stable isotopes ($\delta^{15}N$) from actively collected NO_2 were quantified, and contributions to total NO_x were estimated using a mixing model, incorporating the mean $\delta^{15}N$-NO_x from each emission source and from the *a priori* source apportionment reported in the California Air Resources Board's NO_x inventory.

These results revealed that soil emissions are a substantial source, representing 35% and 21% of the total NO_x inventory for the Imperial and Coachella Valleys, respectively, or 30% on average for the entire air basin. These estimates indicate a tenfold underestimation of soil NO_x emissions on average by the current California Emissions Projection Analysis Model (CEPAM), with the largest discrepancies observed during spring and summer, periods of substantial biogenic activity.

Crucially, this study adopts a community-engaged approach in collaboration with Comité Cívico del Valle and Western Service Workers Association, two influential community organizations that were instrumental in developing my community-based participatory research skills. Two dedicated sections within the dissertation delve into the comprehensive community engagement strategies employed, emphasizing inclusivity, local knowledge integration, discussion of successes and struggles, and participatory decision-making processes. Furthermore, the research documents a transformative mural art project co-created with community members at Sacramento's Southside Community Garden, illustrating the intersection of environmental science and public art in conveying complex environmental issues to diverse audiences. Through a collaborative paint-by-numbers event, residents actively contributed to the artistic process, fostering a sense of ownership, and understanding of how our food system impacts their daily lives. These projects strengthened my community engagement skills and allowed me to practice alternative methods for scientific dissemination. This inclusive methodology enhances the broader impact of the research, creating an empowering relationship between academia and the local community.

Chapter 1: Deducing Atmospheric Conditions that Contribute to Elevated Pollution Events in the Salton Sea Air Basin

Abstract

Public agency regulators of the Salton Sea Air Basin (SSAB) have struggled to comply with the National Ambient Air Quality Standards (NAAQS) for three federally regulated air pollutants: ozone, $PM_{2.5}$, and PM_{10}. To better understand the meteorological factors influencing regional air pollution, seasonal, annual, and diurnal trends in both meteorological conditions and air pollutant climatologies were examined. Through this analysis it was revealed that ozone exceedance days tend to originate from localized sources and are strongly dependent on atmospheric dynamics and temperature-dependent precursor emissions. The observed ozone weekend effect supports a NO_x-limited regime, meaning that ozone production is heavily dependent on NO_x availability, which emphasizes the need for addressing unregulated sources of NO_x pollution like those from agricultural soils. Additionally, strong correlations of $PM_{2.5}$ with NO_x, PM_{10}, and CO, indicate that influences from combustion sources, secondary formation, and mechanical processes are all sources of $PM_{2.5}$ production in Calexico, the main city of $PM_{2.5}$ nonattainment on the southern border. In winter months, low ventilation accumulates localized $PM_{2.5}$ emissions. Source apportionment of $PM_{2.5}$ was assessed using non-negative matrix factorization of data from the Chemical Speciation Network (CSN) site in Calexico. The CSN data analysis for Calexico identifies biomass burning as the dominant source of high $PM_{2.5}$ concentrations, followed by agricultural soils and dust entrainment. Further, analysis of PM_{10} exceedance days indicates that high wind speeds, primarily westerly, are a critical factor, and the

low $PM_{2.5}/PM_{10}$ ratios suggest minimal contribution from combustion sources. Furthermore, the correlation of PM_{10} with wind speed across various sites underscores the importance of dust resuspension and soil erosion. This comprehensive assessment highlights the complexity of air quality problems in the SSAB and emphasizes the need for targeted and localized air quality management strategies for this region which, despite its low population, suffers some of the worst air pollution impacts in the state of California.

1.1 Introduction

The SSAB is a subsea level basin within the Sonoran Desert in southeastern California and is comprised of the Imperial Valley in the south and Coachella Valley in the north. The Salton Sea connects the two valleys and occupies the deepest point of the basin, which is bounded by the Peninsular Ranges to the west, and to the north and east by the Transverse Ranges. Additionally, this region is downwind of two large metropolitan cities—Los Angeles and Mexicali, Mexico. Characteristically, this basin receives on average less than 4 inches of precipitation per year, typically occurring in the winter months due to the passage of extratropical cyclones, or in the summer months because of monsoonal intrusions in the southern region of the basin (Ives, 1949). Daily average temperatures range from 12°C in the winter months and greater than 32°C in summer months, with summertime highs exceeding 40°C regularly. Near surface air enters the region from the San Gorgonio pass and flows towards the southeast down the valley, but as the valley widens south of the Salton Sea, westerly airflow begins to dominate.

Air pollution often results from the interaction between two primary components: chemical production and transport. These processes are contingent on a given region's climatology, synoptic scale meteorology, atmospheric dynamics, topography, human activity,

and natural ecological processes. In 1970, the Clean Air Act was authorized and requires the EPA to establish NAAQS to protect public health and to regulate hazardous air pollutant emissions; today, there are six federally regulated air pollutants. The Salton Sea Air Basin (SSAB) has struggled to meet NAAQS. It is currently in nonattainment for ozone (O_3) and particulate matter with a diameter ≤ 10 μm (PM_{10}). In 2023, the EPA deemed the SSAB in attainment for fine particulate matter (i.e., particulate matter with a diameter ≤ 2.5 μm, $PM_{2.5}$), however, this attainment was short-lived due to EPA lowering the annual $PM_{2.5}$ NAAQS from 12.0 μg/m^3 to 9.0 μg/m^3 (US EPA, 2024). For $PM_{2.5}$, the primary annual NAAQS requires for $PM_{2.5}$ not to exceed 9.0 μg/m^3 (EPA, 2024), based on an annual mean, averaged over 3 years, while the 24-h NAAQS requires $PM_{2.5}$ not to exceed 35.0 μg/m^3 based on the 98th percentile, averaged over 3 years. The NAAQS for ozone requires that the ozone design value (ODV) not exceed 70 ppb; an ODV is defined as the 3-year average of the fourth highest maximum daily 8-hour average (MDA8) ozone concentration. Further, there is but one federally regulated NAAQS for PM_{10}, which states that the 24-h average should not exceed 150 μg/m^3 more than once per year on average over 3 years.

Despite its relatively low population compared to nearby urban areas like Los Angeles and San Diego, the region experiences about a dozen ozone exceedance days per year in the south (Calexico) and up to 50-60 in the north (Palm Springs). Additionally, the daily $PM_{2.5}$ National Ambient Air Quality Standard (NAAQS) is frequently exceeded, especially in the south, with daily values often reaching 50-70 μg/m³ (California Air Resources Board, 2024a). O_3 formation is driven by photochemical reactions involving nitrogen oxides (NO_x) and volatile organic compounds (VOCs) under sunlight. There are various sources of O_3 precursors, including mobile sources (e.g., vehicles and trucks), stationary sources (e.g., industrial activities), and biogenic sources. Sources

of $PM_{2.5}$ in the SSAB include agricultural activities, such as tilling and burning, as well as industrial emissions, vehicle exhaust, and secondary organic aerosols.

Air pollution is the second leading risk factor for premature mortality globally (Institute for Health Metrics and Evaluation, 2021). Both acute and chronic exposure to these air pollutants have been associated with negative health effects, including respiratory and cardiovascular issues and diseases (Al-Hemoud et al., 2018; Caiazzo et al., 2013; Dominici et al., 2006; Hao et al., 2015; Kim et al., 2020; Madl et al., 2010). During the peak of the pandemic, Imperial County suffered from the highest mortality and contraction rates from COVID-19 per capita in the state (The New York Times, 2023), a consequence believed to be partly due to the chronic exposure to air pollutants (Borro et al., 2020; Garcia et al., 2022; Johnston et al., 2019; Marian et al., 2022). In addition, this region is characterized by high rates of poverty, language barriers, impaired water quality, and various other environmental and socio-economic injustices (OEHHA, 2023).

Conventional wisdom seems to be that the region's ozone and $PM_{2.5}$ issues are dominated by exogenous sources: in the Imperial Valley, pollutants come from the greater San Diego/Tijuana area and the border town of Mexicali, while in the Coachella Valley, pollutants are carried from the Los Angeles Basin (EPA, 2022, 2023; Mendoza et al., 2010; Shi et al., 2009; Watson & Chow, 2001). However, despite statewide efforts to reduce pollution sources in surrounding urban pockets, especially due to the efforts of the Clean Air Act to reduce combustion sources, O_3 and $PM_{2.5}$ reductions in the SSAB have been minimal, indicating that localized sources may be influencing their continued nonattainment. Many of the remaining areas in California struggling to comply with current ozone and $PM_{2.5}$ air quality standards are rural, agriculturally active

regions; therefore, these sources must be considered in future management practices (Almaraz et al., 2018; Oikawa et al., 2015).

Warm year-round temperatures make the Imperial Valley one of the most productive agricultural regions in California, the largest year-round irrigated area in the nation, with an estimated economic output of over two billion dollars annually (California Department of Food and Agriculture, 2023). In addition, the Coachella Valley is home to 135 golf courses which require regular seeding, fertilization, and irrigation. Consequently, the SSAB is home to some of the largest soil NO_x emissions (Almaraz et al., 2018; Lieb et al., 2024; Parrish et al., 2017), a precursor to both ozone and particulate nitrate, with surplus nitrogen inputs in the region which have increased 10-20-fold over the past century (Byrnes et al., 2020). In addition, agricultural tilling is a source of particulate matter in the region (Imperial County Air Pollution Control District, 2018). Despite evidence of the significance of soil NO_x in the region, inadequate effort has been made to address this issue. Further, this region is home to the Salton Sea, a saline lake at risk of desertification due to increasing imbalances between inflows and evaporation that have resulted in water level declines by about 13 m since the 1950s. This drastic change has resulted in 124 km^2 of newly exposed lakebed, which threatens to exacerbate air pollution and public health concerns due to the potential for increasing emissions of particulate matter (Abman et al., 2024; Johnston et al., 2019; Jones & Fleck, 2020; Pacific Institute, 2024). The production of soil NO_x and particulate matter are likely to increase due to increased agricultural activity and climate change, putting these already disadvantaged communities at higher risk of respiratory and cardiovascular damage. Therefore, addressing both meteorological phenomena and pollution sources that contribute to poor air quality in the region is crucial.

Moreover, PM_{10} is often generated from natural sources like dust storms, which are common in the arid climate of the SSAB, and are further exacerbated by various anthropogenic activities such as diminished agricultural runoff into the Salton Sea (Abman et al., 2024). Additionally, human activities, including agricultural operations, construction, and unpaved road/ATV travel, contribute to elevated PM_{10} levels (Imperial County Air Pollution Control District, 2018; H. Li et al., 2015). The exposed lakebed of the Salton Sea, due to receding water levels, has become a significant source of dust, further aggravating PM_{10} pollution (Frie et al., 2017; Johnston et al., 2019; Jones & Fleck, 2020). The episodic nature of PM_{10} pollution, driven by both natural and human factors, makes regulatory measures challenging. Addressing PM_{10} requires a multifaceted approach that includes mitigating dust from agricultural activities and improving land management practices. Furthermore, community engagement and investment in green infrastructure, such as windbreaks and wetland restoration, could help reduce the impact of wind-blown dust in the region (Bradley & Yanega, 2018).

To understand the components that influence air quality exceedances, it is important to first understand the region's typical atmospheric conditions. Diurnal, seasonal, and annual climatologies are developed in this work for various air pollutants and meteorological conditions from the years 2009-2023 using existing air monitors from the California Air Resources Board (CARB). This climatology is used to understand the relationship between monitored air pollutants and meteorological conditions. Additionally, normalized anomalies were calculated for days that exceeded the NAAQS for O_3, $PM_{2.5}$, and PM_{10}. Moreover, data from the Chemical Speciation Network site located in Calexico was used to apportion sources of $PM_{2.5}$ using non-negative

matrix factorization (NMF). Clarifying the components that influence poor regional air quality will allow for improvement in measurement practices.

1.2 Methods

1.2.1 Climatology Trends

To investigate regional air quality and meteorological trends, hourly data was obtained from the California Air Resources Board's (CARB) air quality and meteorology data query tools for the years 2009-23 (except for $PM_{2.5}$, which only had sufficient data from 2014-23) (California Air Resources Board, 2024a, 2024b); the meteorological parameters under investigation were temperature, scalar wind speed, U and V wind components (westerly/zonal and southernly/meridional, respectively), vector mean wind direction, and specific and relative humidity, while the air pollutants under analysis included O_3, $PM_{2.5}$, PM_{10}, CO, and NO_x.

1.2.2 Normalized anomaly (σ) calculations

Sites from the CARB air monitoring network (Figure 1.1) were used to calculate normalized anomalies (σ) for various meteorological and pollution parameters of ozone, $PM_{2.5}$, and PM_{10} concentrations. Because of the strong seasonal (monthly) dependence of most AQ and meteorological parameters, we present deseasonalized normalized anomalies, calculated using Equation 1.1:

$$\sigma = \frac{x - \bar{x}}{sd} \tag{1.1}$$

where *x* represents the 24-h averages for each variable, $\bar{x}$ is the monthly average over the 14-year period, and anomalies are normalized by the monthly-averaged standard deviation (*sd*) across the 14 years. The normalized anomalies were primarily analyzed on days that exceeded

the NAAQS (70 ppb, 35 μg/m^3, and 150 μg/m^3 for ozone, $PM_{2.5}$, and PM_{10}, respectively) to identify any significant meteorological or pollutant outliers that occurred during these extreme pollution episodes. We consider the normalized anomalies to be somewhat significant if σ ≥ 0.4 (or σ ≤ -0.4) and very significant if σ ≥ 1 (or σ ≤ -1); these values can be found in Tables S1.2, S1.5, S1.6a, and S1.6b. Equation 1.2 below shows the calculation for SE where *sd* is the standard deviation and *n* represents the number of available datapoints for a given variable.

$$SE = sd/\sqrt{n} \quad (1.2)$$

Because of the strong diurnal behavior of the thermally forced circulations in the SSAB, we also use an analogous (non-normalized) de-diurnalized ozone value in our pollution rose analysis of Section 1.4.1.

Figure 1.1. CARB sites used for the meteorological and air pollution climatology studies. Note that Imperial Valley sites begin at Bombay Beach and move south. The sites north of the Salton Sea are within the Coachella Valley, *except for Banning*, which is a part of the South Coast Air Basin but is used as a reference point for the study.

1.2.3 Correlation coefficient (R^2) calculations

Correlation coefficients (R^2) were calculated for ozone and the aforementioned meteorological and pollutant components. This parameter was calculated between ozone MDA8 and T_{max}, daytime scalar average wind speed, daytime U and V components, and 24-h average relative and specific humidity, $PM_{2.5}$, PM_{10}, NO_x, and CO for the months of April through September, since ozone formation peaks during the afternoon and in the warmer months. Coefficients for $PM_{2.5}$ and PM_{10} were not significant and therefore were not reported. Statistically significant correlation coefficients are indicated by a p-value of less than or equal to 0.05, and these values can be found in Tables S3 and S4.

1.2.4 Chemical Speciation and Source Apportionment of $PM_{2.5}$

To better identify sources that contribute to $PM_{2.5}$ production, data from the Chemical Speciation Network (CSN) in Calexico, CA (the only site in the SSAB) was utilized (US EPA, 2016b) from 2009-2023 (one full 24-hr sample approximately every 6 days for a total of 718 data points). Daily measurements of $PM_{2.5}$ mass concentrations were obtained from the CSN. A continuous time series was constructed, using the corrections described in Malm and Hand (2007) based on IMPROVE protocols for reconstruction of dry mass concentrations (Malm & Hand, 2007). Specifically, dry $PM_{2.5}$ mass concentrations are computed using the following equations:

$$PM_{2.5} = 1.37[SO_4^{2-}] + 1.29[NO_3^-] + [POM] + [EC] + [Soil] + [Sea\ Salt], \quad (1.3)$$

$$POM = 1.4[OC], \quad (1.4)$$

$$\text{Soil} = 2.2[Al] + 2.49[Si] + 1.94[Ti] + 1.63[Ca] + 2.42[Fe] \quad (1.5)$$

$$\text{Sea Salt} = 1.8[Cl^-] \quad (1.6)$$

where sulfate (SO_4^{2-}) is assumed to be fully neutralized to ammonium sulfate ($(NH_4)_2SO_4$), nitrate (NO_3^-) is assumed to be in the form of ammonium nitrate (NH_4NO_3), and organic carbon (OC) is included as particulate organic matter (POM). The EPA describes the calculation of organic carbon (OC) and elemental carbon (EC), since there are multiple measurements of each, and the following equations are used:

$$OC = OC1 + OC2 + OC3 + OC4 + OP \quad (1.7)$$

$$EC = EC1 + EC2 + EC3 - OP \quad (1.8)$$

where OP represents pyrolyzed organic carbon. OP is measured using two methods: thermal optical reflectance (TOR) and thermal optical transmittance (TOT). TOR measures the change in reflectance of the sample surface as it is heated, while TOT measures the change in transmittance, or light passing through, as the sample is heated. Both methods of measurement are necessary to fully depict the OP concentrations since surface reflectance might underestimate OP in the sample's interior, while transmittance might overestimate it if the interior changes are more pronounced than the surface. Therefore, "OC" and "EC" are reported as OC_TOR, OC_TOT, EC_TOR, or EC_TOT depending on the OP measurement. These measurements give strikingly different results, so defining them separately is important. This method of reconstructing $PM_{2.5}$ has good agreement with measured $PM_{2.5}$ concentrations, with a slope of 1.01 and R_2 of 0.83 (Figure S1.1).

In addition to chemical speciation, non-negative matrix factorization (NMF) was used for source apportionment of $PM_{2.5}$. Source apportionment aims to extract the source contributions

and profiles of *p* factors from the speciated concentrations of $PM_{2.5}$ using mass balance analysis, which can be written to account for all *m* chemical species in the *n* samples as contributions from *p* independent sources:

$$x_{ij} = \sum_{k=1}^{p} g_{ij} f_{kj} \quad (1.9)$$

where x_{ij} is the j^{th} chemical species concentration measured in the i^{th} sample, g_{ik} is the airborne contribution of material from the k^{th} source contributing to the i^{th} sample, and f_{kj} is the concentration of the j^{th} species from the k^{th} source (Hopke, 2016). The CSN data was used in this NMF to determine the sources of $PM_{2.5}$ in Calexico. Once the factorization was completed and the sources were identified, we then looked at the 90th percentile and 98th percentile days to see the dominant sources of pollution. This will allow for a better understanding of which sources may result in nonattainment days, allowing for policy makers to focus on these sources in regulatory decisions.

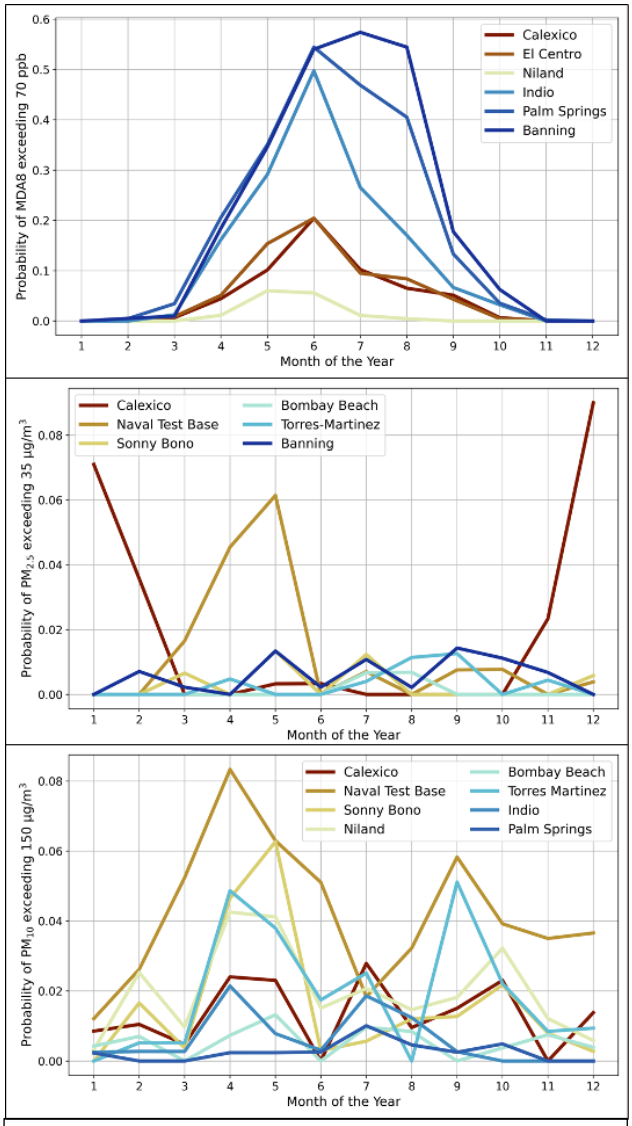

Figure 1.2. The probability of NAAQS exceedance for ozone (top), $PM_{2.5}$, and PM_{10} based on monitoring site.

1.3. Regional Climatology

It is crucial to understand the environmental factors that contribute to O_3, $PM_{2.5}$, and PM_{10} pollution, especially the climatological, seasonal, and diurnal trends. Figure 1.2 shows the probability of MDA8, $PM_{2.5}$ and PM_{10} daily NAAQS exceedances (70 pbbv, 35 µg m^{-3}, and 150 µg m^{-3}, respectively) at each site, illustrating the seasonal patterns of air pollution extremes in the SSAB. This figure shows the highest likelihood of ozone exceedances in June at most sites, but also July in Banning (which is downwind of the LA air basin). They are more than twice as prevalent in the Coachella Valley relative to the Imperial Valley. Figure 1.2 also shows that winter months in Calexico and spring at the Naval Test Base are most likely to have exceedances. Furthermore, while there is a lot of variability between sites for PM_{10} exceedances, sites around the Salton Sea are most likely to experience PM_{10} exceedances, especially in spring and fall.

1.3.1 Wind

Establishing the typical wind patterns helps clarify the mesoscale meteorological influences on regional air pollution transport and processing and can aid in understanding the interregional impacts of pollution events. Monthly wind roses have been prepared using wind data from ten of the California Air Resources Board sites during 2009-2023, showing monthly averaged wind patterns (Section S1.1). Due to the presences of the large body of water at the center of the valley, separating the Imperial and Coachella Valleys, a sea/lake breeze is regularly observed and represents the dominant influence on diurnal wind patterns within the valley. Because of the thermal nature of this circulation, it is especially pronounced in the summer months.

Beginning in the Southern Imperial Valley, there are three main meteorology sites in Calexico, El Centro, and Imperial (refer to Fig. 1.1). Calexico is located about 40 miles south-southeast of the Salton Sea along the Mexican border and experiences westerly and northwesterly winds, the strongest of which are observed during the late winter and spring. A wind reversal occurs in the warmest months when southeasterly flow strengthens and dominates due to the North American monsoon (Adams & Comrie, 1997) bringing moist air from the Gulf of California into the valley. El Centro is located northwest of Calexico and northerly and westerly winds are observed in the fall and winter, with larger wind gusts coming from the west. In early spring, we observe a strengthening of the westerly until early summer, when the monsoonal flow from the southeast dominates in the warmest months of July and August. The effect of the monsoonal flow is reduced in the evening, when the winds veer to south-westerly with nighttime drainage flows likely strengthened by prevailing westerlies. El Centro experiences extreme westerly wind events in the spring and early summer, with wind speeds exceeding 9 m/s. Further, wind speeds measured in El Centro are higher than other monitoring sites within the air basin (Figure 1.3). It is likely that the high wind speeds result from downslope acceleration of flow channeled through the lowest point in the north-south transect of the Peninsular Range, a point referred to as the "El Centro Gap" (Evan, 2019). Additionally, Imperial, the meteorology site located just 7 km north of El Centro, experiences less intense wind gusts, but otherwise the general winds are comparable to El Centro and Calexico. CARB sites located along the perimeter of the Salton Sea are in Sonny Bono, Bombay Beach, the Naval Test Base, and on the Torres-Martinez tribal land. Winds in these regions are largely characterized by daytime sea breezes from the Salton Sea followed by nighttime downslope/downvalley winds/land breezes.

The Coachella Valley is comprised of two major CARB sites: Indio, which is northwest of the Salton Sea, and Palm Springs, which is located at the northernmost point of the Salton basin just on the east side of the San Gorgonia (i.e., Banning) pass. Both sites observe generally weaker winds dominated by northwesterlies channeled in through the pass but exhibit a daytime up-valley wind outside of the spring when the channel flow is strongest due to the sea/lake breeze. Lastly, Banning, in the San Gorgonia gap, is dominated by westerlies throughout the year which are driven by the large-scale pressure gradient channeled through the terrain (Fig. S1.10), except during the wintertime high pressure events which reverse the pressure gradients.

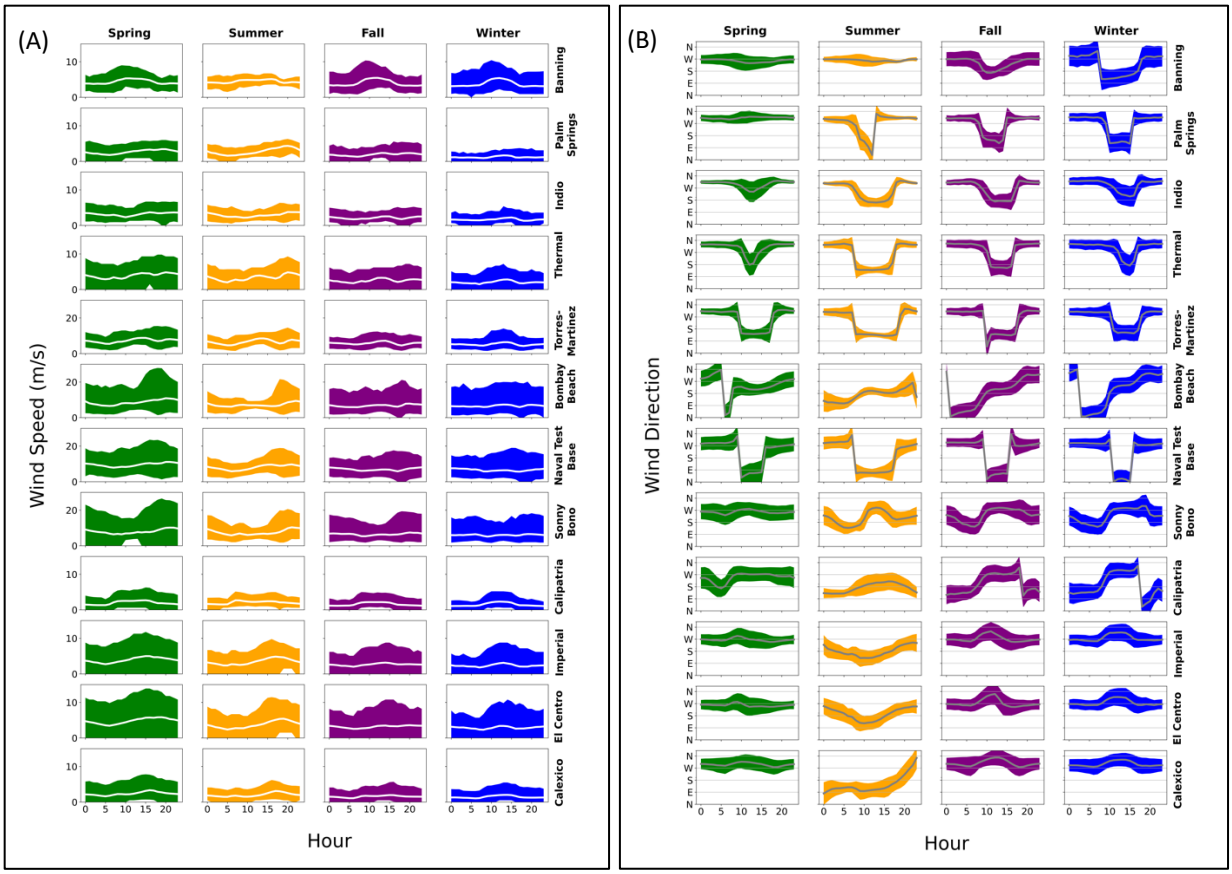

Figure 1.3. (A) Seasonal diurnal scalar average wind speed. White lines indicate the seasonal average while the colored area represents the upper 95th percentile and lower 5th percentile. (B) Seasonal diurnal wind direction.

Grey lines indicate the seasonal average while the colored area represents the standard deviation of the wind direction.

1.3.2 Ozone

Ozone production is seasonal by nature, with the highest concentrations usually observed in the summer months due to the peak in actinic fluxes, more frequent air stagnation under high pressure systems, increased emissions of anthropogenic and biogenic VOCs, as well as the thermal degradation of PAN, a significant temporary sink for NOx in polluted environments (Porter & Heald, 2019). Photochemical production of near-surface ozone is also dependent on temperature-dependent chemical reaction rates. However, in regions of the US with strong temperature-ozone correlations, the temperature-dependent chemistry and emissions have been shown to make up less than half of the relationship, while mass transport yields the majority (~60%) (Kerr et al., 2019). Kerr et al. (2019) found regions in the southern US near bodies of water, such as the lower Mississippi Valley, the Texas Gulf Coast, and the Salton Sea, to exhibit very weak correlations between T and O3, very similar to our findings tallied in Tables S3 & S4 ($0.01 < R2 < 0.11$). Here other factors are more important in determining the highest ozone concentrations. For example, stratospheric intrusion events are particularly influential in the southwestern US (Škerlak et al., 2014; Zhang et al., 2020) which may explain why the second highest month of O_3 exceedance probability is May, closer to the peak in the stratospheric influx of O_3, for some of the sites in the interior of the SSAB (e.g., Indio & El Centro, Fig. 2).

The persistence of elevated near-surface ozone concentrations has been an issue for decades, originally dominated by anthropogenic sources in the urban regions of California (Haagen-Smit, 1954). Air quality regulations resulted in large reductions in the anthropogenic

emissions of ozone precursors (mostly NO_x and reactive organic gases or non-methane volatile organic compounds), considerably lowering the ambient ozone concentrations over the decades (Parrish et al., 2017). However, several rural regions of California still exceed the 2015 NAAQS for ozone, including the Salton Sea Air Basin (Parrish et al., 2017, 2024). With reference to Table 1.1 and Figure 1.4 (ODV), it is apparent that there has been little improvement in ODV concentrations over the last decade in the SSAB (apart from Niland), indicating that anthropogenic combustion sources are likely no longer the determining factor in ozone nonattainment. While Niland's ozone pollution seems to be improving over the past decade, the rate of ozone decline has slowed at all other sites (especially since ~2016), and a positive slope is observed in Calexico and Banning since 2012. Unregulated sources like agricultural NOx emissions and managed landscapes like golf courses, or natural phenomena like stratospheric intrusion and subsidence on the lee side of the Pacific high, may be significantly responsible for continued nonattainment challenges (Carrow, 1997; Parrish et al., 2017, 2024; Škerlak et al., 2014; Zhang et al., 2020). Referring to Table S1.1 and Figure S1.2, which show trends in annual NO_x averages from 2009-2023, it is apparent that, outside of Calexico, the regulatory decline in NO_x concentrations is mostly absent over the past 7 years, indicating that the threshold of reduced mobile source emissions has likely been obtained and unregulated sources of NO_x need more focus to reach attainment goals. Further investigation is necessary to understand the impact of mass transport and to confirm whether stratospheric intrusion is a dominant factor, but several studies have implied that soil NO_x emissions in the SSAB are massively consequential (Almaraz et al., 2018; Lieb et al., 2024; Oikawa et al., 2015; Wang, Ge, et al., 2021) and will need to be addressed in order to further air quality and environmental justice goals in the region.

Table 1.1. Slopes and correlation coefficients (R^2) for Figure 1.4, split into two decades to show the changes in trends. The slopes represent the change in ODV per year.

		Calexico	El Centro	Niland	Indio	Palm Springs	Banning
2000-2011	Slope (ppb/yr)	-0.99	-1.08	-0.43	-0.79	-0.84	-1.46
	R^2	0.24	0.74	0.25	0.42	0.45	0.56
2012-2023	Slope (ppb/yr)	0.24	-0.98	-1.91	-0.53	-0.44	0.46
	R^2	0.41	0.57	0.76	0.27	0.56	0.39

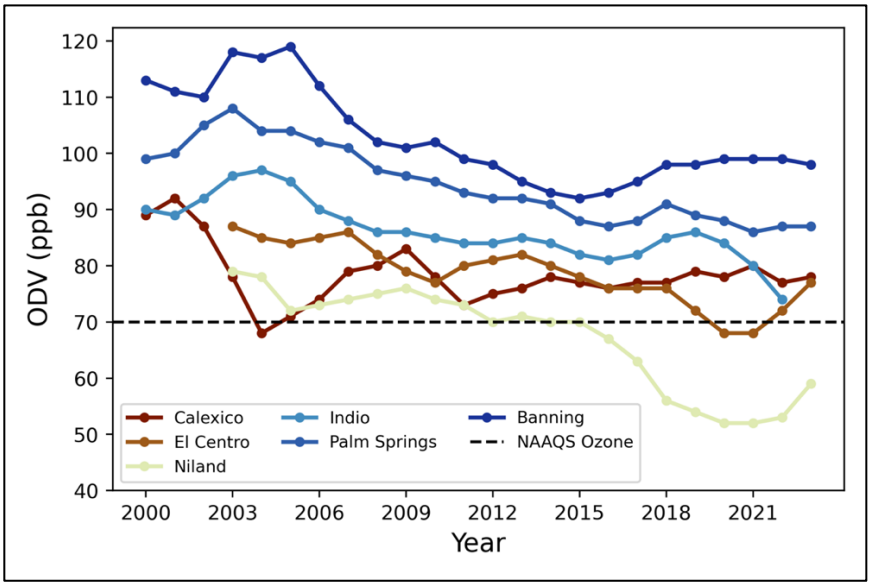

Figure 1.4. Ozone design values (ODV) for the six CARB sites in the Salton Sea Air Basin from 2000-2023. The NAAQS for ozone is denoted by the dashed black line at 70 ppb.

1.3.3 $PM_{2.5}$

Imperial County has recently been reviewed by the EPA, deeming the county in attainment for the 2012 $PM_{2.5}$ standard by its December 31, 2021 "Moderate" area attainment date (EPA, 2023). However, this attainment was short lived due to EPA lowering the annual $PM_{2.5}$ NAAQS from 12.0 µg/m^3 to 9.0 µg/m^3; as it currently stands, the $PM_{2.5}$ design value for Imperial County is 11.0 µg/m^3 (EPA, 2023). To examine climatological trends in $PM_{2.5}$ seasonally and

diurnally, data was analyzed from six CARB sites for the years 2014-2023—these years were chosen based on sufficient availability of $PM_{2.5}$ data. After examining climatological monthly average trends, it is apparent that $PM_{2.5}$ exceedances are concentrated on either end of the basin: Banning in the north and the Southern Imperial Valley at the Calexico site. $PM_{2.5}$ monthly averages exceed the annual NAAQS of 9.0 $\mu g/m^3$ every month except for March in Calexico (Figure 1.5). Aside from late spring/early summer exceedance at the Naval Test Base site, Banning is the only other site with monthly climatological averages that exceed the annual NAAQS, and this occurs from April to October, indicating a predominance of photochemical production of secondary aerosols. All other sites attain the annual NAAQS and observe summertime maximums—Calexico is the only site within the valley that observes maximum $PM_{2.5}$ concentrations in the winter. During winter, cold-air pools (CAP) are common in mountain valleys during periods of light wind, high atmospheric pressure, and low insolation and are associated with surface-based temperature inversions (Daly et al., 2009; Lareau et al., 2013). When these stagnant air masses persist, the local emissions from combustion, burning, and any agricultural sources of $PM_{2.5}$ accumulate within the stagnant air (Silcox et al., 2011). Monitoring sites along the Salton Sea (Sonny Bono, Naval Test Base, Bombay Beach, and Torres-Martinez) are not a part of the U.S. EPA Air Quality System, so long-term trend analysis for PM2.5 design values is not reported.

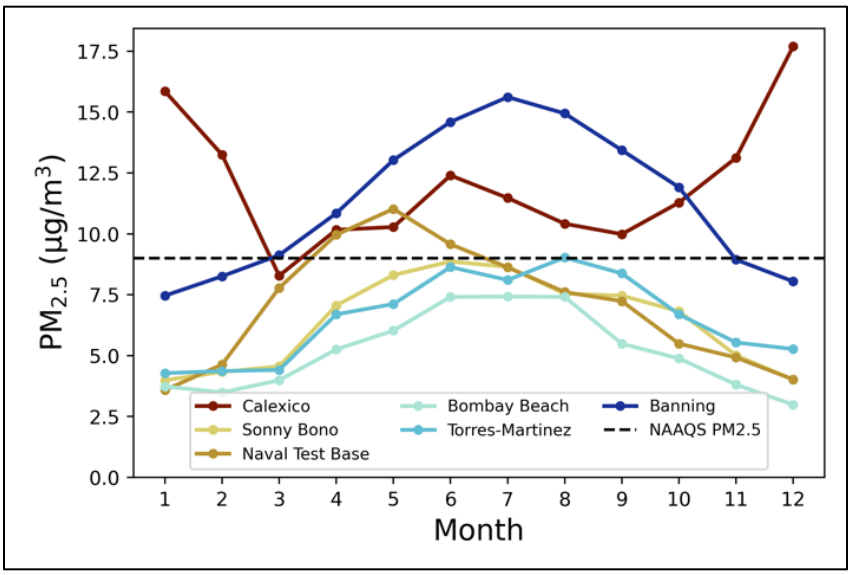

Figure 1.5. Climatological monthly averages for $PM_{2.5}$ were calculated using 24-h average $PM_{2.5}$ concentrations for 2014-23 (as available). The 1-year 2024 National Ambient Air Quality Standard (NAAQS) is denoted by the black dashed line.

Diurnal profiles of seasonal $PM_{2.5}$ concentrations were also prepared to examine the times which most influence $PM_{2.5}$ exceedances, with reference to the 24-h average NAAQS of 35 µg m^{-3} (Figure 1.6A). Referring to the seasonal diurnal averages (represented by the thick white line), routine exceedances are observed in Mexicali, Mexico during the winter. In addition, $PM_{2.5}$ maxima were observed in the mornings and evenings as a response to diurnal changes in the mixing height and possibly source timing of cooking and heating combustion. Referring to seasonal deviations, Naval Test Base and Sonny Bono, two sites located on the southwestern and southern sides of the Salton Sea, respectively, observe high $PM_{2.5}$ events during spring evenings. This may be related to strong evening westerly winds observed in the spring and emissions from the Salton Sea and surrounding playa (Evan, 2019; Freedman et al., 2020; Frie et al., 2019). In addition, Calexico observed similar fall/winter diurnal trends with $PM_{2.5}$ compared to the two Mexicali monitoring sites, although with much lower concentrations. Figure 1.7 shows hourly

$PM_{2.5}$ deviations from the diurnal mean, where wintertime wind directions are primarily westerly and northwesterly, exceptionally larger than average $PM_{2.5}$ concentrations occur on days when winds are southeasterly, indicating that Mexicali could be a principal source for $PM_{2.5}$ production during the wintertime $PM_{2.5}$ events. Further investigation of regional wind patterns was performed for a concise understanding of interregional air pollution influences.

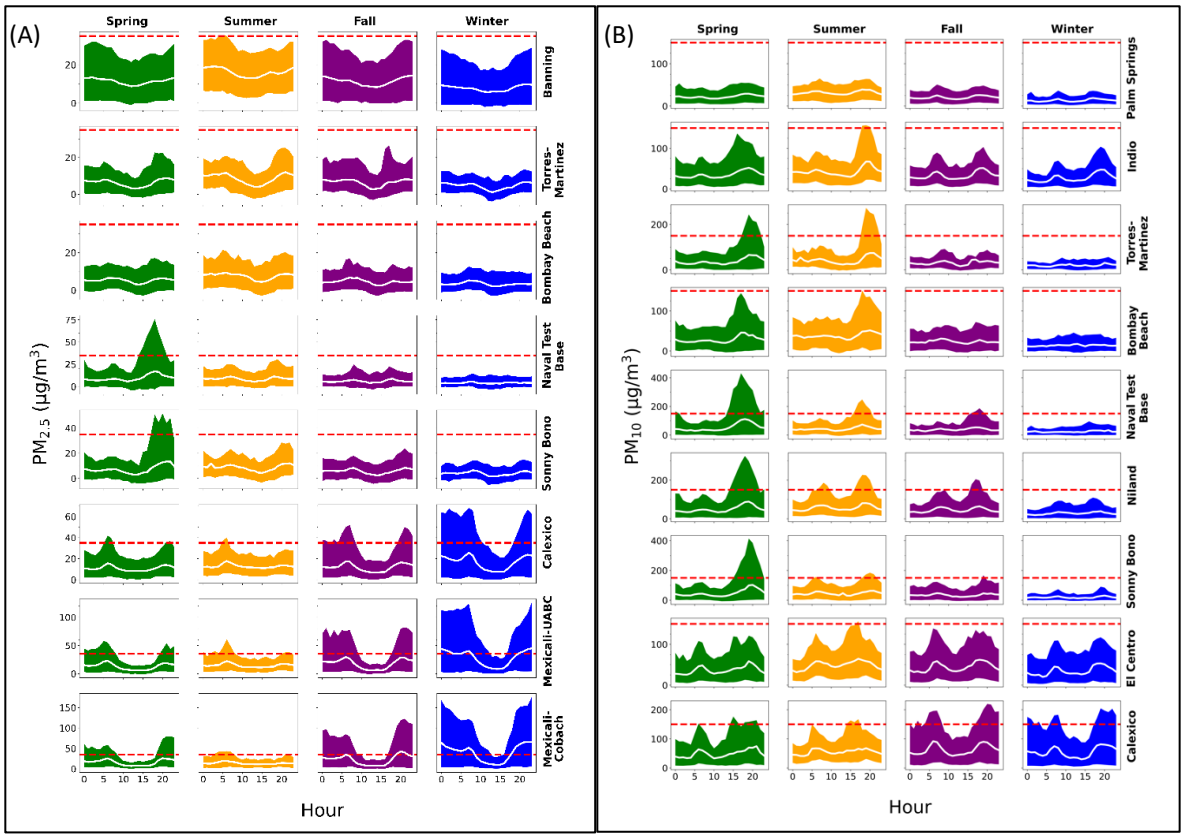

Figure 1.6. Seasonal diurnal averages for (A) $PM_{2.5}$ and (B) PM_{10} concentrations at each site in the Imperial and Coachella Valleys ($PM_{2.5}$ also includes measurements from Mexicali). Note that the white line represents the seasonal average $PM_{2.5}$ concentration, while the colors represent the upper 95th percentile and lower 5th percentile. The dashed red line represents the NAAQS for 24-h $PM_{2.5}$ concentrations, which should not exceed 35 µg/m^3. (Spring = MAM, Summer = JJA, Fall = SON, Winter = DJF).

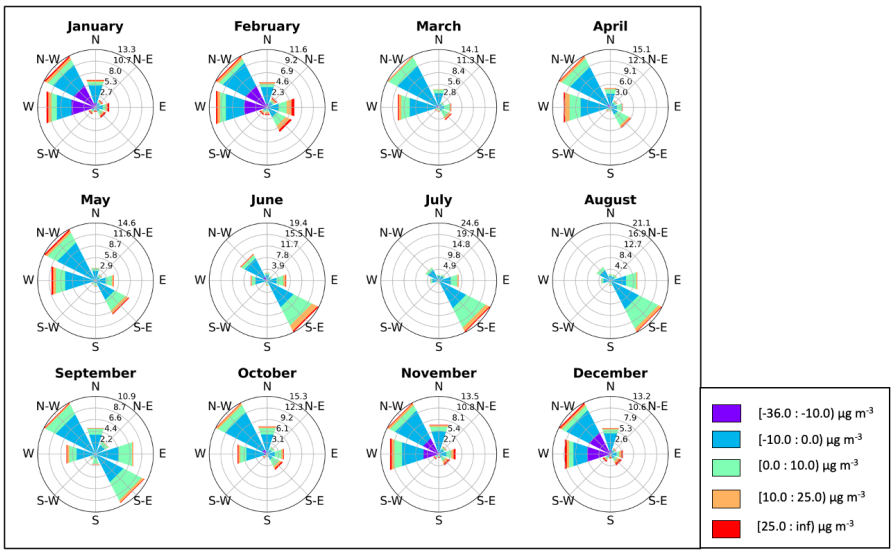

Figure 1.7. $PM_{2.5}$ pollution roses for Calexico. The colors represent *hourly $PM_{2.5}$ deviations* from the mean.

1.3.4 PM_{10}

The SSAB is in "Serious" nonattainment for PM_{10}, which is typically associated with dust, soot, metals, and salts. PM_{10} is known to have negative health implications due to short and long-term exposure. These particles can be inhaled and deposited throughout the upper airways of the lungs, potentially causing tissue damage and lung inflammation, which can adversely affect respiratory and cardiovascular health (California Air Resources Board, 2023). Negative health implications to PM_{10} exposure can include reduced lung function (D'Evelyn et al., 2021); worsening of asthma and other respiratory diseases; increased hospitalization and emergency department visits; faster disease progression; and reduced life expectancy (California Air Resources Board, 2023).

To analyze climatological trends for annual and diurnal PM_{10} patterns, sites from CARB for the years 2009-2023 were used. Referring to the climatological monthly average trends (Figure 1.8A), it is apparent that high PM_{10} concentrations are most frequently observed in Calexico and at the sites surrounding the Salton Sea. Calexico and Torres-Martinez observe

maximums in the fall, while Sonny Bono and Naval Test Base exhibit a strong peak in April/May. All other sites have a summertime maximum. Because PM_{10} emissions are strongly correlated to wind speed, it is important to understand the seasonal fluctuations of wind speed that may be influencing these events and ultimately leading to the strong seasonal variability between sites. Seasonal diurnal patterns of PM_{10} at the different sites are shown in Figure 1.6B. It is apparent that in the springtime, every site south of Palm Springs shows a pronounced peak in PM_{10} concentrations in the late afternoon/early evening, and referring to Figure 1.3, these events are associated with relatively strong westerly (northwesterly in the Coachella Valley) flow. Wind patterns are discussed in more detail in Section 1.3.1 and relationships to wind speed are discussed in Section 1.4.3.

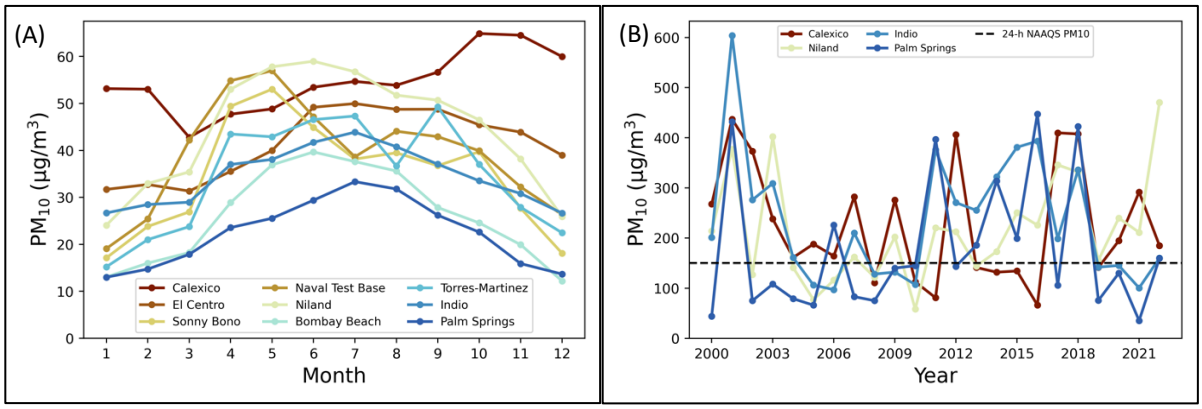

Figure 1.8. (A) Monthly climatological mean concentrations of PM_{10} for each of the CARB sites. (B) PM_{10} design values for the 24-h average NAAQS for available sites.

Further, annual PM_{10} design values for the 24-h average NAAQS are shown for available sites in Figure 1.8B. There is significant variability in the PM_{10} data since exceedances are often associated with extreme events like windstorms. In 2020, the EPA approved Imperial County's State Implementation Plan (SIP) for PM_{10} attainment, claiming that anthropogenic sources of PM_{10} are being mitigated as to not exceed the PM_{10} standard. However, the two Imperial County

sites in Figure 1.8B are exceeding the NAAQS, and there does not appear to be any significant long-term trend in PM_{10} DV. Therefore, understanding the factors that exacerbate these exceedances is crucial.

1.4. Results and Discussion

1.4.1 Normalized anomalies and correlation coefficients (R^2) for ozone

Six sites from CARB were used to calculate normalized anomalies and correlation coefficients for ozone and various meteorological and pollution parameters. Three sites belong to the Imperial Valley (i.e., Calexico, El Centro, and Niland), and three sites belong to the Coachella Valley (i.e., Indio, Palm Springs, and Banning, although Banning is not a part of the SSAB). The number of exceedance days, normalized anomalies, and SE for each site during the 2009-2023 timeframe is shown in Table S1.2. Additionally, correlation coefficients (R2) were calculated for ozone and various meteorological and air pollutant components for the months of April through September (Table S1.3 and S1.4).

Based on the analysis of normalized anomalies in Calexico (Table S1.2), ozone exceedance days are characterized by warmer than average temperatures, low (more northerly) wind speed, and low humidity (68^{th}, 23^{rd}, and 34^{th} percentiles, respectively). Because of the reasons outlined in Section 1.3.2, it is generally expected to see ozone exceedances occurring when temperatures are high, however, Table S1.3 shows that the linear relationship between MDA8 is weakly correlated with the maximum daily temperature from April-September therefore temperature is not the dominant factor influencing ozone exceedances day-to-day. We interpret the average deviations of T, wind speed/direction, and humidity to be evidence of atmospheric dynamics and temperature-dependent precursor emissions influencing extreme values of ozone. For example,

low humidity is consistent with the deep stratospheric transport into the deep boundary layers common in the US southwest as illustrated in Škerlak et al. (2014) and discussed in Section 1.3.2.

Additionally, although southeasterly monsoonal winds are most frequent during the warmest months in the Imperial Valley (July/August, which have lower exceedance probabilities than May/June when the winds are westerly/northwesterly, Fig. 1.2), conditions of stagnant and dry air indicate that ozone exceedances are not predominantly related to transport from Mexicali, Mexico. This is a very consequential finding because international transport is often assumed to be the primary contributor to ozone pollution in the Imperial Valley (EPA, 2022). Figure 1.9 shows that hourly ozone deviations from the diurnal means in Calexico are larger on days where winds are predominantly northwesterly (Table S1.2 also shows the correlation with northerly, $V < 0$, winds). Further, CO concentrations on ozone exceedance days in Calexico are average, neither elevated nor low, which may indicate that traditional combustion processes are not the dominant source of ozone precursors.

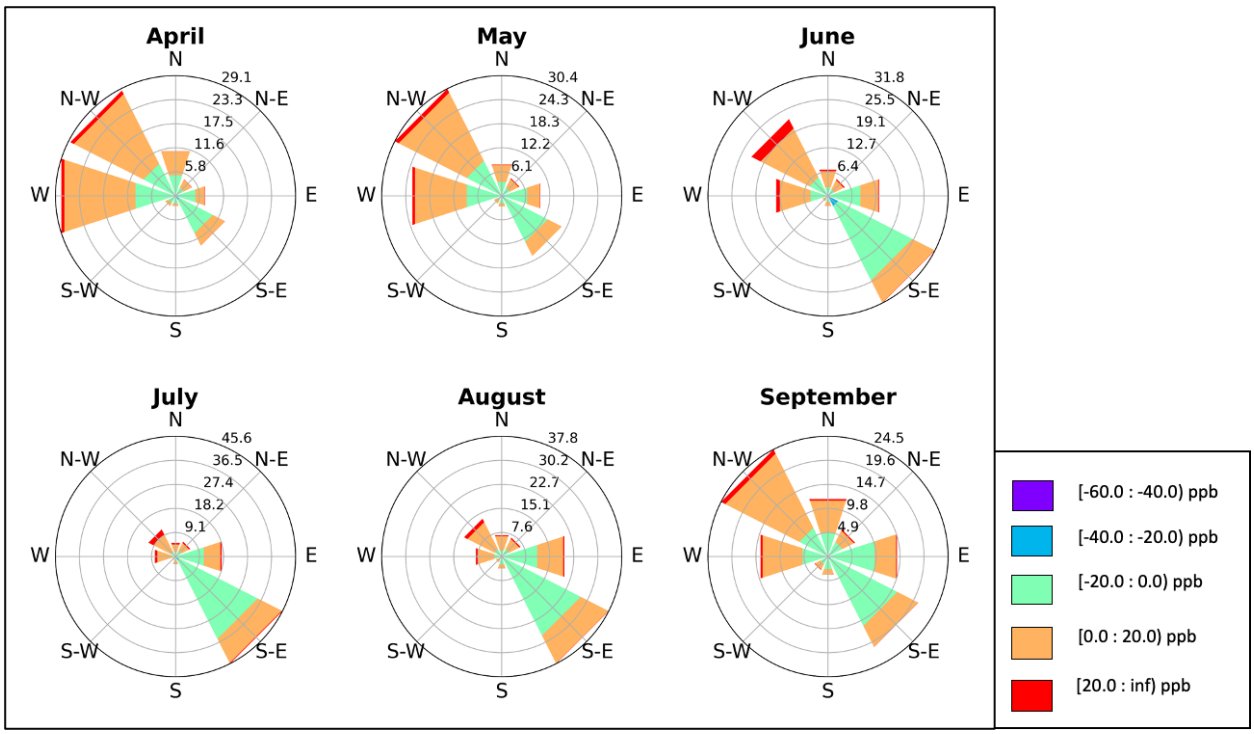

Figure 1.9. Ozone pollution roses for Calexico during June-September. The colors represent *hourly ozone deviations* from the mean.

Looking at the weekday vs weekend differences in ozone levels, or the "weekend effect", helps to understand the ozone production sensitivity to NO_x reductions and the role that vehicle emissions play in ozone levels. Typically, sites dominated by background ozone (e.g., unregulated anthropogenic sources, biogenic sources, and baseline ozone) or long-range transport have similar weekday/weekend O_3, while sites dominated by local/regional anthropogenic O_3 sources do not (Heuss et al., 2003). Heuss et al. investigated the weekend effect for Calexico during ozone season (April-September) from 1996-1997, which showed that the region observed lower O_3 on weekends. This indicates a NO_x-limited regime in which the production of ozone is principally limited by the availability of NO_x rather than that of VOCs. In comparison, Figure S1.3A shows the weekend effect for Calexico during ozone seasons from 2014-2023, evincing a consistent trend of lower O_3 on weekends. Thus, it appears that Calexico is still NO_x-limited, and the average

Sunday diurnal cycle has not changed much in concentration, although weekday concentrations of ozone have decreased by 5-10 ppb since the late 90's. Therefore, we see that the reduction of mobile source emissions, mostly NO_x from heavy duty diesel vehicles (Marr & Harley, 2002), does reduce the average ozone concentration during the weekend. Figure S1.4A shows the expected decline in observed NO_x concentrations on Sundays in comparison to weekday concentrations. El Centro observes the most ozone exceedances in the Imperial Valley, and like Calexico those high ozone days are characterized by relatively warm, weak and more northerly wind, and dry conditions. However, unlike Calexico, O_3 exceedances in El Centro co-occur with high NO_x, $PM_{2.5}$, CO, and $PM_{2.5}/PM_{10}$ concentrations (82^{nd}, 80^{th}, 79^{th}, and 71^{st} percentiles, respectively). El Centro has a similar weekend effect to Calexico (Figure S1.3B), however, because El Centro's ozone exceedances are characterized by high CO, NO_x, and $PM_{2.5}$ this may indicate that combustion processes are significant, which could include local domestic mobile source emissions and agricultural equipment (H. Li et al., 2015).

Nonetheless, Imperial County is agriculturally active year-round, meaning elevated NO_x emissions may result from soil emissions of NO. Agricultural NO_x emissions have not been regulated despite many studies that have shown their significance in agricultural areas, especially the Imperial Valley (Almaraz et al., 2018; Lieb et al., 2024; Luo et al., 2022; Oikawa et al., 2015; Sha et al., 2021). Agricultural soil NO_x emissions are dependent on fertilizer inputs, soil moisture, and temperature. The dependence of temperature is exponential up until about 35-40°C where emissions tend to plateau due to heat stress (Wang, Ge, et al., 2021; Yienger & Levy, 1995). A recent study by Lieb et al., 2024 estimated that agricultural soils contribute 34.7% on average to the Imperial County NO_x budget. The sensitivity of ozone production to NO_x [δO_3 MDA8/δNO_x]

based on the weekend effect (Figs. S1.3-S1.4) in Calexico is 1.05 ppb of O_3 per ppb of NO_x. The average NO_x concentration from April-September is 6.1 ppb, meaning about 2.1 ppb NO_x originate from agricultural soils according to the Lieb et al. (2024) study. In response to soil NO_x production then, about 2.2 ppb O_3 is formed on average during ozone season. In a NO_x-limited regime, increases in NO_x concentrations from agricultural activity can lead to higher concentrations of ozone, pushing the region further away from attaining the NAAQS.

Modeling studies have shown globally that stratospheric contribution to the tropospheric ozone budget is similar in magnitude to net photochemical production (Roelofs & Lelieveld, 1997; Stevenson et al., 2006). In fact, some stratospheric mass transport happens as a result of deep stratosphere-troposphere exchange (STE), when ozone is transported from the stratosphere into the planetary boundary layer (Škerlak et al., 2014, specifically their Fig. 5). These events have a strong seasonal dependence and peak in the spring in the midlatitudes but occur throughout the year and are a particularly important factor in ozone exceedances in the Southwestern US and the SSAB (Parrish et al., 2024; Zhang et al., 2020). Stratospheric air is characterized by low water vapor, and drier than normal conditions are observed at most of the sites on ozone exceedance days, with negative correlations observed for specific humidity in the summer months (Tables S1.3 and S1.4). According to Škerlak et al., (2014), the boundary layers that are most impacted by stratospheric intrusion are within the US southwest and the Tibetan Plateau, specifically in subtropical deserts near regions of high orography, and tropopause ozone concentrations are highest in the spring and summer months. The SSAB is east of the Peninsular Range, and much of the range's ridge line is between 1.5-3 km in height (Evan, 2019); the proximity of this mountain range to the desert creates a mountain valley circulation that promotes deep

tropospheric mixing. High orography and low air density combined with intense heating leads to deep convective boundary layers, and the deeper the boundary layers, the farther the vertical mixing reaches into the free troposphere, bringing down these elevated ozone concentrations. In addition, subtropical deserts observe the largest summertime boundary layer heights due to dry convection, again mixing down these higher ozone levels. These factors combined with the strong subsidence associated with mountain-valley circulation makes the Salton Sea Air Basin a prime location for deep STE and elevated background ozone concentrations.

In the Coachella Valley, ozone exceedances are much more frequent, but without strong correlations (Table S1.4) or significant normalized anomalies (Table S1.2), it is difficult to identify specific conditions that influence ozone exceedance events. It is likely that ozone exceedances in the Coachella Valley are a mixture of anthropogenic combustion sources, both local and interregional, as well as background ozone and biogenic sources (i.e., agriculture, golf courses, fertilized lawns). Agricultural emissions may be the most influential at the Indio monitoring site due to its proximity to the agriculturally active eastern Coachella Valley. Weekend effects in the Coachella Valley at Indio and Palm Springs O_3 monitoring sites also show a NO_x-limited regime (Fig. S1.4C & D). Lieb et al., 2024 estimated that agricultural soils contribute 21.0% on average to the Imperial County NO_x budget. The sensitivity of ozone production to NO_x [δO_3 MDA8/δNO_x] based on the weekend effect (Figs. S1.3-S1.4) in Palm Springs is 6.95 ppb of O_3 per ppb of NO_x. The average NO_x concentration in Palm Springs during ozone season is 2.4 ppb, meaning about 0.5 ppb originates from soils. In response, we expect to see 3.5 ppb O_3 formed on average.

To summarize, ozone pollution in the Imperial Valley seems to result primarily from localized emissions and depend strongly on temperature-dependent precursor emissions and

atmospheric dynamics. While interregional transport from Mexicali, Mexico is a source, ozone concentrations that deviate higher than average during ozone season dominant when northwesterly winds are observed, further suggesting that basin-wide sources of ozone dominate. Furthermore, the Coachella Valley observes many more ozone exceedance days than the Imperial Valley, in part due to the proximity of highly urbanized areas, with agriculture and managed landscapes (e.g., golf courses) likely contributing to the production of ozone precursors. The SSAB is a NO_x-limited regime, meaning that increases in NO_x emissions will increase the production of ozone, causing the NAAQS for ozone to be pushed further away from attainment. To mitigate the exacerbation of these conditions and reduce issues of exposure to over-burdened populations, unregulated sources of ozone precursors (e.g., agriculture, golf-courses) should be addressed.

1.4.2 Normalized anomalies for $PM_{2.5}$

Monthly mean normalized anomalies and correlation coefficients were calculated using data from CARB for 2014-2023. Normalized anomalies on days that exceed 24-hr $PM_{2.5}$ NAAQS of 35 $\mu g/m^3$, along with the standard deviation of the mean (SE) can be found in Table S1.5. Correlation coefficients were not included due to their low values, since the frequency of $PM_{2.5}$ exceedance days is low. In Calexico, NO_x and PM_{10} concentrations on $PM_{2.5}$ exceedance days have very strongly related anomalies, as well as CO and the $PM_{2.5}/PM_{10}$ ratio (92^{nd}, 85^{th}, 97^{th}, and 86^{th} percentiles, respectively). Sources of NO_x are likely dominated by combustion processes in the winter however, soil NO_x sources may be an important factor even during the winter months (Lieb et al., 2024). Because of the moderate fall and winter temperatures, the primarily planting season in the Imperial Valley occurs from September to April, meaning that fertilization

dominates during this period (Byrnes et al., 2020; Lieb et al., 2024; Watson & Chow, 2001; Yienger & Levy, 1995). Additionally, particulate nitrate accounts for 22% of the $PM_{2.5}$ mass chemical speciation on these exceedance days (Figure S1.5), likely linked to higher-than-average NO_x concentrations. During the winter months, the daytime atmospheric lifetime of NO_x is significantly extended due reduced actinic flux. Coupled with high ammonia concentrations from agricultural activities and livestock, the production of particulate nitrate is an important source of $PM_{2.5}$ (Granella et al., 2024). Source apportionment and chemical speciation of $PM_{2.5}$ in Calexico is discussed further in Section 1.4.4.

Four of the six $PM_{2.5}$ sites are along the perimeter of the Salton Sea. The first site is in the Northern Imperial Valley in Sonny Bono, and $PM_{2.5}$ exceedances (n = 6) were associated with strong northwesterly winds, higher than average temperatures, and exceptionally high PM_{10} concentrations (wind speed, temperature, and PM_{10} were in the 96^{th}, 76^{th}, and 100^{th} percentiles, respectively). However, with few data points and missing data, these values have a high degree of uncertainty, see Table S4 (SE ≥ 0.3). Few exceedance days paired with these normalized anomalies indicate that the $PM_{2.5}$ pollution in Sonny Bono may be a result of exceptional weather events. Further, there is a strong positive correlation between $PM_{2.5}$ and PM_{10}—these factors, in combination with the normalized anomaly data, may be indicative of meteorological influence on emissive compounds and playa dust from the Salton Sea (Frie et al., 2017). On the western side of the Salton Sea the Naval Test Base $PM_{2.5}$ monitor is located, which observed 36 exceedances during the period. These exceedances were associated with strong westerly winds and again very high levels of PM_{10}—scalar average wind speed and PM_{10} were in the 95^{th} and 100^{th} percentiles, respectively. Springtime exceedances (Figure 1.5) dominate because of

synoptically forced downslope winds from the Peninsular Range located west of the site (Evan, 2019). It is also worth noting that at sites with wind dominated PM exceedances, the $PM_{2.5}/PM_{10}$ does not seem to change significantly during high events, indicating that these sizes are comparably enhanced by aeolian dust. Bombay Beach is a site located on the eastern side of the Salton Sea, however, only 4 exceedances occurred at this site during the timeframe and analysis of normalized anomalies did not produce significant results. Lastly, in Banning, $PM_{2.5}$ exceedances were strongly associated with high humidity and NO_x levels (80^{th} percentile), consistent with secondary aerosol formation in the summer season. Winds in Banning are overwhelmingly westerly during the summer and springtime, situated in the eastern end of the LA basin; therefore, these exceedance days are likely related to interregional transport of urban $PM_{2.5}$ and precursors like NO_x and VOCs.

In summary, the $PM_{2.5}$ exceedance in the SSAB is primarily concentrated in Calexico and results from localized sources due to stagnating conditions. These sources are discussed further in Section 1.4.4. Additionally, $PM_{2.5}$ exceedances in regions immediately surrounding the Salton Sea seem to be heavily impacted by strong wind events and high PM_{10} levels. And just upwind of the Coachella Valley, Banning's $PM_{2.5}$ levels are highest in the summertime under the humid conditions affected by interregional transport of urban $PM_{2.5}$ and its precursors (e.g., NO_x and its oxidation products). The causes of $PM_{2.5}$ exceedances in the SSAB vary significantly across the valley, suggesting that mitigation strategies should be tailored to the specific needs of each region.

1.4.3 Normalized anomalies for PM_{10}

Monthly mean normalized anomalies for PM_{10} exceedance days were calculated using CARB data from 2009 to 2023 and are shown in Table S1.6a&b. Correlation coefficients (R^2) were not reported due to their insignificance. There are four PM_{10} monitors (Table S1.6a) in Imperial County and four in the Coachella Valley (Table S1.6b). The sites from the Salton Sea down across the Imperial Valley all share a similar pattern: high wind speeds, primarily westerly in direction, and high $PM_{2.5}$ but low $PM_{2.5}/PM_{10}$ ratios. Calexico, Indio, and Palm Springs exceedances exhibit lower than average NO_x, CO, and (mostly) O_3 concentrations, indicating that combustion sources are likely not contributing to these PM_{10} events, but instead are related to extreme wind events and thus ventilation of the trace gas pollutants. Because of this, PM_{10} composition is likely primarily crustal material.

The analysis highlights the complex interplay between meteorological factors and pollutant sources driving PM_{10} concentrations. Understanding these relationships is crucial for developing targeted air quality management strategies. Specific actions might include local emission controls, especially in urban areas where combustion sources likely contribute, and dust mitigation strategies, especially surrounding the Salton Sea.

1.4.4 Chemical Speciation Network Data Analysis: Calexico

The EPA's Chemical Speciation Network (CSN) was utilized to determine the chemical speciation of $PM_{2.5}$ in Calexico, CA—the site with the most $PM_{2.5}$ exceedance days in the SSAB. To understand how the speciation varies seasonally, Figure 1.10 shows the average seasonal chemical speciation for 2009-2023. In the winter months (DJF), there is a stronger than average concentration of nitrate, while in warmer months, sulfates have a larger contribution. The

concentrations of each chemical species can be found in Table S1.7. The chemical speciation data was also assessed during $PM_{2.5}$ exceedances, shown in Figure S1.5. Here, we see that organic carbon, nitrates, and soil comprise the majority of the $PM_{2.5}$ on exceedance days, or when $PM_{2.5}$ concentrations exceed the 24-h NAAQS of 35 µg/m^3. This makes sense because most exceedance days occur in the winter months.

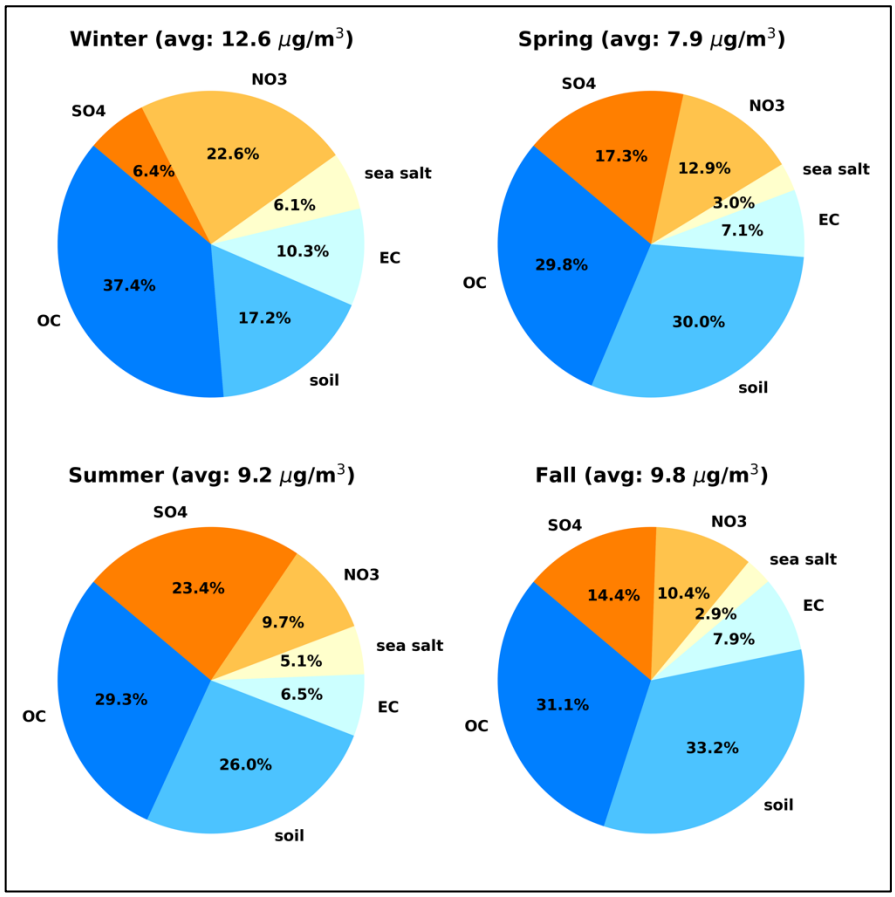

Figure 1.10. Chemical speciation of $PM_{2.5}$ in Calexico, CA averaged by season for the years 2009-2023.

The NMF analysis yielded five identifiable factors based on factor profiles: biomass burning, motor vehicle exhaust, agricultural soils, industrial, and dust. Factor contribution and profiles were normalized to one to facilitate source apportionment and profile interpretability. Each factor was unique in its particle distributions as well as its elemental composition (Figure

1.11), and our analysis was compared to a detailed source characterization study from Watson and Chow (2001). The composition of factor 1 was fairly consistent with their assessment of vegetative burning, with OC as the most abundant species. OC accounted for ~80% of the total mass and the OC/TC ratio was 0.82, much higher than the ratio for motor vehicle profiles. Sources of biomass burning in the Imperial Valley include agricultural field burning, domestic trash burning, and residential wood combustion, with field burning being the strongest emitter (Watson & Chow, 2001). Aside from OC and EC, other markers of biomass burning mentioned by Watson and Chow (2001) were less than 5%.

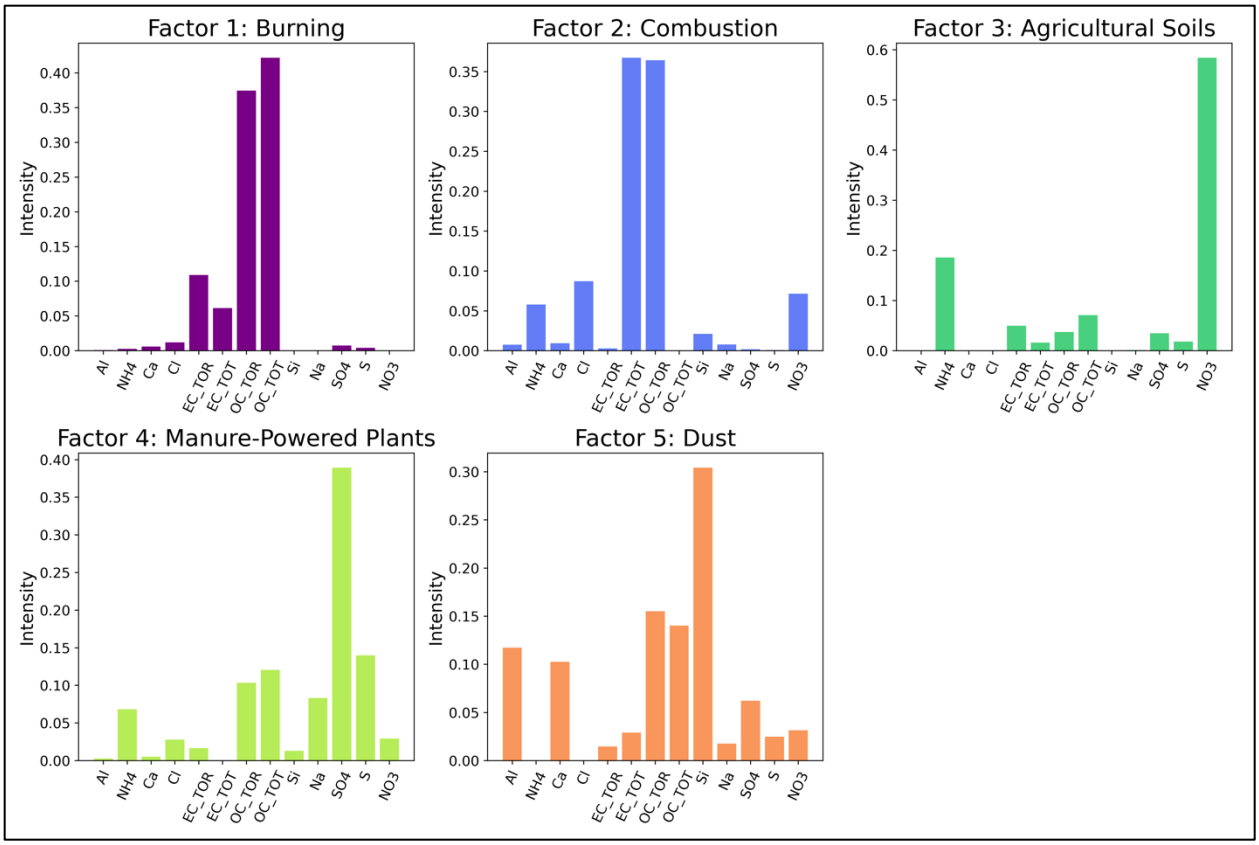

Figure 1.11. Positive Matrix Factorization was performed on the chemical speciation $PM_{2.5}$ data in Calexico, CA for the years 2009-2023.

Factor 2's composition was consistent with Watson and Chow (2001)'s analysis of motorized vehicle combustion, although the relative normalized contributions differed. It's important to note that Watson and Chow (2001) analyzed several field samples of data, whereas we are looking at long-term factorizations (2009-2023). Markers for motorized vehicle combustion include high contributions of OC, EC, and chlorine. Watson and Chow (2001) observed a strong profile of sulfate; however, we see a larger influence of ammonium nitrate. Factor 3 seems to indicate a large signal of ammonium nitrate small signatures (<10%) from EC, OC, sulfur, and sulfate. This profile was not observed in the Watson and Chow (2001) analysis, but due to the about 1:3 ratio of ammonium to nitrate, we believe that this factor represents particulate nitrate that originates from agricultural soils. Low concentrations of EC and OC may be indicative of organonitrate and organosulfate compounds.

Furthermore, factor 4 corresponds to Watson and Chow's assessment of industrial source emissions, specifically a manure-fueled power plant located upwind in El Centro, CA. The largest chemical component was sulfate (~39%), similar to the contribution measured by Watson and Chow. Lastly, factor 5's strong signatures of silicon (Si), aluminum (Al), and calcium (Ca) are all crustal components that indicate a dust source. In addition, organic carbon—a natural component of crustal material—is likely enhanced by road dust and soil sources of crop debris, burn residue, and agricultural chemicals (e.g., pesticides, herbicides, fungicides) (Watson & Chow, 2001).

To assess the contribution of each source to $PM_{2.5}$ exceedance, we selected from the dataset the days in which 24-h average $PM_{2.5}$ concentrations were greater than or equal to the 24-h NAAQS of 35 $\mu g/m^3$ (i.e., 98^{th} percentile). The results are shown in Figure 1.12. Mobile source

combustion, biomass burning, and agricultural soils tend to dominate as producers of $PM_{2.5}$ for Calexico. However, because the CSN data is only collected every six days, there are only 12 measurements used to calculate this, thereby increasing the uncertainty of this assessment. To increase the number of data points, we performed a similar analysis for the 90th percentile of the data (n = 80 days), which shows that biomass burning is the dominant source of the upper end of $PM_{2.5}$ concentrations, followed by agricultural soils and dust.

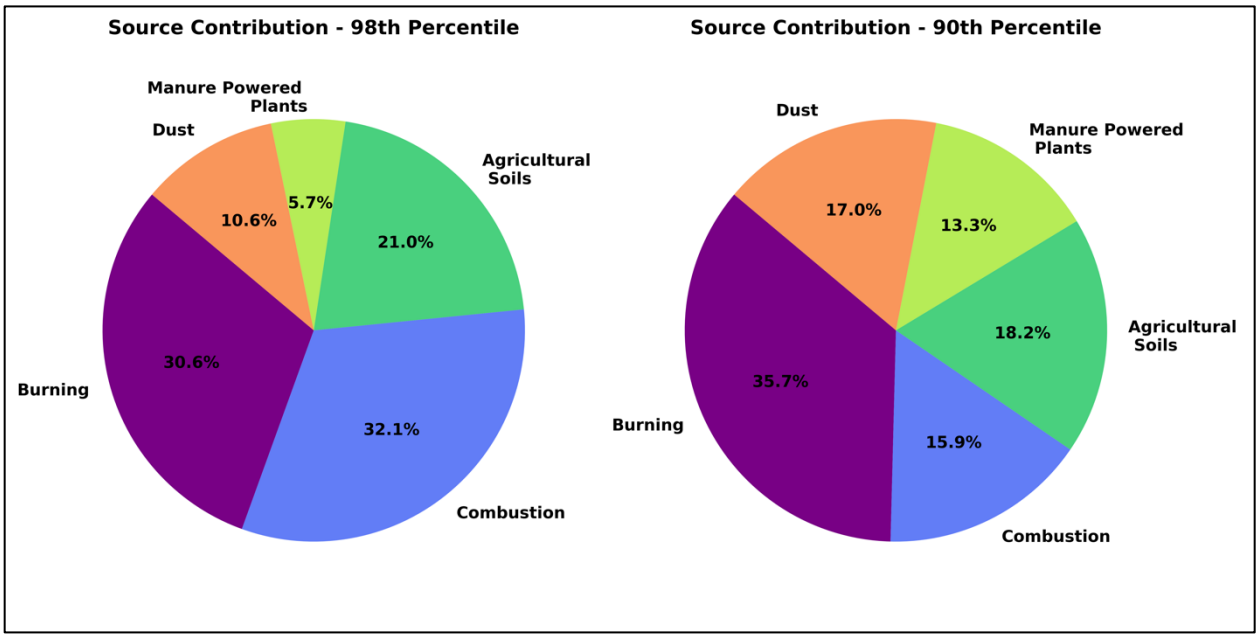

Figure 1.12. (A) Shows the source contribution to $PM_{2.5}$ exceedance days (i.e., 98th percentile, concentration ≥ 35 µg/m^3) in Calexico, CA. (B) Shows the source contribution to the upper 10th percentile of $PM_{2.5}$ measurements in Calexico, CA.

To address the continued nonattainment of $PM_{2.5}$ in Calexico, further work is necessary to reduce the impact of burning, agricultural soil NO_x emissions, and dust entrainment. Additionally, several mitigation strategies can be implemented, including stricter burning regulations, regulations on agricultural practices, and dust control measures. Enforcing stricter burning regulations and the reduction of burning during critical air quality periods may mitigate

commercial burning sources, while the conversion to alternative heating sources may reduce residential burning. Extensive procedures on ways to manage agricultural practices are outlined in section 2.5. Furthermore, soil stabilizers and vegetative cover in fallow farmlands or around the Salton Sea may reduce dust entrainment and help mitigate wind erosion. By implementing these strategies, Calexico can make significant progress toward achieving $PM_{2.5}$ attainment and improving the health and well-being of its residents.

1.5 Supplementary Tables

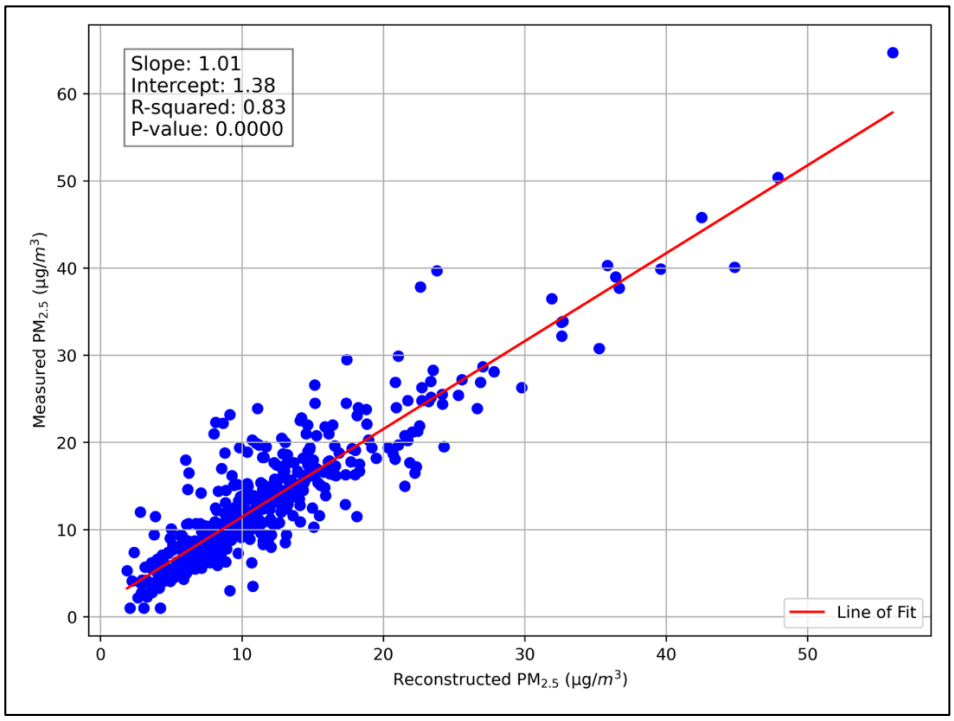

Figure S1.1. Reconstructed $PM_{2.5}$ concentrations compared to CSN measured $PM_{2.5}$ concentrations measured in Calexico, CA.

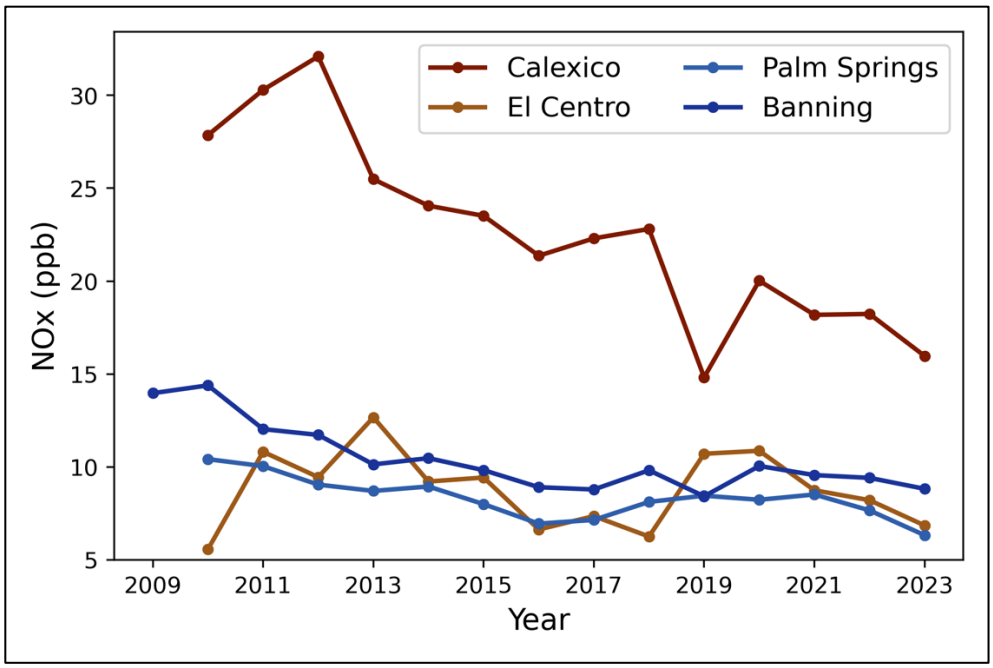

Figure S1.2. NO_x annual averages for the CARB sites in the Salton Sea Air Basin from 2009-2023.

Table 1.1. Comparing the trends of changes in NO_x concentrations.

Site	2009-2016			2017-2023		
	Slope	R^2	%-NO_x/yr	Slope	R^2	%-NO_x/yr
Calexico	-1.47	0.67	-5.57	-0.88	0.40	-4.65
El Centro	0.01	0.00	0.11	0.02	0.00	0.24
Palm Springs	-0.52	0.92	-5.86	-0.12	0.10	-1.54
Banning	-0.71	0.91	-6.21	0.02	0.00	0.22

Section S1.1. Hourly wind roses for each meteorological site in the Salton Sea Air Basin. The legend to the right of each represents scalar wind speed.

Figure S1.1.1 Monthly wind rose for Calexico

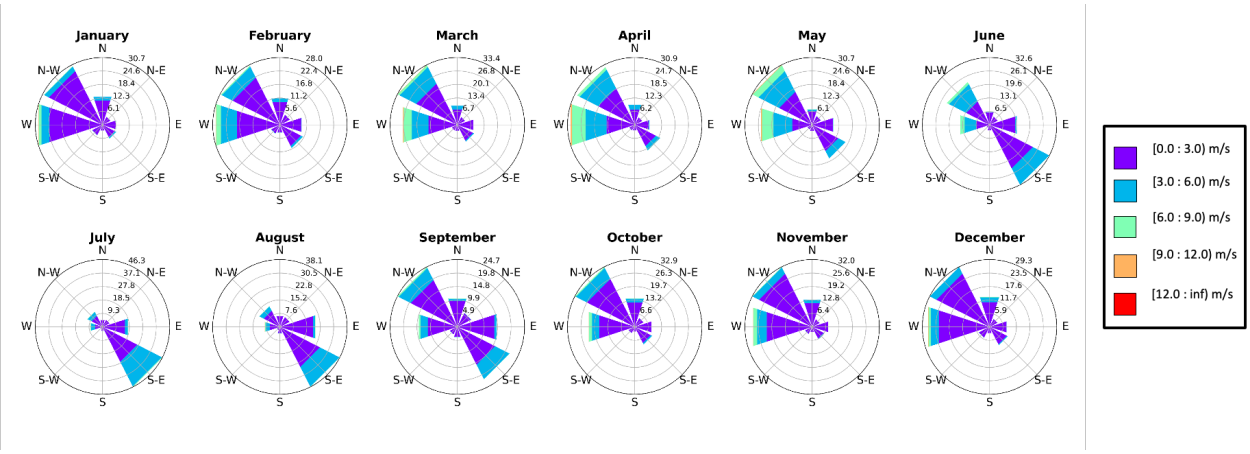

Figure S1.1.2 Monthly wind rose for El Centro

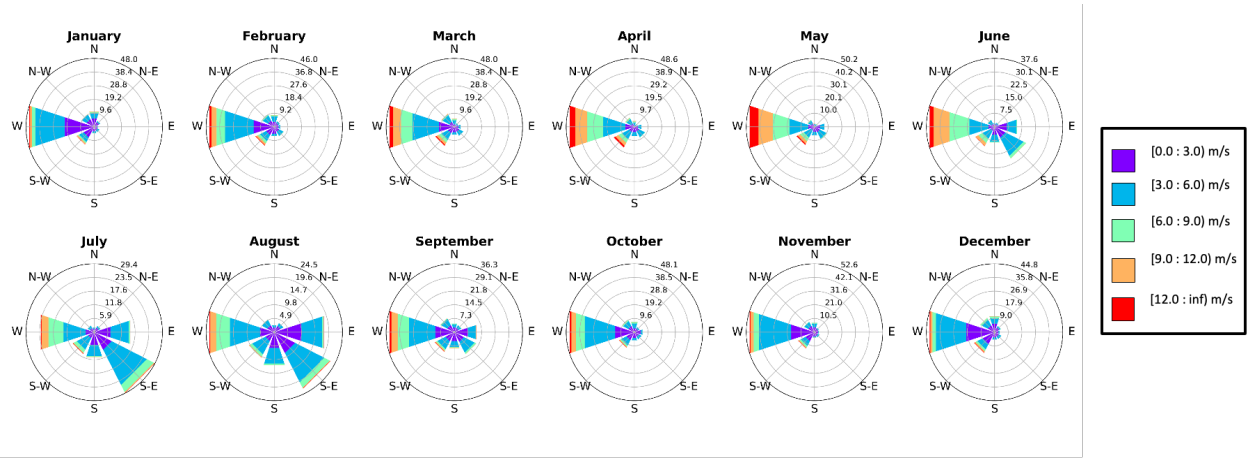

Figure S1.1.3 Monthly wind rose for Imperial

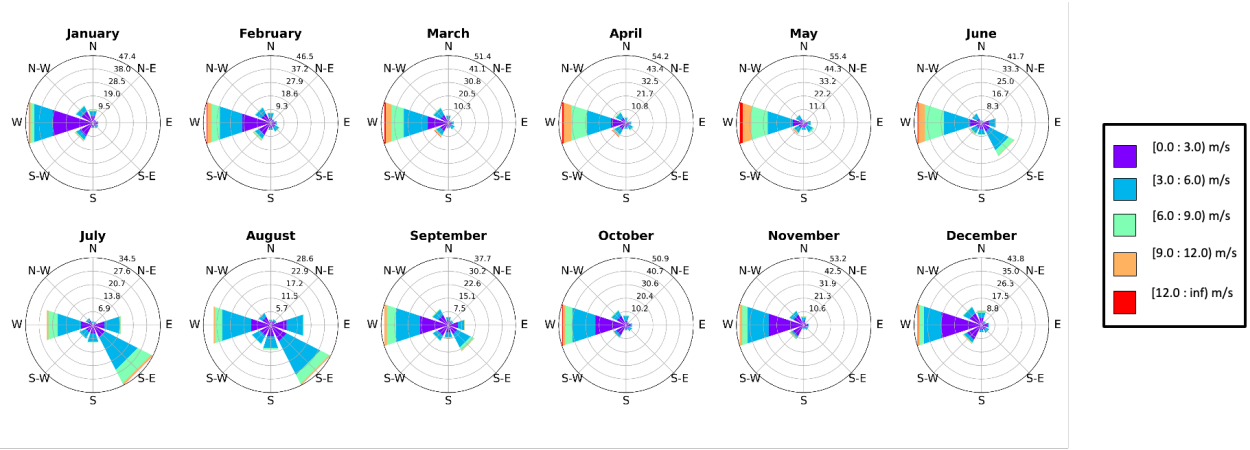

Figure S1.1.4 Monthly wind rose for Sonny Bono

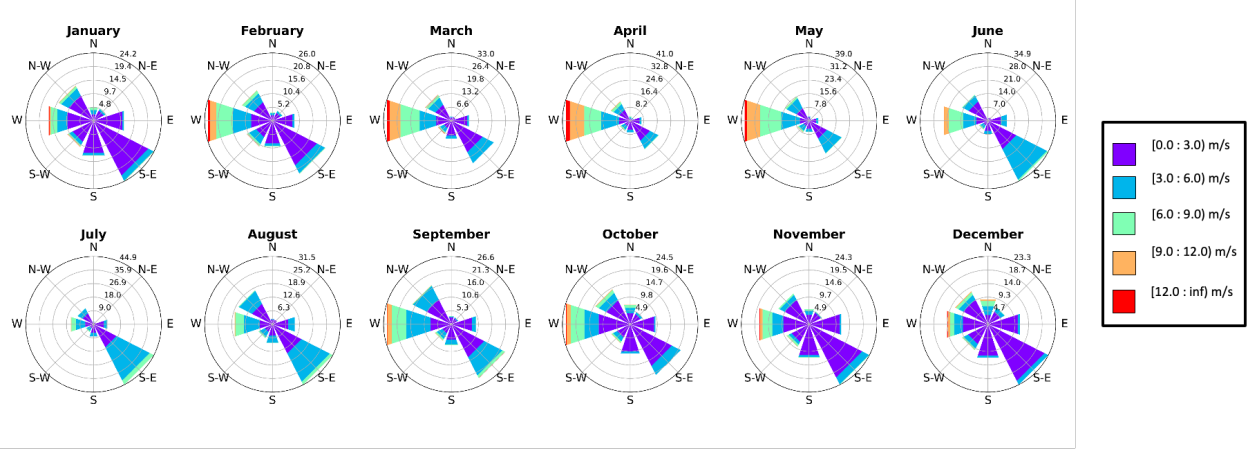

Figure S1.1.5 Monthly wind rose for Naval Test Base

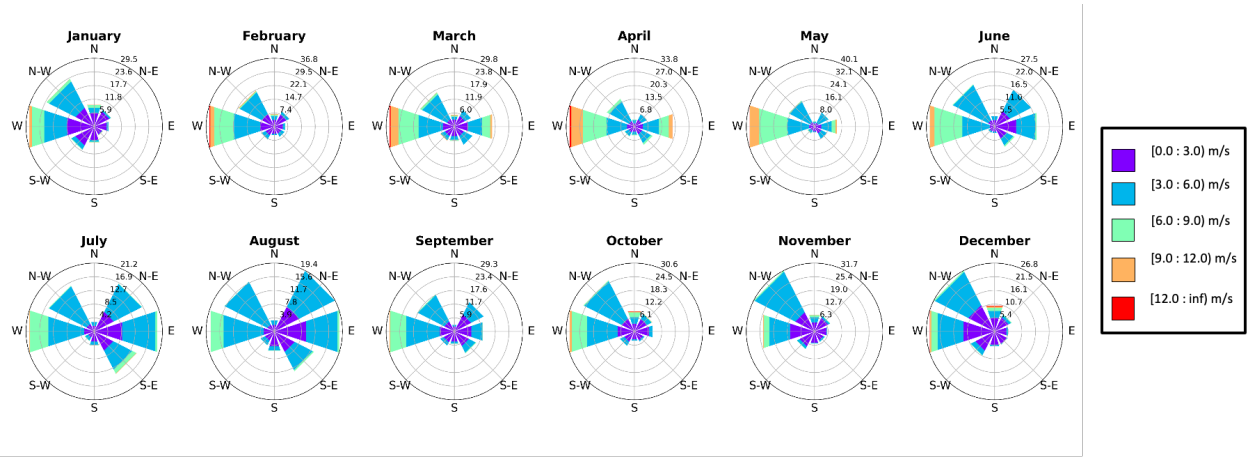

Figure S1.1.6 Monthly wind rose for Bombay Beach

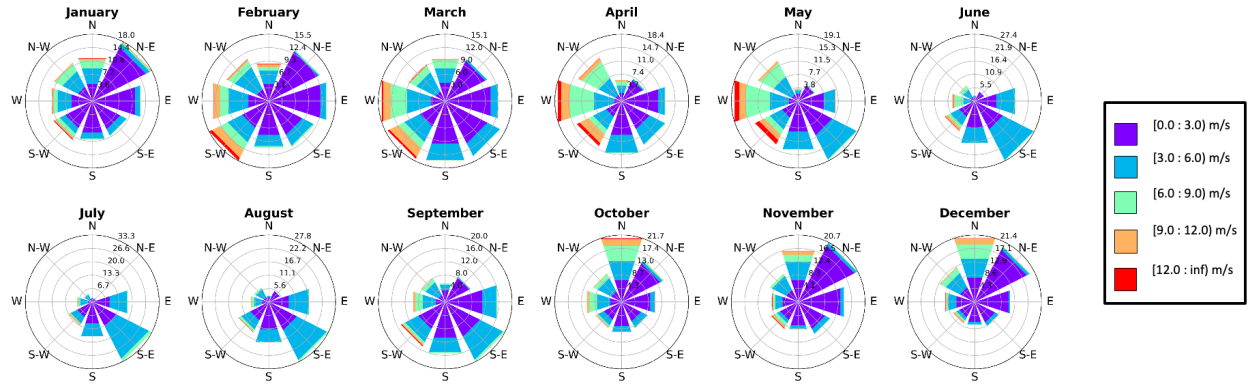

Figure S1.1.7 Monthly wind rose for Torres-Martinez

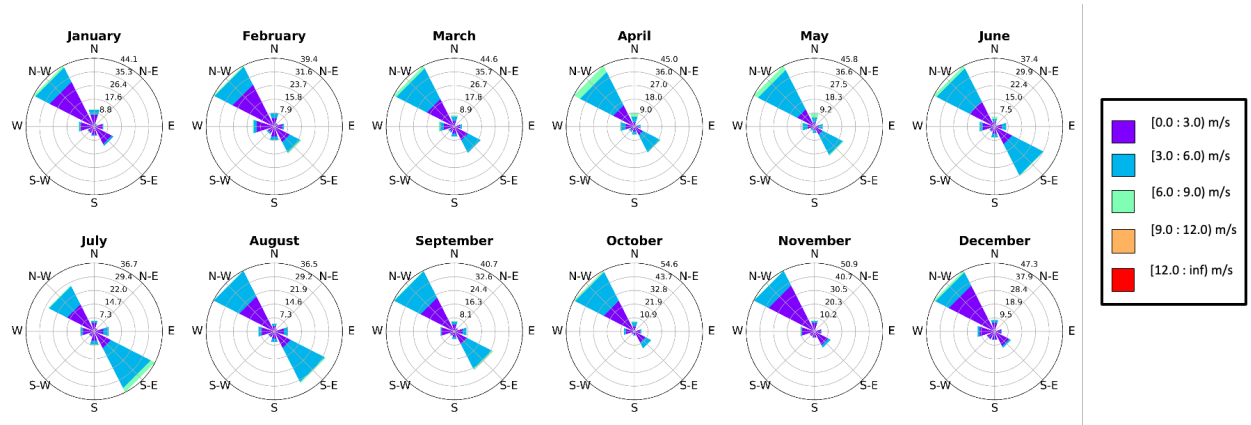

Figure S1.1.8 Monthly wind rose for Indio

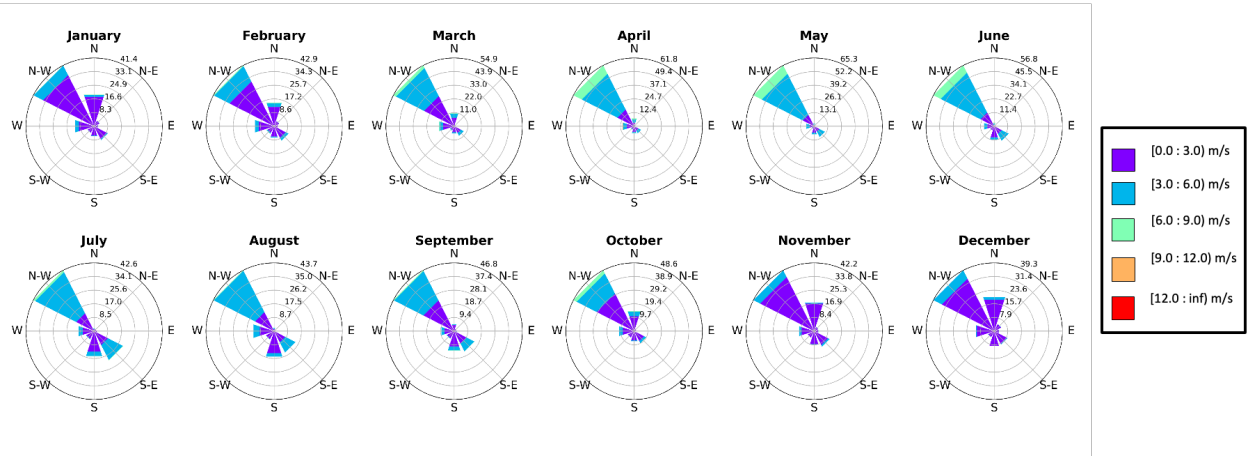

Figure S1.1.9 Monthly wind rose for Palm Springs

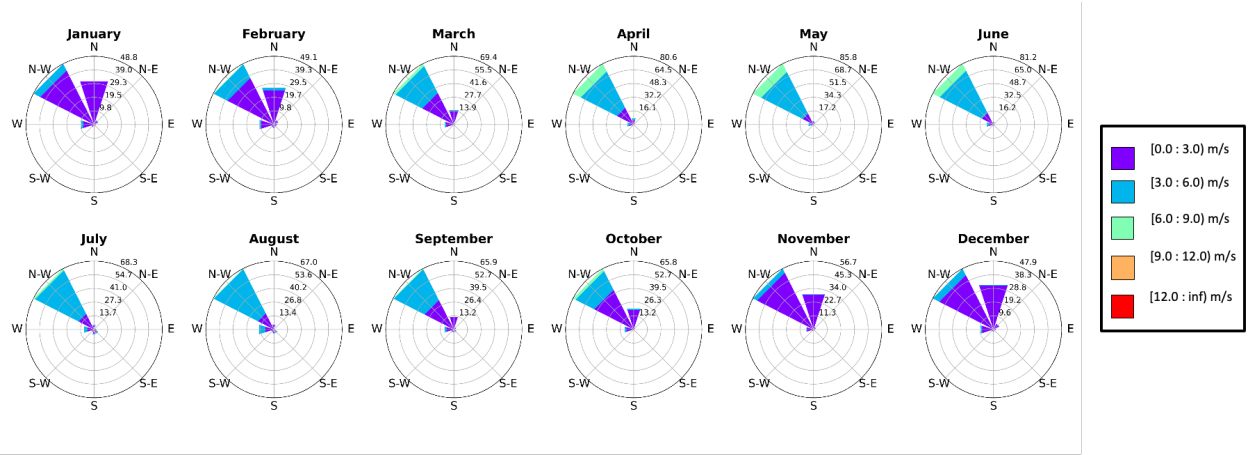

Figure S1.1.10 Monthly wind rose for Banning

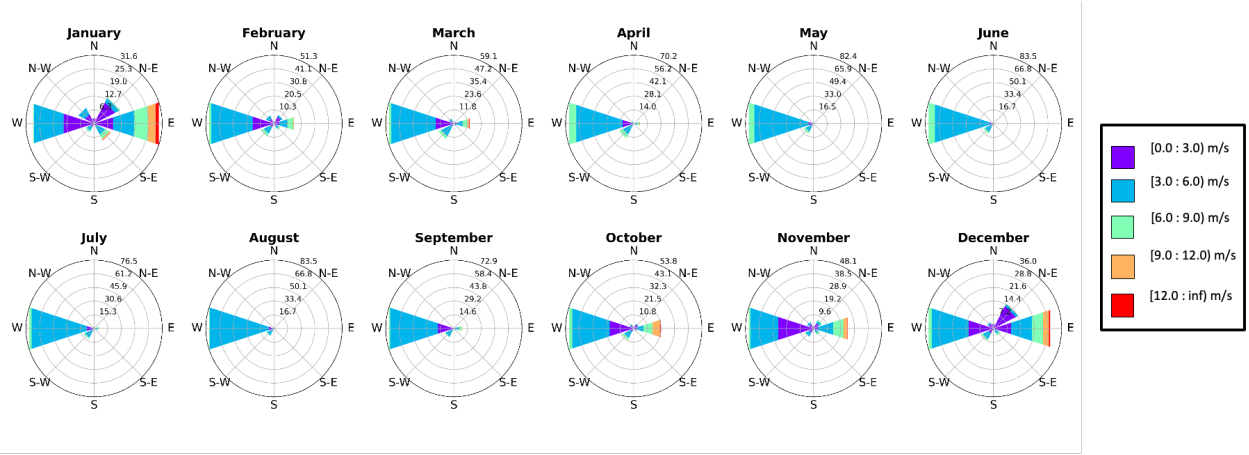

Table S1.2. Normalized anomalies for the Salton Sea Air Basin for CARB monitoring sites on days that exceed the O_3 NAAQS of 70 ppb during 2009-21. Monitors for analysis were selected by their proximity to the ozone monitoring sites (within a subregion). An asterisk (*) beside the number indicates that the monitor used for this measurement was based on the nearest neighboring air monitor in the subregion. Cells containing an N/A denote that there was not sufficient data available to perform the analysis, while NM denotes that there is no monitor for the region. Standard error (SE)for the normalized anomalies is also reported.

	Calexico	El Centro	Niland	Indio	Palm Springs	Banning
n exceedance days	241	264	55	546	761	1073
Temp (°C)	0.51* SE = 0.1	0.47 SE = 0.1	0.21 SE = 0.1	0.30 SE = 0.0	0.42 SE = 0.1	0.46 SE = 0.0
Scalar Avg Wind Speed (m/s)	-0.68 SE = 0.0	-0.49 SE = 0.0	0.22* SE = 0.1	0.00 SE = 0.1	-0.11 SE = 0.1	-0.20 SE = 0.0
U Vector Wind Direction	0.08 SE = 0.0	-0.20 SE = 0.0	-0.16* SE = 0.5	0.16 SE = 0.1	-0.02 SE = 0.1	-0.07 SE = 0.0
V Vector Wind Direction	-0.21 SE = 0.0	-0.20 SE = 0.0	-0.03 SE = 0.2	-0.04 SE = 0.1	0.04 SE = 0.1	-0.24 SE = 0.0
Specific Humidity (g H_2O/kg air)	-0.37* SE = 0.1	-0.23 SE = 0.1	N/A	-0.24 SE = 0.1	-0.02 SE = 0.1	0.07 SE = 0.0
Relative Humidity (%)	-0.51* SE = 0.1	-0.41 SE = 0.1	N/A	-0.35 SE = 0.0	-0.02 SE = 0.0	-0.24 SE = 0.0
PM_{10} (µg/m^3)	0.09 SE = 0.1	0.26* SE = 0.1	0.23 SE = 0.1	0.05 SE = 0.0	0.05 SE = 0.0	NM
$PM_{2.5}$ (µg/m^3)	0.38 SE = 0.1	0.66* SE = 0.1	N/A	0.25* SE = 0.0	0.14* SE = 0.0	0.35 SE = 0.0
NO_x (ppb)	0.27 SE = 0.1	0.82 SE = 0.1	NM	0.15* SE = 0.0	0.27 SE = 0.0	0.37 SE = 0.0
NO_2 (ppb)	0.45 SE = 0.1	0.93 SE = 0.1	NM	0.20* SE = 0.0	0.33 SE = 0.0	0.42 SE = 0.0
CO (ppm)	-0.01 SE = 0.1	0.58* SE = 0.1	NM	0.11* SE = 0.0	0.19 SE = 0.0	NM
$PM_{2.5}/PM_{10}$	0.38 SE = 0.1	0.44* SE = 0.1	N/A	N/A	N/A	N/A

Table S1.3. Correlation coefficients (R^2) and slopes (m) for the Imperial Valley ozone sites calculated for the months of April through September during 2009-19. Cells containing an NM

denote that there was no monitor for that specific variable. Additionally, correlation coefficients were considered statistically significant if their p-values were less than or equal to 0.05. Correlation coefficients with a p-value greater than 0.05 are marked with a strikethrough.

	Calexico		El Centro		Niland	
	R^2	m	R^2	m	R^2	m
T_{max} (°C)	0.01	0.15	0.03	0.38	0.06	-0.57
Daytime Scalar Average Wind Speed (m/s)	0.06	-1.85	0.01	-0.47	0.04	0.68
Daytime U Wind Component	0.05	1.03	~~0.00~~	0.07	0.01	0.33
Daytime V Wind Component	0.12	-2.81	0.00	-0.25	0.02	0.56
24-h Avg Specific Humidity (g H_2O/kg air)	0.23	-1300	0.12	-911	0.15	-1300
24-h Avg RH (%)	0.26	-0.46	0.14	-0.36	0.04	-0.34
24-h Avg NO_x (ppb)	~~0.00~~	-0.03	~~0.00~~	-0.05	NM	NM
24-h Avg NO_2 (ppb)	0.00	0.13	~~0.00~~	-0.07	NM	NM
24-h Avg $PM_{2.5}$ ($\mu g/m^3$)	0.01	0.23	0.08	0.61	0.01	0.38
24-h Avg PM_{10} ($\mu g/m^3$)	0.02	-0.03	~~0.04~~	0.01	0.00	-0.01
24-h Avg CO (ppm)	0.01	4.87	NM	NM	NM	NM

Table S1.4. Correlation coefficients (R^2) and slopes (m) for the Coachella Valley ozone sites calculated for the months of June through September during 2009-19. Cells containing an NM denote that there was no monitor for that specific variable. Additionally, correlation coefficients were considered statistically significant if their p-values were less than or equal to 0.05. Correlation coefficients with a p-value greater than 0.05 are marked with a strikethrough.

	Indio		Palm Springs		Banning	
	R^2	m	R^2	m	R^2	m
T_{max} (°C)	0.04	0.38	0.11	0.62	0.33	1.21

Daytime Scalar Average Wind Speed (m/s)	0.04	-1.87	0.01	-1.11	0.02	-2.26
Daytime U Wind Component	~~0.00~~	-0.17	~~0.00~~	-0.35	0.02	0.65
Daytime V Wind Component	0.01	0.38	0.01	0.60	0.04	-2.77
24-h Avg Specific Humidity (g H_2O/kg air)	0.15	-1300	0.01	-300	0.03	925
24-h Avg RH (%)	0.18	-0.41	0.10	-0.29	0.14	-0.25
24-h Avg NO_x (ppb)	NM	NM	0.01	0.54	0.06	0.82
24-h Avg NO_2 (ppb)	NM	NM	0.02	0.77	0.11	1.20
24-h Avg $PM_{2.5}$ ($\mu g/m^3$)	0.02	0.28	NM	NM	0.16	0.87
24-h Avg PM_{10} ($\mu g/m^3$)	~~0.00~~	-0.01	~~0.00~~	0.02	NM	NM
24-h Avg CO (ppm)	NM	NM	0.06	37.6	NM	NM

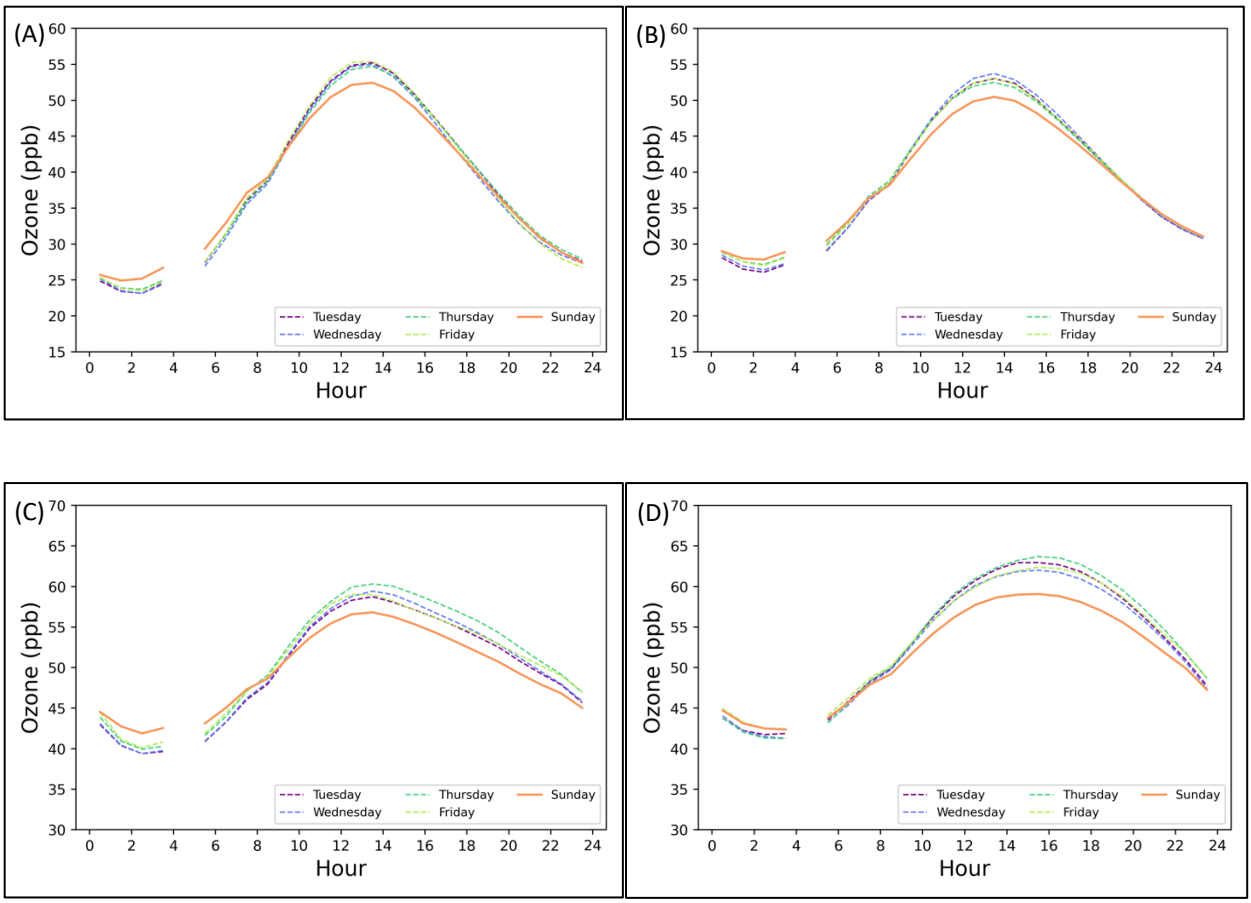

Figure S1.3. The weekend effect for the average hourly ozone concentrations in (A) Calexico, (B) El Centro, (C) Indio, and (D) Palm Springs from 2014-2023. Data at 4 am is not available due to routine calibration. Both Monday and Saturday were not included to account for transitions between the weekend and weekday.

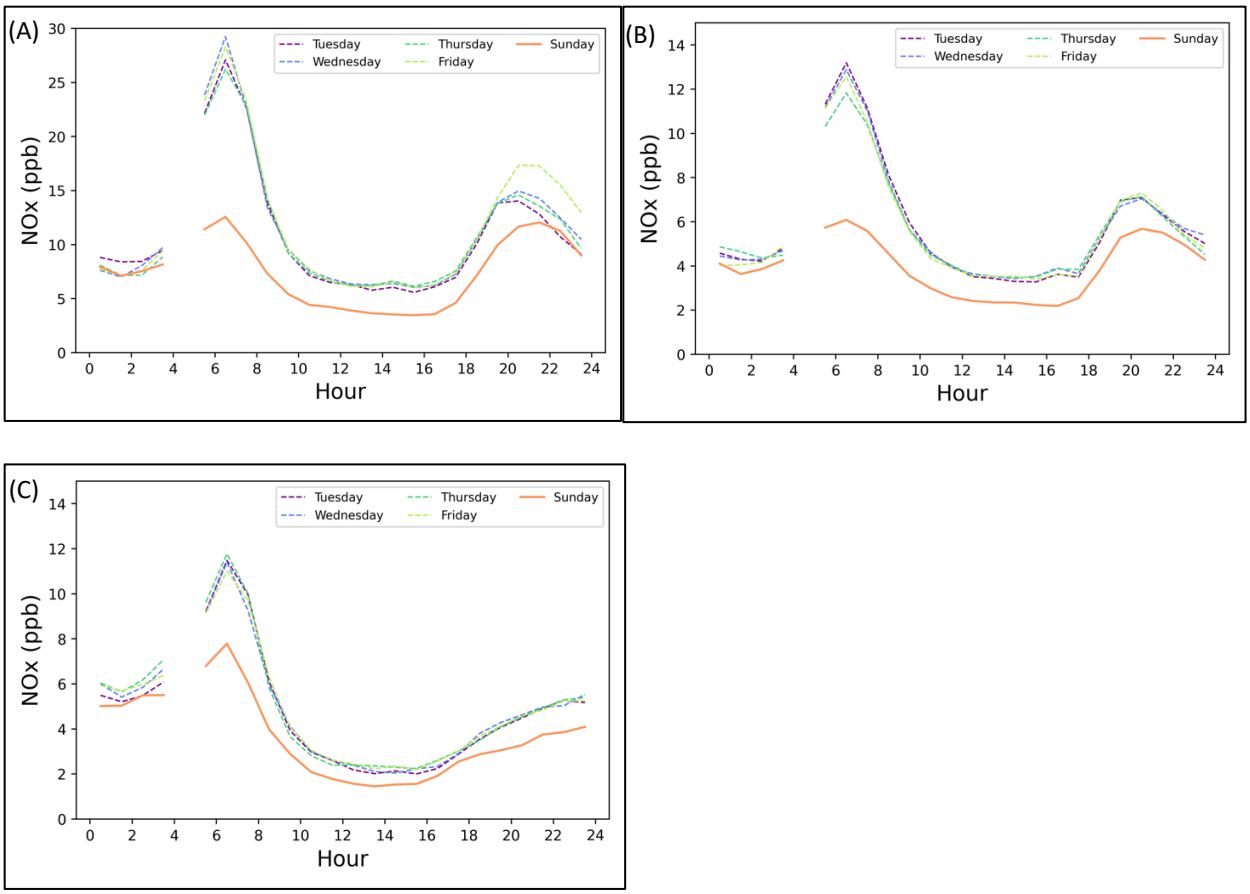

Figure S1.4. The weekend effect for average hourly NO_x concentrations in (A) Calexico, (B) El Centro, and (C) Palm Springs from 2014-2023. Data at 4 am is not available due to routine calibration. Both Monday and Saturday were not included to account for transitions between the weekend and weekday.

Table S1.5. Normalized anomalies for the Salton Sea Air Basin for CARB monitoring sites on days that exceed the $PM_{2.5}$ NAAQS of 35 µg/m^3 during 2009-21. Monitors for analysis were selected by their proximity to the $PM_{2.5}$ monitoring sites. An asterisk (*) beside the number indicates that the monitor used for this measurement was based on the nearest neighboring air monitor in the subregion. Cells containing an N/A denote that there was not sufficient data available to perform the analysis, while NM denotes that there is no monitor for the region. Standard error (SE) for the normalized anomalies is also reported.

	Calexico	Sonny Bono	Naval Test Base	Bombay Beach	Torres-Martinez	Banning
n exceedance days	67	6	36	4	9	31
Temp (°C)	-0.23* SE = 0.2	0.73 SE = 0.5	0.09 SE = 0.28	N/A	-0.37* SE = 0.37	-0.22 SE = 0.2
Scalar Avg Wind Speed (m/s)	-0.61 SE = 0.1	1.99 SE = 0.6	1.91 SE = 0.2	0.70 SE = 2.6	N/A	0.01 SE = 0.3
U Vector Wind Direction	-0.64 SE = 0.1	1.24 SE = 1.2	1.92 SE = 0.2	-0.85 SE = 0.1	N/A	-0.17 SE = 0.4
V Vector Wind Direction	-0.59 SE = 0.1	1.43 SE = 0.29	0.41 SE = 0.2	0.93 SE = 0.5	N/A	-0.37 SE = 0.2
Specific Humidity (g H_2O/kg air)	-0.12* SE = 0.1	0.06 SE = 0.3	-0.26 SE = 0.2	N/A	0.99* SE = 0.4	0.80 SE = 0.3
Relative Humidity (%)	-0.08* SE = 0.1	-0.18 SE = 0.4	-0.3 SE = 0.2	N/A	1.03* SE = 0.2	0.70 SE = 0.3
PM_{10} (µg/m^3)	2.10 SE = 0.2	5.61 SE = 3.5	4.48 SE = 0.9	-0.28 SE = 0.5	N/A	NM
NO_x (ppb)	1.55 SE = 0.1	NM	NM	NM	0.15* SE = 0.4	0.76 SE = 0.2
NO_2 (ppb)	1.36 SE = 0.2	NM	NM	NM	-0.08* SE = 0.4	0.84 SE = 0.2
CO (ppm)	1.06 SE = 0.1	NM	NM	NM	-0.01* SE = 0.2	NM
$PM_{2.5}/PM_{10}$	1.00 SE = 0.1	0.13 SE = 0.6	-0.63 SE = 0.1	10.93 SE = 2.6	N/A	N/A

Table S1.6a. Normalized anomalies for the Salton Sea Air Basin for CARB monitoring sites on days that exceed the 24-hour PM_{10} NAAQS of 150 µg/m^3 during 2009-21. Monitors for analysis

were selected by their proximity to the $PM_{2.5}$ monitoring sites. An asterisk (*) beside the number indicates that the monitor used for this measurement was based on the nearest neighboring air monitor in the subregion. Cells containing an N/A denote that there was not sufficient data available to perform the analysis, while NM denotes that there is no monitor for the region. Standard error (SE) for the normalized anomalies is also reported.

	Calexico	Sonny Bono	Niland	Naval Test Base
n exceedance days	34	64	79	126
Temp (°C)	-0.34 SE = 0.2	0.31 SE = 0.3	-0.06 SE = 0.1	-0.06 SE = 0.1
Scalar Avg Wind Speed (m/s)	1.55 SE = 0.2	1.72 SE = 0.3	2.24* SE = 0.2	1.46 SE = 0.1
U Vector Wind Direction	0.94 SE = 0.4	1.54 SE = 0.3	1.80* SE = 0.3	1.33 SE = 0.1
V Vector Wind Direction	0.83 SE = 0.2	0.76 SE = 0.2	0.89* SE = 0.3	0.19 SE = 0.2
Specific Humidity (g H_2O/kg air)	0.01 SE = 0.2	0.01 SE = 0.2	0.44 SE = 0.1	-0.03 SE = 0.1
Relative Humidity (%)	-0.04 SE = 0.2	-0.25 SE = 0.2	0.36 SE = 0.1	0.02 SE = 0.01
$PM_{2.5}$ (µg/m^3)	2.56 SE = 0.4	4.29 SE = 1	4.69* SE = 0.6	2.09 SE = 0.2
NO_x (ppb)	-0.64 SE = 0.2	NM	NM	NM
NO_2 (ppb)	-0.63 SE = 0.2	NM	NM	NM
O_3 MDA8 (ppb)	-0.09 SE = 0.02	NM	-0.00 SE = 11	NM
CO (ppm)	-0.48 SE = 0.1	NM	NM	NM
$PM_{2.5}/PM_{10}$	-1.19 SE = 0.2	-0.56 SE = 0.3	NM	-1.16 SE = 0.1

Table S1.6b. PM_{10} normalized anomalies and SE continued.

	Bombay Beach	Torres-Martinez	Indio	Palm Springs
n exceedance days	16	50	28	13
Temp (°C)	0.39 SE = 0.3	-0.38* SE = 0.1	-0.19 SE = 0.4	-1.20* SE = 0.2
Scalar Avg Wind Speed (m/s)	1.78 SE = 0.4	1.54 SE = 0.3	2.00 SE = 0.8	-0.59 SE = 0.5

U Vector Wind Direction	0.29 SE = 0.6	1.08 SE = 0.3	-0.71 SE = 0.8	-0.92 SE = 0.1
V Vector Wind Direction	0.41 SE = 0.8	-1.71 SE = 0.3	-1.14 SE = 0.9	1.00 SE = 0.0
Specific Humidity (g H_2O/kg air)	0.34 SE = 0.8	0.00* SE = 0.2	0.41 SE = 0.5	1.25* SE = 0.1
Relative Humidity (%)	0.27 SE = 0.8	0.11 SE = 0.3	0.60 SE = 0.2	1.25* SE = 0.2
$PM_{2.5}$ ($\mu g/m^3$)	2.33 SE = 0.5	2.71 SE = 0.4	2.48* SE = 0.7	3.60* SE = 2.7
NO_x (ppb)	NM	NM	-0.68* SE = 0.1	-0.76 SE = 0.2
NO_2 (ppb)	NM	NM	-0.72* SE = 0.1	-0.91 SE = 0.2
O_3 MDA8 (ppb)	NM	NM	-0.73 SE = 0.2	-0.94 SE = 0.3
CO (ppm)	NM	NM	NM	-0.76 SE = 0.3
$PM_{2.5}/PM_{10}$	-1.07 SE = 0.1	-1.43 SE = 0.1	-0.97* SE = 0.2	-1.05* SE = 0.5

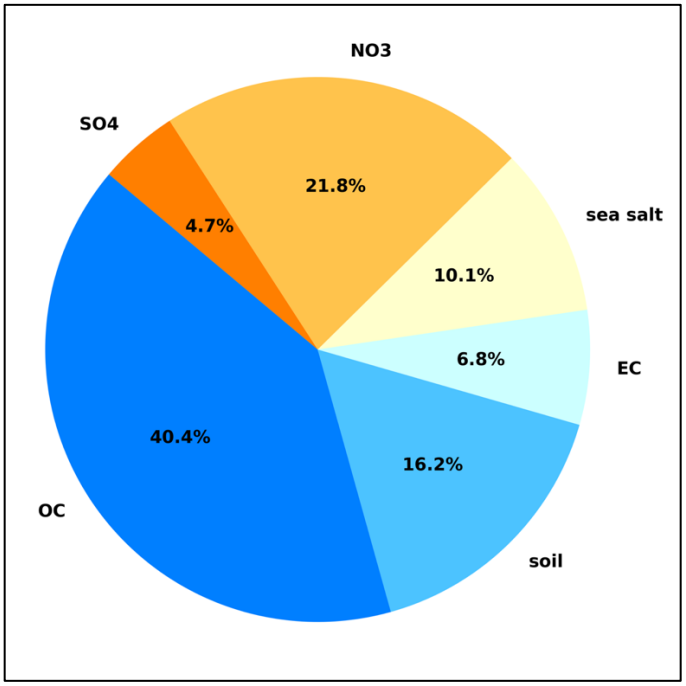

Figure S5. Chemical speciation of $PM_{2.5}$ 98th percentile averaged for the years 2009-2023.

Table S1.7. Restructured chemical speciation seasonal compositions.

Season	OC ($\mu g/m^3$)	Soil ($\mu g/m^3$)	EC ($\mu g/m^3$)	Sea Salt ($\mu g/m^3$)	NO_3 ($\mu g/m^3$)	SO_4 ($\mu g/m^3$)	Average $PM_{2.5}$ ($\mu g/m^3$)	Average $PM_{2.5}/PM_{10}$
Winter	4.71 (37.4%)	2.16 (17.2%)	1.29 (10.3%)	0.77 (6.1%)	2.85 (22.6%)	0.81 (6.4%)	12.60	0.27
Spring	2.35 (29.8%)	2.37 (30.0%)	0.56 (7.1%)	0.23 (3.0%)	1.02 (12.9%)	1.37 (17.3%)	7.91	0.23
Summer	2.70 (29.3%)	2.40 (26.0%)	0.60 (6.5%)	0.47 (5.1%)	0.90 (9.7%)	2.16 (23.4%)	9.23	0.26
Fall	3.04 (31.1%)	3.25 (26.0%)	0.77 (6.5%)	0.28 (5.1%)	1.02 (9.7%)	1.41 (23.4%)	9.78	0.21
Mean	3.20	2.55	0.81	0.44	1.45	1.44	9.88	0.24

Chapter 2: Nitrogen Isotopes Reveal High NO_x Emissions from Arid Agricultural Soils in the Salton Sea Air Basin

Abstract

Air quality management commonly aims to mitigate nitrogen oxide (NO_x) emissions from combustion, reducing ozone (O_3) and particulate matter (PM) pollution. Despite such efforts, regulations have recently proven ineffective in rural areas like the Salton Sea Air Basin of Southern California, which routinely violates O_3 and PM air quality standards. With over $2 billion in annual agricultural sales and low population density, air quality in the region is likely influenced by the year-round farming activity. We conducted a source apportionment of NO_x (an important precursor to both O_3 and PM) using nitrogen stable isotopes of ambient nitrogen dioxide (NO_2), which revealed a significant contribution from soil-emitted NO_x to the regional budget. The soil source strength was estimated using a mixing model based on the mean δ^{15}N-NO_x from each emission category in the California Air Resources Board's NOx inventory. Our annual average soil emission estimate for the air basin was 11.4 ± 4 tons/d, representing ~30% of the extant NO_x inventory, 10 times larger than the state's inventory for soil emissions. Unconstrained environmental factors such as nutrient availability, soil moisture, and temperature have a first-order impact on soil NO_x production in this agriculturally intensive region, with fertilization and irrigation practices likely driving emission variability. Without spatially and temporally accurate data on fertilizer application rates and irrigation schedules, it is difficult to determine the direct impacts that these variations have on our observations. Nevertheless, comparative analysis with previous studies indicates that soil NO_x emissions in the Imperial Valley are significantly

underrepresented in current inventories, highlighting the need for more detailed and localized observational data to constrain the sizeable and variable emissions from these arid, agricultural soils.

2.1 Background

The modern nitrogen cycle was formed around 2.7 billion years ago when microbial processes evolved with robust natural feedbacks and controls (Canfield et al., 2010). The biosphere contains a mixture of nitrogen compounds with various physical and chemical properties and lifetimes. These compounds include molecular nitrogen (N_2), ammonia/ammonium (NH_3/NH_4^+), nitrous oxide (N_2O), nitric oxide and nitrogen dioxide ($NO + NO_2 = NO_x$), nitrous acid/nitrite (HNO_2/NO_2^-), nitric acid/nitrate (HNO_3/NO_3^-), and organic nitrogen. The presence of these compounds, aside from inert N_2, is highly variable and is largely dependent on the microbiome in a given region (Rooker, 1977).

Anthropogenic activity has significantly influenced the nitrogen cycle (Rooker, 1977). In the late 19th century, the first gasoline-fueled combustion engines were produced for commercial use. Additionally, in the last century there has been development of new agricultural practices to satisfy global demand for food due to the creation of synthetic fertilizers using the Haber-Bosch process. These activities have resulted in negative environmental implications, including destruction of natural lands as well as air and water pollution.

Nitrogen oxides ($NO_x = NO + NO_2$) are a central precursor to ozone (O_3) and particulate matter (PM), both of which are federally regulated criteria pollutants, known to negatively impact human health and the environment (Caplin et al., 2019; Di et al., 2017). NO_x is produced through natural, biogenic, and anthropogenic processes, although a critical distinction is necessary.

Natural sources of NO_x occur without influence from human activity, such as lightning or weather-induced wildfires. Biogenic NO_x is naturally occurring and is produced by living organisms through microbial nitrification/denitrification cycles in soils. Further, anthropogenic NO_x results from human activities such as fossil fuel combustion in vehicles and power plants. However, these natural processes can be affected by anthropogenic activity, such as biomass burning in agricultural systems, human-ignited wildfires in poorly managed landscapes, and microbial denitrification in soils from fertilized croplands.

Anthropogenic combustion sources have traditionally been the primary focus of air quality management practices, as they have historically been the dominant source of NO_x emissions, with biogenic processes accounting for only about 20% of the global NO_x budget, on average (Fowler et al., 2013; Hu et al., 2017; Jaeglé et al., 2005; Miyazaki & Eskes, 2013; Song et al., 2022; Stevenson et al., 2006; van Vuuren et al., 2011). These practices have largely reduced precursor emissions, yet several of the United States' worst-air quality districts remain in rural regions (Almaraz et al., 2018; Parrish et al., 2017), including the Imperial and Coachella Valleys of Southern California. These valleys together constitute the Salton Sea Air Basin (SSAB), which is currently nonattainment for the O_3, $PM_{2.5}$, and PM_{10} National Ambient Air Quality Standards (NAAQS). Interregional transport from larger metropolitan areas is often blamed (California Air Resources Board (CARB), 2022; Chow et al., 2000; Environmental Protection Agency (EPA), 2020a, 2020b, 2022, 2023; Mendoza et al., 2010) hewing to the traditional paradigm of combustion dominant sources. This issue is a serious matter of environmental injustice because residents of Imperial County are 86% Latino and 21% of residents live below the poverty line (U.S. Census Bureau, 2023). Additional burdens these communities face include insufficient housing

availability and poor infrastructure, language barriers, poverty conditions, asthma, and impaired water quality (Anderson et al., 2012; Atkinson et al., 2016; Farzan et al., 2019; Miao et al., 2022; OEHHA, 2023). These factors put residents and farmworkers at risk of respiratory damage and diseases like asthma and COVID-19 (Borro et al., 2020; Comunian et al., 2020; Farzan et al., 2019). In fact, Imperial County held both the highest infection and mortality rates per capita in California from COVID-19 throughout the height of the pandemic (Los Angeles Times, 2023; The New York Times, 2023). Members of the rural Eastern Coachella Valley also suffer from similar socioeconomic and environmental injustices (OEHHA, 2023).

The SSAB is an agriculturally active desert responsible for more than $2 billion in annual agricultural sales due to mild temperatures and abundant sunshine in the winter, allowing for year-round production; top commodities include but are not limited to hay, alfalfa, dates, lettuce, broccoli, and livestock production (California Department of Food and Agriculture (CDFA), 2022). However, growing crops in sandy soil is challenging and can require anthropogenic land modifications such as carbon-based soil amendments, heavy application of inorganic fertilizers, and intensive irrigation. This is primarily due to the soil's texture, with larger particle diameters and lower organic carbon composition, resulting in poor retainment of water and nutrients necessary for plant growth (J. Huang & Hartemink, 2020). Tillage is often required for agricultural production in sandy soils, which can result in structural damage to the soil that leads to compaction and hard-setting soils that are difficult to cultivate when dry, as well as entrainment of particulate matter (J. Huang & Hartemink, 2020; H. Li et al., 2015; Moore et al., 2015). Hard-setting soils have high soil strength that is not suitable for root growth or shoot development. Consequently, this requires frequent soil-wetting through irrigation practices, especially in

summer months when temperatures regularly exceed 35°C, and these dry, hot conditions and frequent changes in volumetric soil moisture (VSM) may lead to large, transient soil NO_x emissions (Figures 2.1 and 2.2) (Almaraz et al., 2018; J. Huang & Hartemink, 2020; Wang et al., 2023).

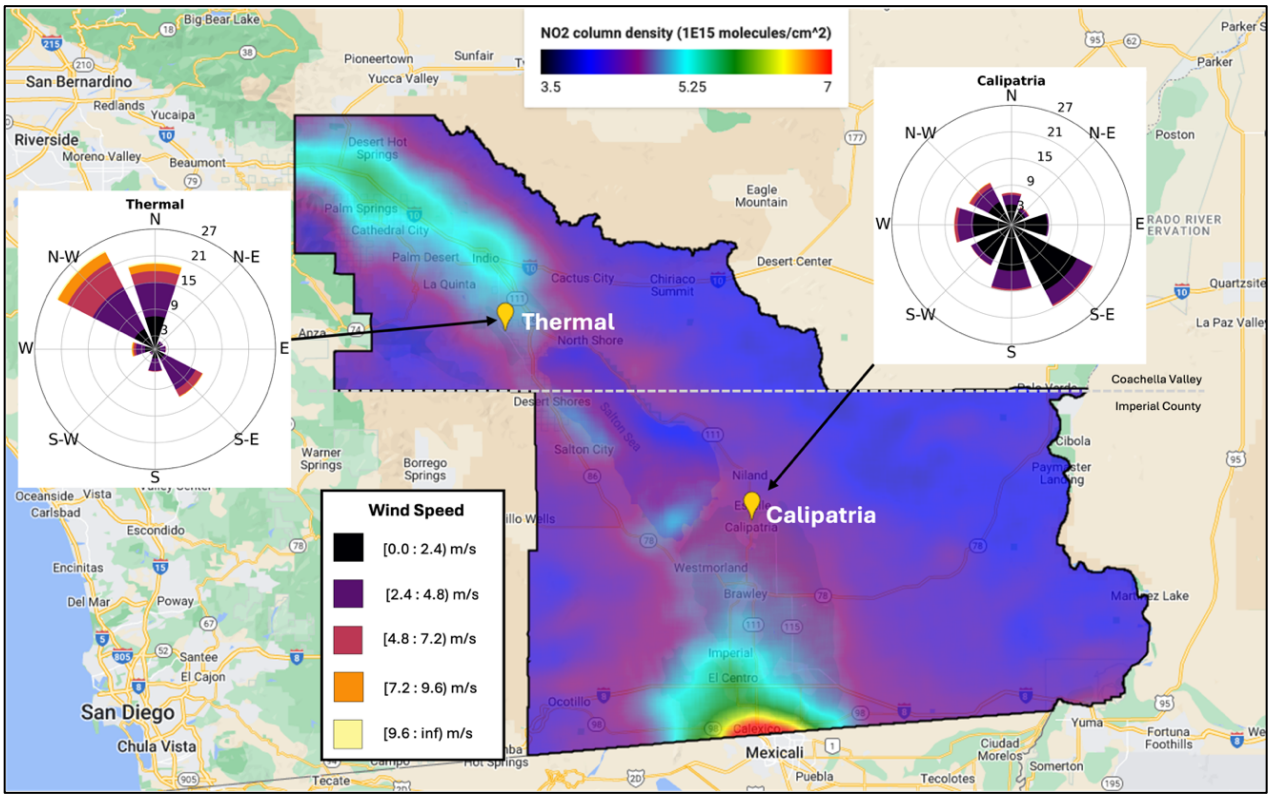

Figure 2.1. NO_2 column density was averaged from June 1, 2022, to May 31, 2023, from TROPOMI satellite data for the Salton Sea Air Basin to show the average spatial variation of NO_2. Calipatria (SE) and Thermal (NW), our two sampling sites, are indicated by a yellow marker. Wind roses for Calipatria and Thermal are also shown.

In addition, inorganic fertilizer amendments are not regulated, leading to over-application and nutrient leaching into the surrounding environment, such as the groundwater, local water sources, and soils (de Vlaming et al., 2004; J. Huang & Hartemink, 2020; Ribaudo et al., 2011; Schroeder et al., 2002). The objective of this work is to understand the implications of agricultural practices on the SSAB's regional air quality. Observations and modeling studies show a massive

expansion of arid lands globally due to climate change, ranging from 2.5 – 6.5 million km^2 by the end of the century, especially in large croplands in the northern hemisphere (Spinoni et al., 2021). Consequently, agricultural production in arid ecosystems will become more prominent (Intergovernmental Panel on Climate Change, 2022), therefore the implications of these practices need to be better understood. Microbes in soils naturally produce nitric oxide (NO), nitrous oxide (N_2O), and nitrous acid (HONO) gases during nitrification and denitrification processes, but their relative amounts are highly uncertain. These processes are dependent on many variables, but most importantly on the availability of reactive nitrogen and oxygen, nitrifying and denitrifying bacteria, soil moisture and pH, and temperature (Firestone & Davidson, 1989; Hall et al., 1996; Oswald et al., 2013; Pilegaard, 2013; E. J. Williams & Fehsenfeld, 1991). Nitrification is a two-step microbial process (shown below) that converts available ammonia (NH_3) into nitrate (NO_3) and involves ammonia-oxidizing and nitrite-oxidizing bacteria (Ward, 2008). NO can be a byproduct in Step 1 under high ammonia concentrations or low oxygen conditions. Irrigation and precipitation events temporarily suppress bacterial activity until water is redistributed or evaporated, restoring oxygen and nutrient availability and resulting in NO pulsing events.

$$2NH_3 + 3O_2 \rightarrow 2NO_2^- + 2H_2O + 2H^+ \quad \text{(Step 1)}$$

$$NO_2^- + H_2O \rightarrow NO_3^- + 2H^+ \quad \text{(Step 2)}$$

Denitrification (step 3) is a redox reaction that reduces nitrate to N_2 gas, typically occurring under anaerobic conditions when bacteria use nitrate as an oxidizing agent in the absence of oxygen (Prosser, 2007). In this process, NO is an intermediate and can be emitted when there is an imbalance in electron donors and acceptors (e.g., not enough organic carbon) or under acidic soil

conditions where denitrifying bacterial activity is inhibited. However, in this step N_2O emissions typically dominate over NO.

$$NO_3^- \rightarrow NO_2^- \rightarrow NO \rightarrow N_2O \rightarrow N_2 \quad \text{(Step 3)}$$

Nitrogen availability in agricultural soils is directly dependent on N fertilizer inputs, meaning overapplication of N fertilizers results in emissive nitrogen gases. Applying excessive ammonia-based fertilizer with insufficient oxygen availability (e.g., when fields are flooded) can result in NO production from nitrification because nitrite is not able to fully oxidize to nitrate. In addition, soil texture influences the relative proportions of N gases released from nitrification and denitrification; denitrification is favored in clay soils while nitrification is favored in freely draining sandy soils, like the ones in the SSAB (Barton et al., 1999; Parton et al., 2001). Soil NO emissions are believed to increase exponentially with temperature, then plateau between 30-40°C, as long as these other soil components are not limiting factors (Pilegaard, 2013; Wang, Ge, et al., 2021; Yienger & Levy, 1995). The exact temperature that these emissions plateau is still debated, however, we believe that the plateau point may be higher in hot agroecosystems like the SSAB, where microbes have likely adapted to the extreme heat (Oikawa et al., 2015).

Further, high pH generally favors microbial ecosystems that promote nitrification and NO production, while acidic fertilized soils produce HONO through chemical equilibrium with nitrite in water (Pilegaard, 2013). However, comparable quantities of HONO and NO emitted from nonacidic soils were found in Oswald et al. (2013) and suggested that HONO may be an unaccounted, yet significant amount of reactive nitrogen released from soil worldwide, particularly dominant in arid and arable environments like the SSAB. This is an important point because the daytime lifetime of HONO with respect to photolysis to NO + OH is around 15

minutes, so any soil emissions will quickly cycle into the photostationary state of O_3-NO-NO_2 and provide an additional source of NO_x to the atmosphere (Wang, Fu, et al., 2021; Xue et al., 2021).

As mobile sources of NO_x decrease due to continued air quality regulatory management, the impact of anthropogenically driven biogenic production of NO_x, specifically from agricultural soils, needs to be understood. The nitrogen stable isotope composition (reported as $\delta^{15}N$) has been a valuable tool for NO_x source apportionment due to differences in $\delta^{15}N$-NO_2 values between anthropogenic and biogenic emission sources (Chang et al., 2018; Felix & Elliott, 2014; Fibiger et al., 2014; Fibiger & Hastings, 2016; Hastings et al., 2013; D. Li & Wang, 2008; Miller et al., 2017; Walters et al., 2015). Ambient $\delta^{15}N$-NO_2 has been shown to be a useful tool of NO_x source apportionment due to its well quantified isotope fractionation factors and because of offsetting isotope effects from the balance between isotope equilibrium and photochemical isotope fractionation (J. Li et al., 2020). Previous ambient $\delta^{15}N$-NO_2 studies have successfully been able to track the influence of highly variable biogenic soil NO emissions impacting the NO_x budget in a small Midwestern city during the summer (Walters et al., 2018), suggesting it could be a powerful tool for constraining biogenic soil emissions in the SSAB.

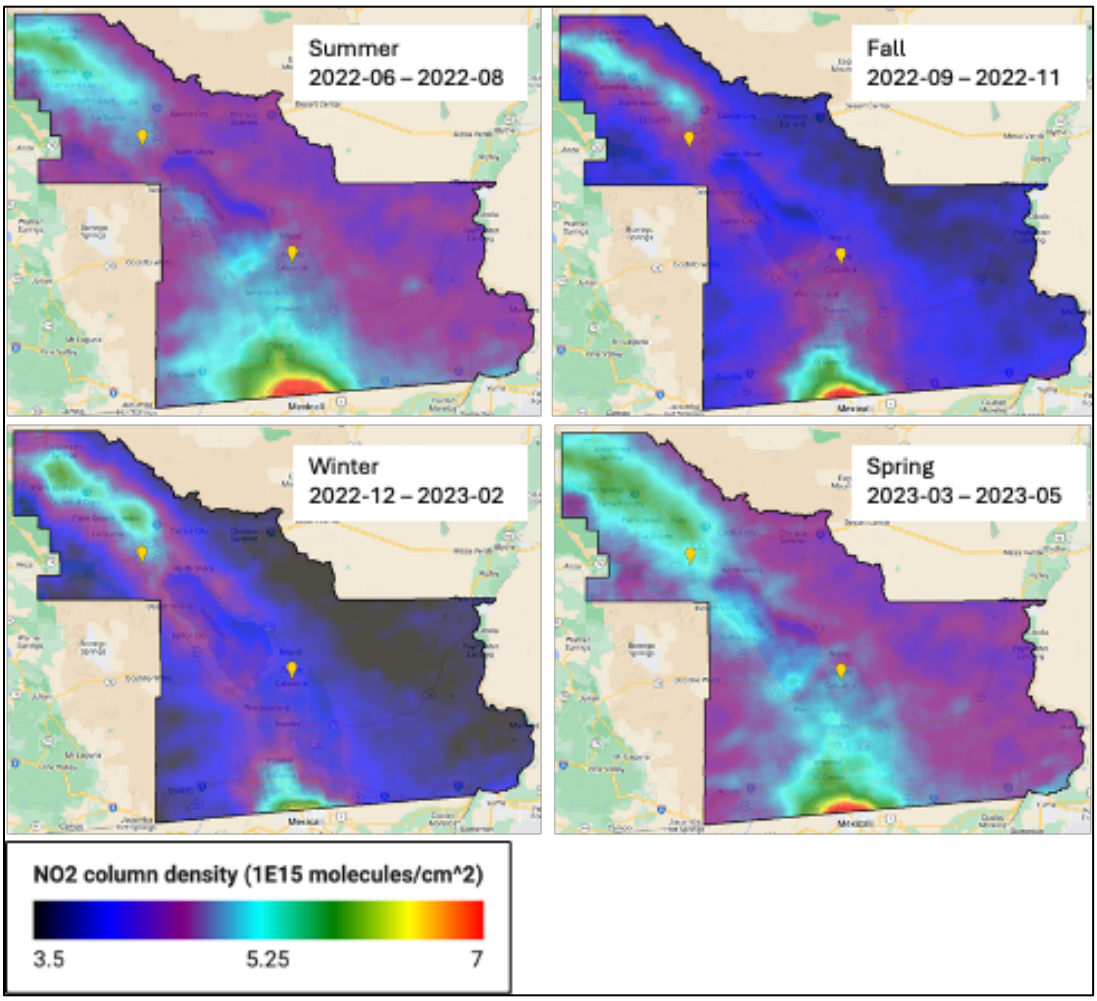

Figure 2.2. Seasonal average NO_2 columns for the Salton Sea Air Basin during our sampling campaign (June 2022 – May 2023), obtained from the TROPOMI Sentinel-5P satellite (NRTI Level 3). Data was processed using Google Earth Engine. Yellow points indicate the two sampling sites Calipatria (SE) and Thermal (NW).

In this study, $\delta^{15}N$ was quantified from NO2 (and total nitrate, $tNO_3 = HNO_3$ + particulate NO_3) actively collected on a Thermo ScientificTM ChemComb® Speciation Cartridge (CCSC). Ambient NO_2 samples were collected in two locations in the SSAB for 10 months and analyzed for $\delta^{15}N$ to quantify the soil source contributions to the region's NO_x inventories. Using our field measured $\delta^{15}N\text{-}NO_2$ values and accounting for nitrogen isotopic fractionation to adjust these values to $\delta^{15}N\text{-}NO_x$, we used a mixing model approach to estimate the soil source strength of the

field observations based on the mean $\delta^{15}N\text{-}NO_x$ from each emission source and from the *a priori* source apportionment reported in CARB's California Emissions Projection Analysis Model CEPAM inventory. Because nitrate is influenced by long-range transport, we do not use tNO_3 as a marker for source apportionment. This study aims to improve our understanding of the sources of persistent air pollution in the SSAB by assessing the current NO_x inventory's estimation of soil NO_x emissions.

2.2 Methods

2.2.1 Sample Collection, Extraction, and Isotopic Analysis

Ambient NO_2 and total particulate nitrate (tNO_3) were collected and quantitatively speciated using a denuder-filter pack active sampling device known as a Chemcomb Speciation Cartridge (CCSC), as previously described (Blum et al., 2020). Briefly, the body of the CCSV contains an inlet with an impactor plate for the removal of coarse particles, a glass transition piece to induce laminar flow, two honeycomb denuders to collect ambient NO_2 gas, and a downstream filter pack (Koutrakis et al., 1993). Denuders were soaked in 10% (v/v) hydrochloric acid (HCl) for 24 hours, then rinsed in triplicate with 18.2 MΩ Millipore water and dried with N_2 gas prior to field preparation. For the collection of NO_2, denuders were coated with 10-mL of 2.5 M potassium hydroxide (KOH) and 25% by weight of guaiacol ($C_7H_8O_2$) using methanol as a solvent, which was allowed to air dry, then capped until assembly for field collection. This mixture selectively binds NO_2 as nitrite (NO_2^-) (Ammann & Saurer, 1999; D. Li & Wang, 2008; Walters et al., 2016; E. L. Williams & Grosjean, 1990). Caps were placed on either end of the denuders for storage until use. This solution was made fresh each time and 10 mL of this solution was applied to each denuder, first removing a single cap, and evenly distributing the solution among the

pores, then re-capping and shaking to distribute the solution evenly. Excess solution was poured into the hazardous waste container and caps were removed so the denuders could dry, then were recapped with clean caps. Following the denuders is a single Nylon filter (Measurement Technologies Laboratory NY47P, 47 mm and 1 µm pore size) for collecting tNO_3. Filters came pre-washed by the manufacturer but were washed again before field sampling: first, filters were placed in a container filled with MQ-H_2O and placed on an orbital shaker for 1 hour. Then filters were dried in low heat for 15-20 minutes and stored in a petri-dish. Ambient air was sampled at a flow rate of 10 LPM using a mass-flow controller (MKS IE50A008304SBVP20) and vacuum pump. Details about chemicals and materials can be found in Table 2.1. Field sampling was performed nearly once a month from June 2022 – April 2023 at two sampling sites in the SSAB (Figure 2.1), one in the Imperial Valley (Calipatria High School in Calipatria, CA) and one in the Coachella Valley (Torres-Martinez air station in Thermal, CA). This project incorporated community engagement and citizen science; Comité Cívico del Valle (CCV), a grassroots community organization based in Imperial County that was founded on the principle that "Informed People Build Healthy Communities", served as our community partners. Trained air monitoring technicians from CCV oversaw field set-up and break-down. Sampling was performed for 3-7 days, approximately monthly over ten months (Table S2.1).

Table 2.1. List of materials needed for denuder preparation and CCSC setup and extraction.

Chemical/material	**Manufacturer**	**Grade/description**
Potassium hydroxide	Thermo-Fisher Scientific	Flake, 85%
Methanol	Thermo-Fisher Scientific	99.8+%, ACS reagent
Guaiacol	Thermo-Fisher Scientific	99+%
Sulfanilaminde	Sigma Aldrich	99+%

N-(1-Naphthyl) ethylenediamine dihydrochloride (NED)	Sigma Aldrich	>98%
Vanadium (III) chloride	Sigma Aldrich	
Sodium nitrite	Sigma Aldrich	99.999% trace metals basis
Sodium nitrate	Sigma Aldrich	99.999% trace metals basis
Hydrochloric acid	Thermo-Fisher Scientific	ACS certified
Nylon filters	Measurement Technologies Laboratory	47 mm, 1μm pore spaced, prewashed
Whatman filters #1	Sigma Aldrich	
Mass flow controller	MKS	10 LPM

The extraction of NO_2 and tNO_3 was performed with 30-mL and 20-mL of MQ water for the front denuder and nylon filter, respectively, then filtered through vacuum filtration using a Whatman grade 1 filter. Back denuders were used for breakthrough and were not used for analysis. Field blanks were collected for method validation, however, blanks contained negligible concentrations of NO_2 and tNO_3. Nitrate and nitrite concentrations were determined on the UV-Vis using a colorimetric method developed by Doane and Horwath (2003). The rest of the preparation and extraction steps were followed based on the manufacturer's recommendations (Thermo Scientific, 2005).

Immediately after ambient air collections arrived from shipment, denuders were extracted using 30 mL of Milli-Q water and nylon filters were extracted using 20 mL of Milli-Q water. Extracted samples were then filtered via vacuum filtration using a Whatman #1 filter (55 mm). Standards of $NaNO_2$ and $NaNO_3$ for UV-Vis analysis were prepared from 5 μM to 200 μM to ensure the collected concentrations of analyte were within the range. The coloring agent for the nitrite samples were made differently from the nitrate samples. For nitrite, two solutions were prepared, 10% sulfanilamide in 30% HCl: 70% MQ-H_2O, and 1% NED in MQ-H_2O. For UV-Vis

analysis, 1 mL of analyte or standard was added to the cuvette, then 25 µL of sulfanilamide solution was added and the cuvette was capped and inverted to mix. The cuvettes sat for 10 minutes, then 25 µL of the NED solution was added and inverted. Solutions were allowed to sit for 10 minutes before analyzing on UV-Vis. For nitrate, the preparation for the coloring solution was prepared as reported in Doane and Horwath, 2003 (Doane & Horwáth, 2003). After concentrations were determined to be sufficient, nitrite solutions were neutralized using 0.1 M HCl, then isotopic analysis was performed at the UC Davis Stable Isotope Facility (SIF) by the denitrifier method on a GasBench-PreCon-Isotopic Ratio Mass Spectrometer to determine $\delta^{15}N$-NO_2 (Casciotti et al., 2002; Sigman et al., 2001). The pooled standard deviation for the ^{15}N reference was 0.11‰.

The lifetime of aerosols in the atmosphere is typically 5-10 days, meaning the N in particulate nitrate is derived from a large integrated area that spans several air basins across California. Although there was a fair correlation between NO_2 and particulate NO_3 $\delta^{15}N$ values across the experiment (Pearson correlation coefficient of ~0.45), the average for the $\delta^{15}N$-NO_3 samples was ~10 ‰ heavier than for $\delta^{15}N$-NO_2, indicating that the aerosol nitrate was likely more strongly influenced by distant, traditional fossil-fuel combustion sources of NO_x. Additionally, quantifying isotope effects associated with tNO_3 formation is more difficult (Bekker et al., 2023). Uncertainty in knowing exactly where the tNO_3 was produced along its long-range trajectory makes it a much more challenging marker for source apportionment studies, therefore we do not use the tNO_3 data.

2.2.2 Evaluation of $\delta^{15}N$ References

The isotopic signature of nitrogen is expressed in terms of its $\delta^{15}N$, where:

$$\delta^{15}N = (R_{sample}/R_{standard} - 1) \times 10^3$$

In this equation, R represents the $^{15}N/^{14}N$ ratio. The standard is atmospheric N_2, which is considered to have a globally uniform isotopic composition (Högberg, 1997). Studies of the natural variations in $^{15}N/^{14}N$ ratios from different sources are used to apportion sources of NO_x pollution.

A literature review was conducted to evaluate published stable $\delta^{15}N$ isotope ratios for various sources of NO_x, and relevant $\delta^{15}N\text{-}NO_x$ values are summarized in Table 2.2. On average, biogenic soil sources have been observed to have a significantly lower ratio of light $^{15}N/^{14}N$ isotopes than combustion sources. This is a result of various soil NO-producing processes (e.g., nitrification, denitrification, chemodenitrification) stimulated by N amendments, which impart a distinguishable isotopic signature that differs from other measured NO_x emission sources (D. Li & Wang, 2008; Miller et al., 2018; Yu & Elliott, 2017). Biogenic nitrification processes kinetically favor utilizing the lighter N isotope (^{14}N), leading to a more depleted $\delta^{15}N$ (Högberg, 1997; D. Li & Wang, 2008; Yu & Elliott, 2017). These processes are highly variable, as reflected in the large standard deviations reported in the literature (Table 2.2 and Figure 2.3).

Table 2.2. Summary of previously reported $\delta^{15}N\text{-}NO_x$ values sorted by emission source type.

Source type	$\delta^{15}N\text{-}NO_x$	Mean	Standard deviation	References
Mobile source	-8.1‰ to +9.8‰	-2.5‰	2.7‰	Walters, Goodwin, et al. (2015)*, Miller et al. (2017)
Biomass burning	-7‰ to +12‰	1.0‰	4.1‰	Fibiger & Hastings (2016)
Stationary source	-19.7‰ to -13.9‰	-16.5‰	1.7‰	Walters, Tharp, et al. (2015)
Biogenic soil emission	-59.8‰ to -14.2‰	-33.2‰	9.6‰	Li & Wang (2008), Yu & Elliot (2017), Miller et al. (2018)

**Only a portion of the measurements from this paper were used since they were measured with a cold, neutral engine, which wouldn't be relevant for ambient temperatures.*

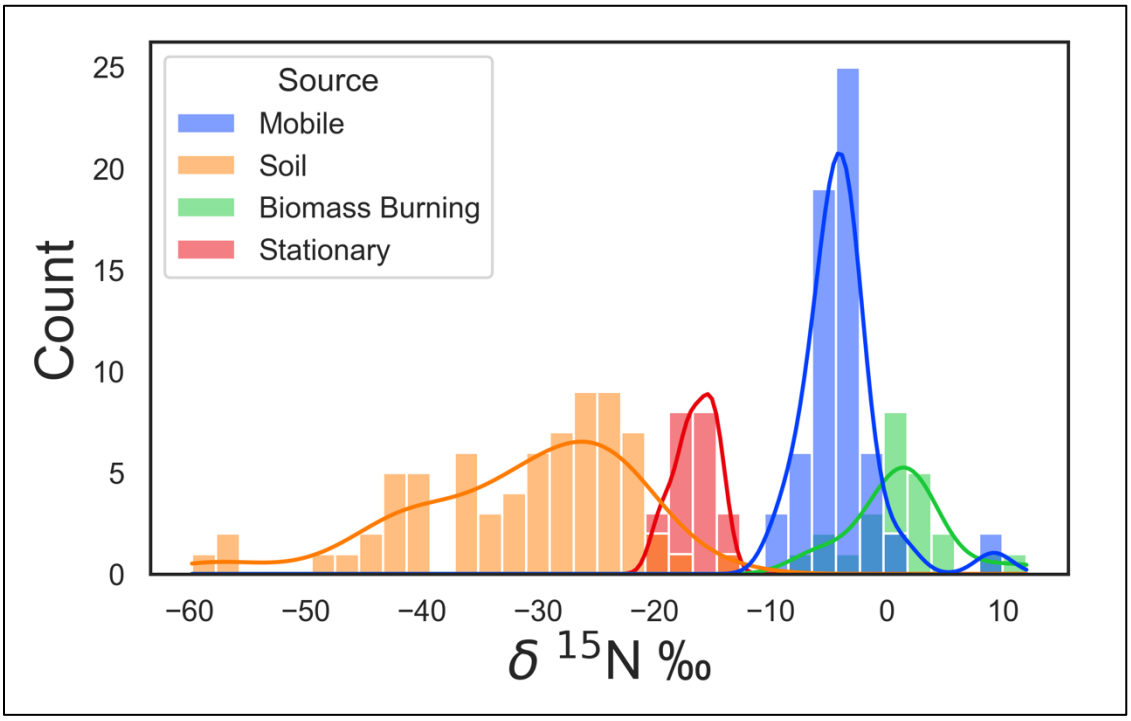

Figure 2.3. Probability distributions for each soil source and their spread of measured isotopic signatures.

It is important to consider the uncertainties of the isotopic signatures for each source due to variations in measurement techniques found in the literature. For this study, passive sampling techniques (Ammann et al., 1999; Felix & Elliott, 2014; Redling et al., 2013) were excluded because the measurement periods were much longer, could allow for a mixture of NO_x sources, and were more difficult to reproduce, ultimately introducing a bias in the $\delta^{15}N\text{-}NO_x$ (Dahal & Hastings, 2016). Additionally, studies on vehicles without catalytic converters were excluded (Heaton, 1990) since catalytic converters are mandatory and regulated through California smog checks. For these reasons, only two publications were used to represent mobile source emissions: Miller et al., 2017 and Walters et al., 2015. Not all measured values reported in Walters et al., 2015 were used because some measurements were taken from engines that were

cold and/or in neutral. Catalytic converters take a few minutes to warm up and work efficiently, and efficient catalytic converters preferentially uptake lighter ^{14}N isotopes (Miller et al., 2017; Walters et al., 2015), leading to heavier ^{15}N emissions. Therefore, cold engines are biased with more negative isotopic signatures and likely do not represent background mobile source emissions measured in the Salton Sea Air Basin. Additionally, both studies were performed in the northeastern US in large metropolitan areas where biogenic sources are believed to be negligible. The reported mean from Miller et al., 2017 was then averaged with the mean of warm and/or driven vehicles from Walters et al., 2015 to represent mobile source $\delta^{15}N\text{-}NO_x$ (Table 2.2). Further, coal burning is not a method of energy production in the Salton Sea Air Basin or surrounding areas, therefore, studies that measured the isotopic signature of NO_x produced through coal combustion have been excluded from our stationary source measurements (Felix et al., 2012; Heaton, 1990). See Section 2.2.3 for uncertainty propagation.

Table 2.3. The 2022 California Emissions Projection Analysis Model (CEPAM) NO_x emission inventory and our estimated soil NO_x adjustments for Imperial County and the Coachella Valley, as well as for the combined SSAB, are shown. The CEPAM inventory is based on an annual average, so we averaged our field estimates for our sampling duration. Also shown are the adjustments to the NO_x inventory based on the average results from our field sampling campaign. The EPA's National Emissions Inventory (NEI) for 2020 is also shown for comparison for Imperial County only.

Source Type	NEI (2020)	CEPAM (2022)			This Study		
	Imperial County (tons/d)	Imperial County (tons/d)	Coachella Valley (tons/d)	SSAB total (tons/d)	Imperial County (tons/d)	Coachella Valley (tons/d)	SSAB total (tons/d)
Mobile	11.9 (72.7%)	12.4 (81.8%)	15.9 (88.2%)	28.3 (85.2%)	12.4 (56.7%)	14.7 (69.9%)	28.2 (62.1%)
Biomass Burning	0.5 (3.1%)	0.1 (0.9%)	0.7 (4.0%)	0.8 (2.4%)	0.1 (0.6%)	0.6 (3.2%)	0.9 (1.9%)

Stationary	1.3 (8.0%)	1.7 (11.4%)	1.3 (7.4%)	3.0 (9.0%)	1.7 (7.9%)	1.4 (5.9%)	3.1 (6.7%)
Biogenic Soil	2.7 (16.2%)	0.9 (5.9%)	0.1 (0.4%)	1.0 (3.0%)	6.7 (34.7%)	4.7 (21.0%)	11.4 (29.2%)
Total NO_x	**16.3**	**15.2**	**18.0**	**33.2**	**21.8**	**22.7**	**45.5**

2.2.3 Soil Source Strength Mixing Model Estimation and Propagation of Uncertainty

A best estimate of the sources of NO_x in the SSAB is compiled in the California Air Resources Board's California Emissions Projection Analysis Model (CEPAM) shown in Table 2.3. CEPAM was used over the EPA's National Emissions Inventory (NEI) because CEPAM is broken into county and air basin, and due to its California focus, should in principle be more accurate. Because chemical and physical processing can induce isotopic fractionation such that $\delta^{15}N$ may not be conserved, isotopic fractionation was calculated to determine $\delta^{15}N\text{-}NO_x$ (Bekker et al., 2023; Freyer, 1991; J. Li et al., 2021; Walters & Michalski, 2015). Specifically, these N isotopic fractionations are associated with the photostationary equilibrium of O_3-NO-NO_2 (Leighton Cycle) and were accounted for using Equations 2.1-2.3 below from Bekker et al., 2023. The influence of $\delta^{15}N$ fractionation associated with NOx cycling is shown in Equation 2.1:

$$\delta(^{15}\square, NO_x) \approx {}^{15}\square\varepsilon\left(\frac{NO_2}{NO}\right) \times \left(1 - f(NO_2)\right) - \delta(^{15}\square N, NO_2) \quad \textbf{(2.1)}$$

where $\delta(^{15}N,NO_2)$ represents our isotopic measurements from the field study, $^{15}\varepsilon(NO_2/NO)$ is the isotope effect associated with NO conversion to NO_2, and $f(NO_2)$ represents the fraction of NO_2 in NO_x. Additionally, the $^{15}\varepsilon(NO_2/NO)$ value represents a combination of Leighton Cycle isotope effects (LCIE) and equilibrium isotope effects (EIE), refer to Bekker et al. (2023) for a detailed explanation. Further, they estimated the relative role of EIE and LCIE in Equation 2.2 and 2.3. The

isotope effects were modeled in previous studies and these estimates were used in our calculations.

$$^{15}\varepsilon\left(\frac{NO_2}{NO}\right) = f_{EIE}(^{15}\varepsilon_{EIE}) + (1 - f_{EIE})(^{15}\varepsilon_{LCIE}) \quad \textbf{(2.2)}$$

$$f_{EIE} = \frac{k(NO_x - EIE)[NO_2]}{k(NO+O_3)[O_3]+k(NO_x-EIE)[NO_2]} \quad \textbf{(2.3)}$$

where *EIE* represents the equilibrium isotope effect and *LCIE* represents the Leighton Cycle isotope effect.

These δ^{15}N-NO_x values were then used to calculate the soil source emission strength (E_s) in Equation 2.4 based on the average δ^{15}N-NO_x of each emission source based on the *a priori* source apportionment reported in the CEPAM NO_x inventory, which is used for regulatory modeling in California. Here, δ_{obs} represents the observed δ^{15}N-NO_x, *i* represents the main source types accounted for in the CEPAM NO_x inventory (where *a, b, c,* and *s* represent mobile, biomass burning, stationary, and soil sources, respectively), α_i represents the proportion each source contributes to the overall CEPAM NO_x inventory, δ_i represents the literature derived δ^{15}N-NO_x for each source (Table 2), and E_{inv} represents the total NO_x budgeted in the CEPAM inventory (in tons/d).

$$E_s = \left(\delta_{obs} - \sum_{a,b,c,s}^{i} \alpha_i \delta_i\right) E_{inv} \Big/ (\delta_s - \delta_{obs}) \quad \textbf{(2.4)}$$

Equation 2.4 assumes that the current CEPAM inventory is correct aside from the soil source because the observed δ^{15}N is (usually) lighter than expected; without adjusting the soil source signature, the CEPAM inventory would indicate a mean δ^{15}N-NO_x of -5.04‰ and -3.11‰ for Imperial County and the Coachella Valley, respectively. Therefore, we solve for the magnitude of the soil source such that the observed δ^{15}N signature can be explained by the sum of the

inventory sources plus the revised soil emissions. This procedure further assumes that the sampled NO_2 is entirely from NO_x (or HONO) emitted from sources within the air basin. Figure 3.1 shows annual NO_2 column data from the European Space Agency's TROPOspheric Monitoring Instrument (TROPOMI) for the year of our sampling.

We propagate the various uncertainties associated with these measurements of sources from the literature to estimate the overall error associated with our calculated soil emissions. Equation 2.5 comes from the propagation of error for the final soil source strength (σ_{E_s}). The analytical uncertainty δ_{obs} (typically < 0.25‰) was ignored because it is an order of magnitude smaller than the standard deviations of the $\delta^{15}N\text{-}NO_x$ measurements for each source (Table 2.2).

$$\sigma_{E_s}^2 = \sum_{a,b,c}^{x} \frac{\alpha_x^2 E_i^2}{(\delta_s - \delta_{obs})^2} \times \sigma_x^2 + \left[\frac{\alpha_s^2 E_i^2}{(\delta_s - \delta_{obs})^2} - \frac{2\left(N - \alpha_s^2 \delta_s E_i^2\right)}{(\delta_s - \delta_{obs})^3} + \frac{N^2 + \alpha_s^2 \delta_s^2 E_i^2}{(\delta_s - \delta_{obs})^4} \times \sigma_s^2\right] \quad \textbf{(2.5)}$$

where $N = \left(\delta_{obs} - \sum_{a,b,c}^{i} \alpha_i \delta_i\right) E_i$

2.3 Results and Discussion

2.3.1 Field Sampling Results

Results of collected $\delta^{15}N\text{-}NO_2$ signatures are shown in Table 2.3. Figure 2.4 displays the soil emission estimates for this field campaign at both sites, comparing the monthly magnitudes to the overall annual CEPAM NO_x inventory. It is apparent that the CEPAM NO_x budget underestimates the soil contribution to ambient NO_x (and consequently to $PM_{2.5}$ and O_3) in both Calipatria (Imperial Valley) and Thermal (Coachella Valley). Soil NO_x contributed 0.3 – 10.1 (mean: 6.7 ± 3) tons/d and 0 – 13.8 (mean: 4.7 ± 4) tons/d throughout the duration of the field sampling for the Calipatria and Thermal sites, respectively. These soil emissions amount to on average 11.4

± 4 tons/d throughout the entire SSAB, an order of magnitude larger than what is represented in the CEPAM inventory (1.0 ton/d).

Table 2.3. Field sampling results for $\delta^{15}N\text{-}NO_2$ and estimated $\delta^{15}N\text{-}NO_x$ based on isotopic fractionation calculations, as well as the results for $\delta^{15}N\text{-}NO_3$ for Calipatria and Thermal.

	Calipatria			Thermal		
	$\delta^{15}N\text{-}NO_2$	$\delta^{15}N\text{-}NO_x$	$\delta^{15}N\text{-}tNO_3$	$\delta^{15}N\text{-}NO_2$	$\delta^{15}N\text{-}NO_x$	$\delta^{15}N\text{-}tNO_3$
Jun 2022	-13.2	-13.6	-0.02	No measurements		
Jul 2022	-13.4	-14.1	-2.6	-14.3	-16.1	-4.5
Aug 2022	-14.4	-14.9	-9.8	-4.6	-8.0	-4.8
Sep 2022	-15.6	-16.6	-3.4	-5.9	-8.0	N/A
Oct 2022	-5.3	-6.1	-1.1	-9.7	-12.0	-8.2
Nov 2022	-12.4	-13.4	-2.9	1.8	0.2	2.8
Dec 2022	-13.3	-14.9	-2.9	-7.5	-9.1	3.4
Jan 2023	-9.6	-11.6	-0.7	-1.5	-3.2	3.9
Feb 2023	-14.8	-15.5	0.1	-11.3	-12.0	2.6
Apr 2023	-16.0	-16.0	-3.4	-6.8	-7.6	1.8
Average	-12.8	-13.7	-2.7	-6.6	-8.4	-0.38

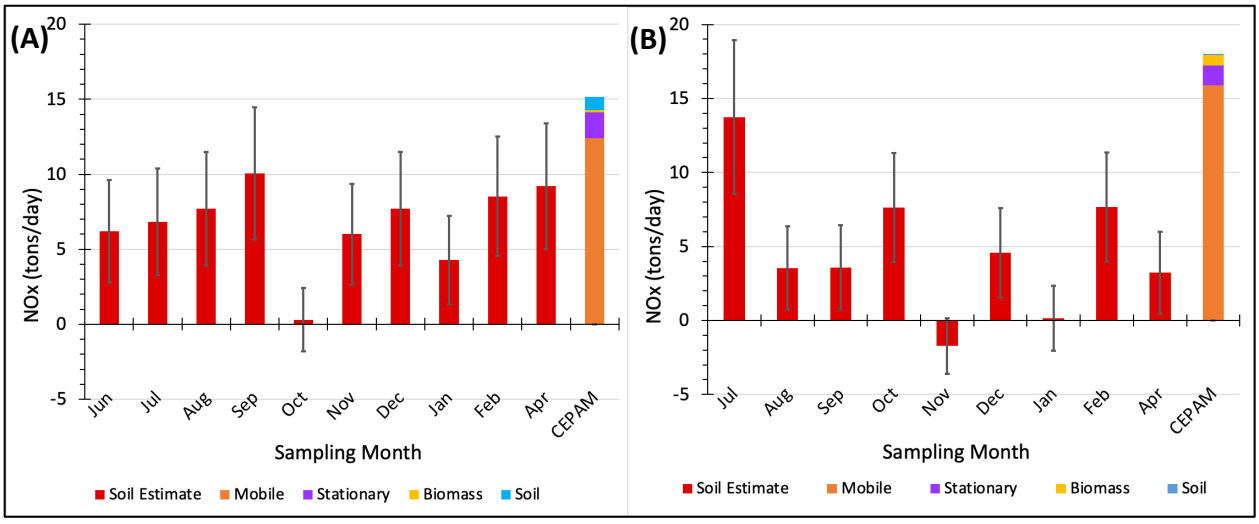

Figure 2.4. The NO_x budget (in tons/day) based on CEPAM2019v1.03 for the year 2022 is shown, which is split into mobile, stationary, biomass burning, and soil emission sources for (A) Calipatria and (B) Thermal. Soil emission estimates from this study are shown in red, and estimated uncertainties are denoted by the error bars. The annual total CEPAM NO_x inventory for Imperial County (A) and the Coachella Valley (B) is presented on the right, where

mobile, stationary, biomass, and soil sources are shown in orange, purple, yellow, and blue. Note that in Thermal for the November sampling, there was a negative estimated soil contribution, but we assume that the soil source was zero for this month and justified this assumption due to the error bar range.

The quantitative basis of our estimates relies on the assumption that the ambient NO_2 at the sampling site comes from sources entirely within the SSAB. Figures 2.1 (and 2.2) show the overall pattern of column NO_2 observed by TROPOMI during its overpass time near 13:30 local time. The general flow throughout the Salton Sea Air Basin (SSAB) is the superposition of three different scales (Figures 2.5 and 2.6). At the basin scale, there is a consistent lake-breeze pattern originating from the Salton Sea during the day, bringing southeasterly winds to Thermal and northwesterly winds to Calipatria, with this pattern reversing at night. On a broader, continental scale, the North American monsoon exerts its influence, characterized by air flow from the Gulf of California, predominantly from the south-southeast. This monsoonal flow is most prevalent during the peak summer months of July and August, mainly affecting the Imperial Valley located south of the Salton Sea. Additionally, on a synoptic scale, the prevailing westerlies interact with the surrounding mountain ranges, creating distinct airflow patterns. The Banning Pass, situated upwind of Palm Springs, channels strong westerly winds, while to the south, gaps in the valley's western rim, formed by the Peninsular Mountain Range, allow these synoptic winds to sweep over the Imperial Valley (Evan, 2019).

Winds in the Coachella Valley average around 4 m/s, with the Thermal site located approximately 75 km downwind from Banning. Banning serves as the eastern outflow point for urban emissions channeled from the Los Angeles basin. The time it takes for these emissions to travel from Banning to Thermal is roughly 4.5 hours, which is comparable to the photochemical lifetime of NOx during the warm season, as noted in previous studies (Beirle et al., 2011). In

contrast, winds in the Imperial Valley tend to be milder. During the monsoon season in July and August, when airflow from Mexicali is prevalent, it takes approximately 5.5 hours for the wind to travel the roughly 50-km distance to Calipatria, with a wind speed averaging around 2.5 m/s. The San Diego/Tijuana urban complex is situated roughly 150 km away and requires over 10 hours for its influence to reach the Imperial Valley. This duration exceeds the photochemical lifetime of NO_x, even during the winter months.

The satellite data illustrates two important aspects of the regional NO_x. First, although there is a flow connection between the Coachella Valley and upwind urban sources in the LA basin (Figure 2.5), the valley plume is distinct and does not appear to represent a decaying tail (especially noticeable in the Fall and Winter maps of Figure 2.5). The Imperial Valley, on the other hand, is only downwind of Mexicali during July/August (Figure 2.6) and yet it exhibits a broad amorphous shape that deviates from the circular symmetry of a concentration field falling off with distance from an urban core. Second, the basin-wide concentrations are greatest during spring/summer when the photochemical lifetime of NO_x is shortest, supporting our finding that agricultural soil sources are significant, especially during the warmest part of the growing season. Regardless of the details of source apportionment for the sampling, Equation 2.4 shows that any influence from urban sources upwind (with their heavier $\delta^{15}N$ fractions) would effectively increase our soil emission estimates, meaning that the values reported here represent lower limits.

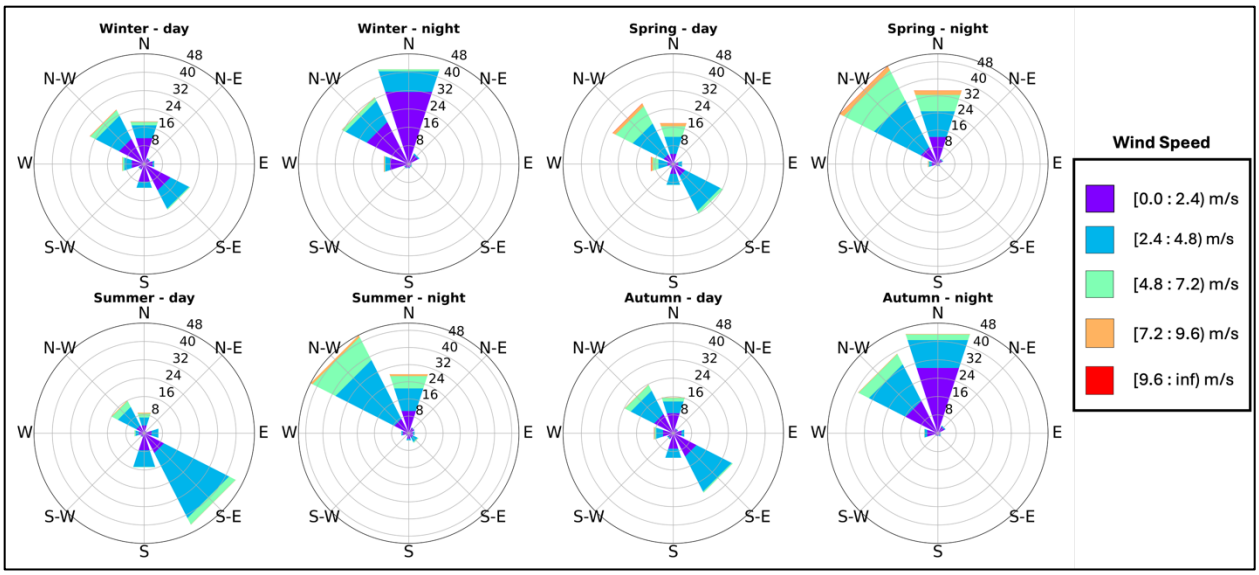

Figure 2.5. Seasonal and diurnal wind patterns are shown for Thermal. Although Thermal is further northwest from Calipatria, influence from the North American Monsoon can be observed in the summer months shown by the southeasterly flow. (Daytime: [06:00 – 18:00]; nighttime: [19:00 – 05:00]).

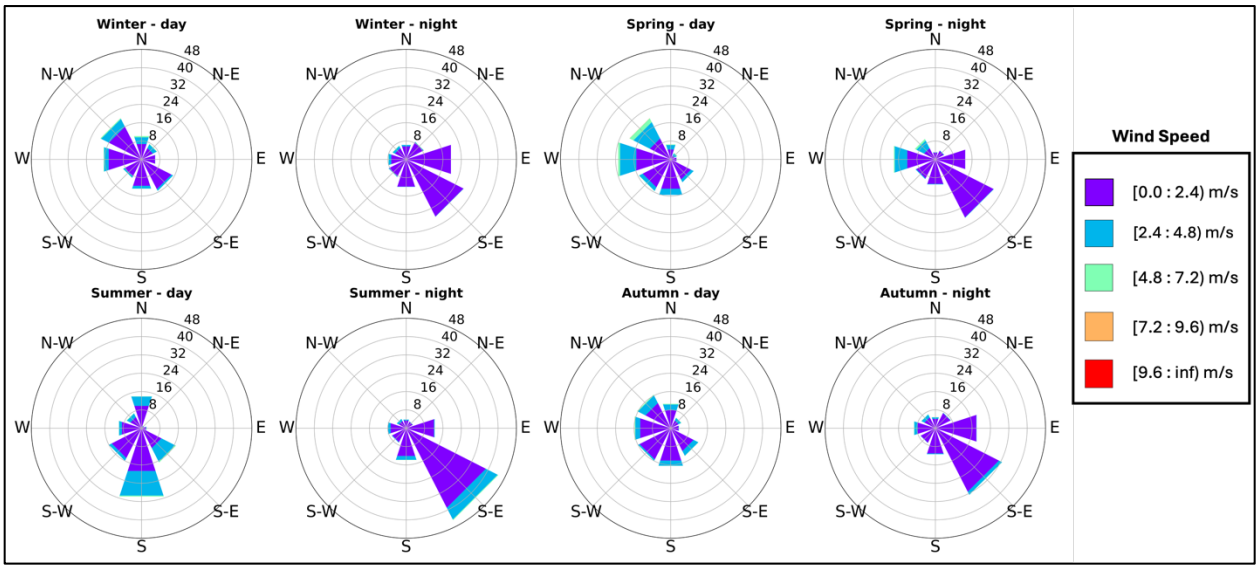

Figure 2.6. Seasonal and diurnal wind patterns are shown for Calipatria. Southerly and southeasterly winds dominate in the summer months due to influence from the North American Monsoon originating from the Gulf of California. (Daytime: [06:00 – 18:00]; nighttime: [19:00 – 05:00]).

2.3.2 Environmental Influences on Soil NO_x Production

To better understand the environmental influences that control the production of soil NO_x, we look at the leading parameters used in modeling estimates; namely nutrient availability, temperature, and soil moisture (Hudman et al., 2012; Yienger & Levy, 1995). Temperature is known to influence soil NO_x production, although the exact dependence at higher temperatures is still debated (Wang, Ge, et al., 2021), and has been observed by satellite over croplands (Wang et al., 2023). Nevertheless, no clear temperature dependence was observed in this study (Figs. 2.4 & 2.7) despite observations ranging from 17-44°C (Supplementary Tables S2.2, S2.3). As an agriculturally active desert, NO_x production is likely limited not principally by temperature as in unmanaged landscapes but by nutrient abundance and soil moisture determined by agricultural activity. In addition, the soil microbes in this high-temperature agroecosystem may have acclimated to the extreme desert heat, so their behavior may vary compared to agricultural ecosystems in more temperate regions (Oikawa et al., 2015).

The role of soil moisture in the production of NO_x is related to both gas diffusivity and microbial activity, with increasing soil water content stimulates nitrification and denitrification. Nitrification peaks 2-3 days after wetting when the amount of excess water and the rate of downward movement have decreased (Oikawa et al., 2015). In addition, extensive dry periods limit substrate diffusion and cause water-stressed nitrifying bacteria to remain dormant, which allows N substrate to accumulate while temporarily suppressing NO emissions (Davidson, 1992; Hudman et al., 2012; Jaeglé et al., 2005). Irrigation reactivates these microbes and redistributes substrate, resulting in NO pulsing events that typically last 1-2 days and can be 10-100 times background emission rates (Hudman et al., 2012; Yienger & Levy, 1995). Moreover, soil NO

emissions have been shown to spike after all rewetting events, even if fertilizer had not been applied within the last 30 days (Oikawa et al., 2015). To further understand the influence of these parameters, we looked at volumetric soil moisture content using NASA's Soil Moisture Active Passive (SMAP) satellite data. Soil moisture tends to be higher on average in the Imperial Valley agricultural lands than in any other region in the air basin (Fig. 2.8). This is because of the region's appropriation of approximately 3 billion m^3 of water from the Colorado River, used primarily for frequent irrigation of its ~200,000 – 275,000 ha of arable soil. This is equivalent to ~150 cm of water over the croplands, whereas the climatological rainfall observed usually only amounts to < 5-10 cm (Supplementary Tables S2.4 and S2.5). Due to the amount of agricultural land in the SSAB and uncertainty of irrigation use per parcel of land and crop type, it is difficult to accurately estimate the contribution of soil re-wetting on our measurements. However, this factor likely contributes to our soil NO_x estimates, but it is unlikely that our ~10 annual samples captured all irrigation variability.

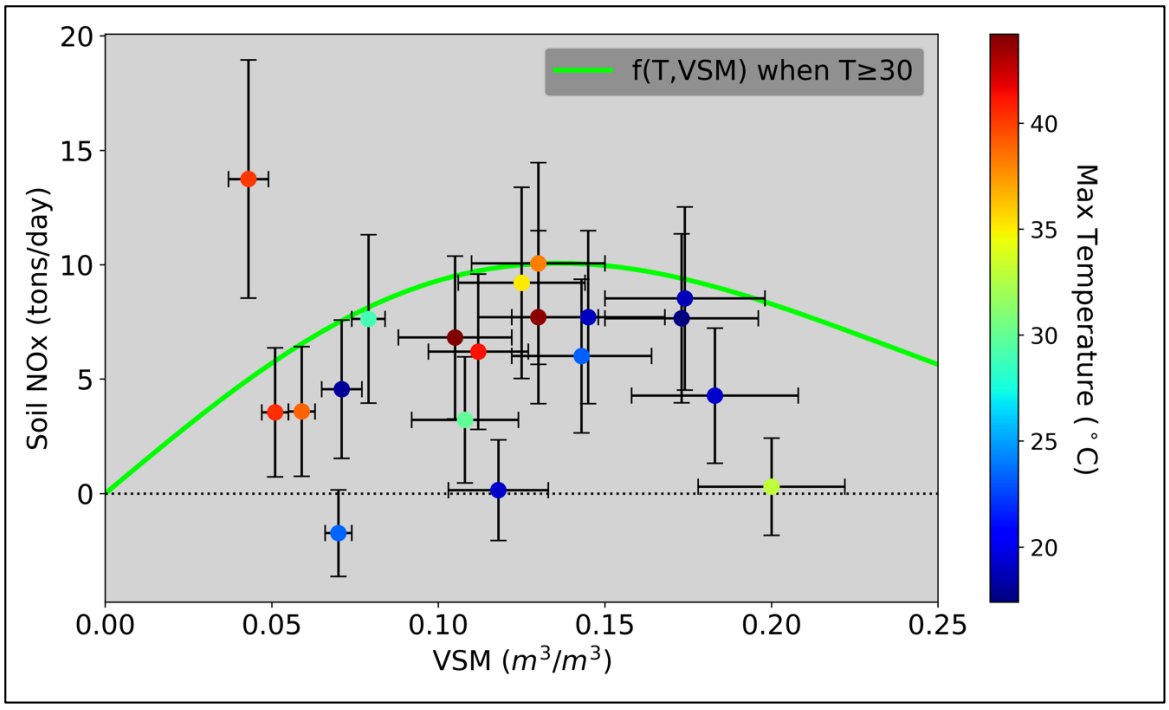

Figure 2.7. Soil NO_x estimates from our field campaign compared to the average VSM and maximum temperature during the measurement period. Maximum temperature was determined for the sampling period from the CARB meteorology station at Calipatria and Thermal. VSM was determined for the Imperial Valley for Calipatria measurements and the Coachella Valley for Thermal measurements using SMAP satellite data, filtered for 4:30 pm (closest time to when T_{max} occurs).

Although Figure 2.7 could be interpreted as exhibiting a crude correspondence between soil NO_x emissions and VSM, temperature only appears to be weakly related, which likely indicates that nutrient availability is the dominant factor controlling soil NO_x production in this heavily agricultural region. According to the California Department of Food and Agriculture (CDFA), N fertilizer sales in Imperial County have increased by 137% since 1991 (California Department of Food and Agriculture (CDFA), 1991, 2022), and an estimated 18-fold since 1930 (Byrnes et al., 2020), much greater than the national average sevenfold increase. In addition, despite being ranked as the 9th highest in county agricultural sales in the state, Imperial County used more N fertilizer than any other county during 2022 (8% of California total), including the top three crop producing counties (Fig. 2.9), likely a result of the insufficient nutrient retainment in sandy soils. When N fertilizer is applied in excess, this increases the likelihood of N gases to be emitted from the soils. A previous study showed that doubling the fertilization amount from 50 kg N ha-1 to 100 kg N ha-1 increased the integrated NOx fluxes by a factor of 5 (Oikawa et al., 2015).

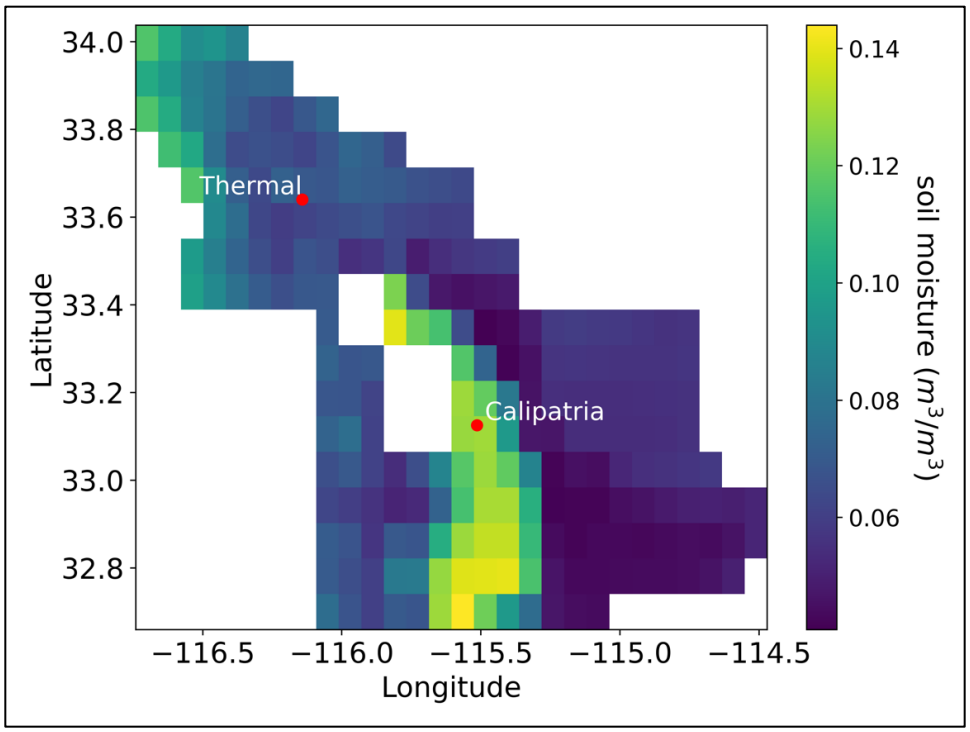

Figure 2.8. Average volumetric soil moisture (VSM) for the SSAB from June 2022 – May 2023, obtained from Soil Moisture Active-Passive (SMAP) satellite data.

Spatially and temporally relevant irrigation and fertilization data are not currently publicly available, therefore it is difficult to assess the direct influence of these leading parameters on the soil NO_x emission variance observed in this study. In Figure 5, we used data from the Trajectories Nutrient Dataset for Nitrogen (TREND-nitrogen) to look at historical N fertilizer applications and legacy N concentrations in Imperial County. N surplus was calculated using TREND-nitrogen, where the county-scale surplus or "legacy" nitrogen (kg N ha^{-1} y^{-1}) is calculated by mass balance from the inputs of atmospheric deposition, fertilizer application, biological N fixation, and human N waste, minus the crop and pastureland N uptake (Byrnes et al., 2020). It is apparent that N fertilizer usage and surplus N in Imperial County has been steadily increasing from 1920 to the present day (Fig. 2.9). Our estimates are based on a small fraction of days in the Salton Sea Air Basin; in our study, we sampled ~39 days in Calipatria and ~43 days in Thermal, accounting for

about 11% of the year. Inspecting the conditions of our 19 sampling intervals with respect to the annual values for VSM and air temperature (Fig. 2.10, Table S2.7), they compare well. Nevertheless, without knowing the exact timing of N amendments to all the cropped area, it is possible that while our estimates of annual average VSM and temperature are not statistically different from the average, the soil emissions, predominately influenced by the fertilizer inputs, may be much higher than our estimates having missed many periods of high fertilization in our sporadic sampling.

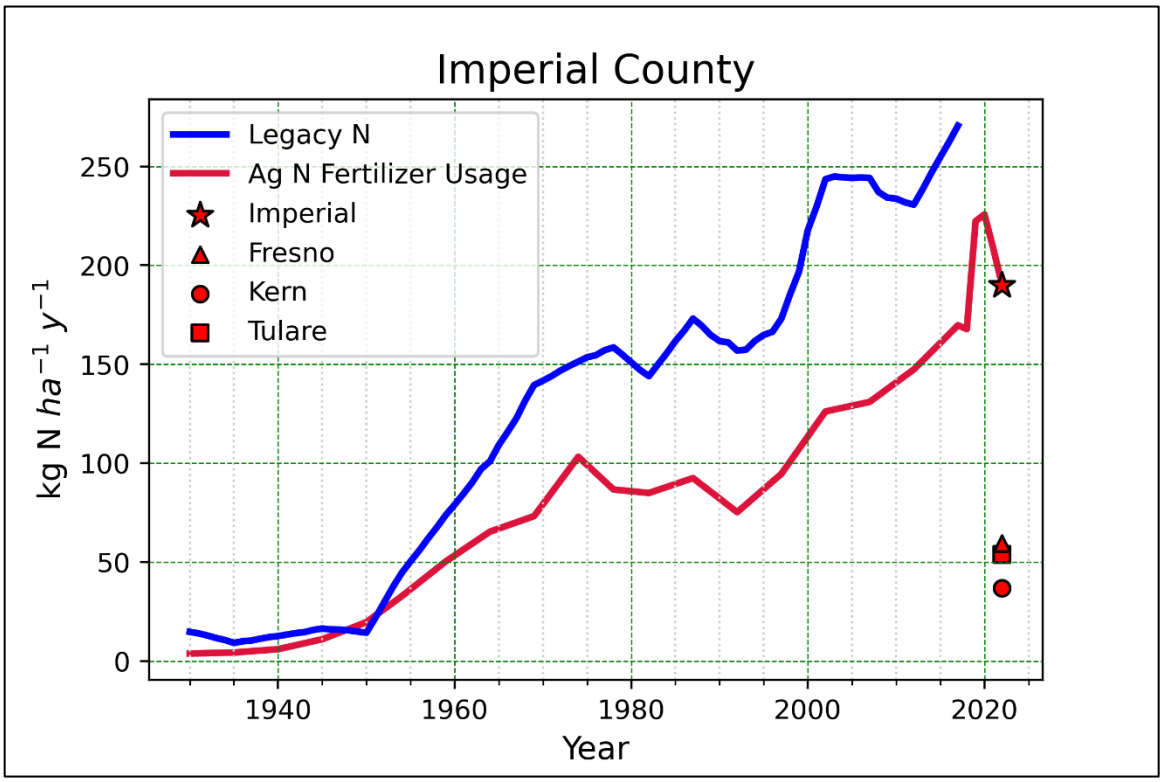

Figure 2.9. Imperial County N fertilizer usage (red) and legacy N history (blue) was prepared using the Trajectories Nutrient Dataset for Nitrogen (TREND-nitrogen) from Byrnes et al., 2020. The agricultural fertilizer use was extended after 2017 using the CDFA agricultural statistics for N fertilizer sales. Fresno, Kern, and Tulare Counties are ranked 1st, 2nd, and 3rd in state agricultural sales, while Imperial County is ranked 9th. Fertilizer usages are reported as kg of N used per hectare of agricultural land.

To understand the overall influence of fertilizer inputs on atmospheric N, we calculated the NO_x flux as a proportion of fertilizer consumption using the net fertilizer usage recorded (California Department of Food and Agriculture (CDFA), 2022). Imperial County purchased 57,630 tons of all nitrogen fertilizer, minerals, and compost in 2022 (California Department of Food and Agriculture (CDFA), 2022). Our annual average soil emission of 6.7 tons NO_x/d in Imperial County implies an average flux of 1.3% of the applied N being released as NO or HONO from agricultural fertilizer inputs. This is squarely within the 0.3-2.5% range reported by Jaeglé et al. (2005). Note that we were unable to quantify this for the Coachella Valley because it is part of the much larger Riverside County and fertilizer sales are only reported county-wide.

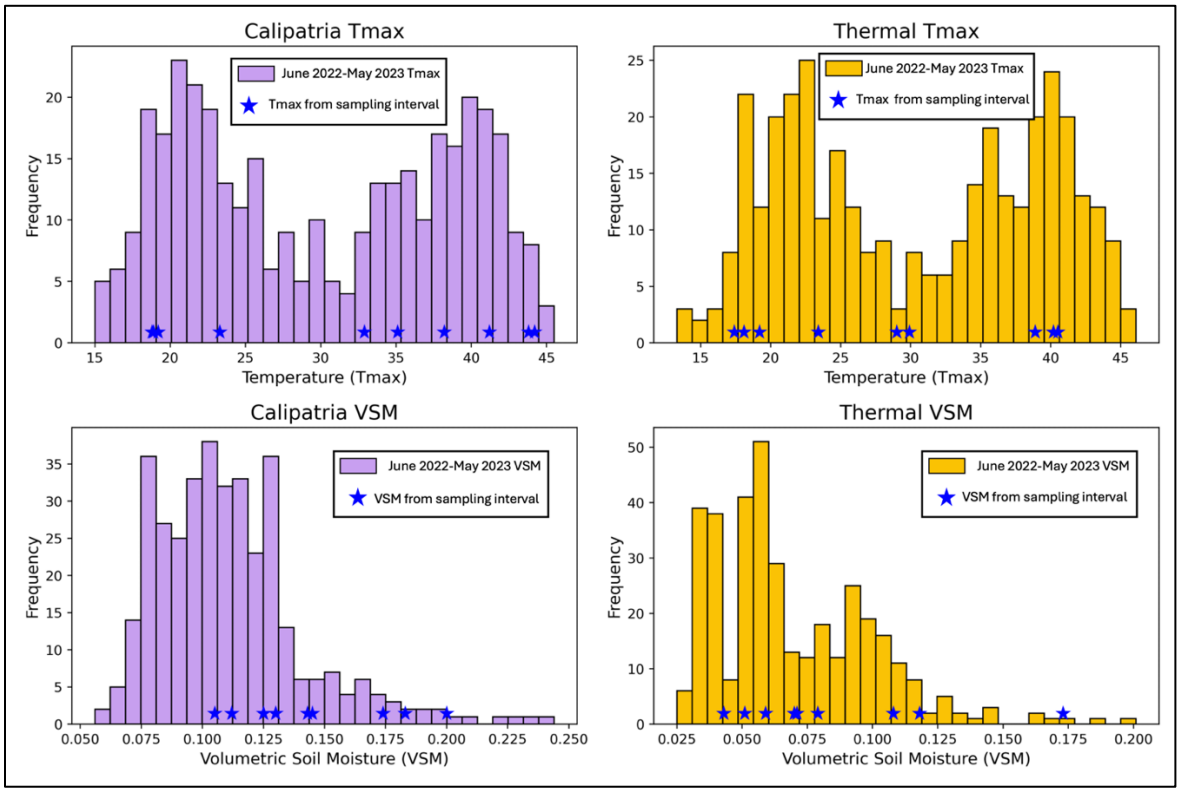

Figure 2.10. Histograms of observed T_{max} and VSM June 2022-May 2023 for Calipatria/Imperial Valley (purple) and Thermal/ Coachella Valley (gold) are reported. Values from our sampling intervals are marked with blue stars.

Furthermore, $\delta^{15}N$ outliers were observed for October in Calipatria and for November and January in Thermal, yielding estimated soil emissions that were effectively zero within the errors of our measurement technique (Fig. 2.4). The outliers measured in October (Calipatria) and November (Thermal) correspond to precipitation events during our measurement periods that likely suppressed NO_x emissions during the short intervals of sampling by wetting the soil to excess temporarily (Fig. 2.11) (Yienger & Levy, 1995). During our sampling interval in January (Thermal), precipitation was negligible, but examining HYSPLIT back trajectories for the interval, it appeared that there was a high-pressure system over the region that may have forced subsidence of cleaner tropospheric air into the Coachella Valley, which is consistent with the sampled NO_x being lower than the monthly average by 5.5 ppb (Supplementary Tables S2.3 and S2.5). However, this circulation did not persist throughout the entire 5-day sampling period, and the February sample was also collected when NO_x was 5 ppb lower than average, so ultimately, we are uncertain as to the exact cause of this near zero soil emissions measured at Thermal in January.

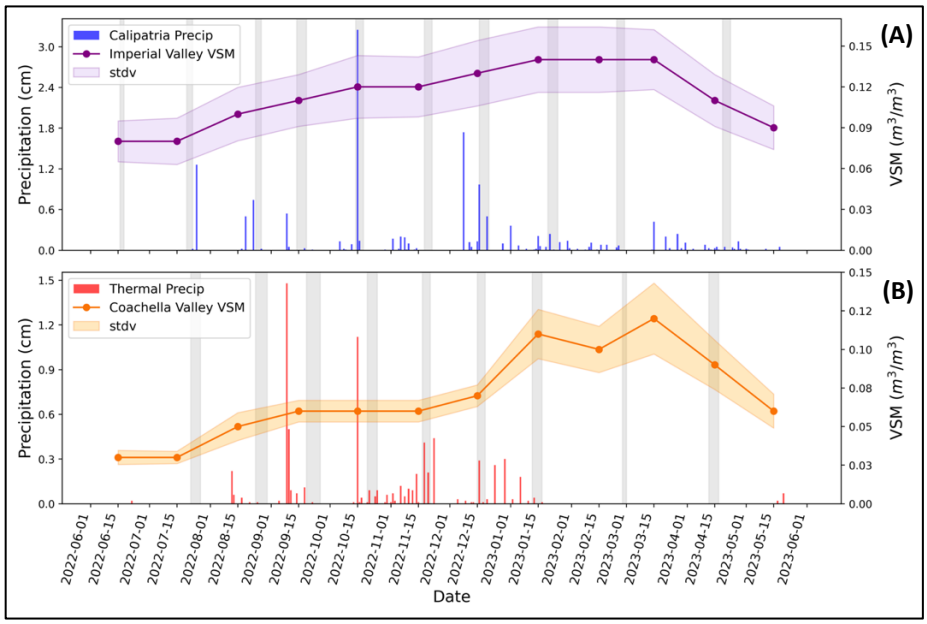

Figure 2.11. Monthly average Volumetric Soil Moisture, VSM (2022-2023, shown as a line plot), and the standard deviation (shown with shading) in (A) Imperial Valley and (B) Coachella Valley compared to the total daily precipitation (2022-2023, shown as bars) at our field sampling sites. Precipitation data was obtained from AQMIS and CIMIS and VSM data was obtained from NASA's SMAP satellite. The grey boxes indicate our sampling dates at each site.

2.3.3 Comparison Between Studies

To further assess the validity of our results for Imperial Valley, we compared our measurements to Oikawa et al. (2015), which found some of the highest soil NO_x emissions on record from chamber studies across the growing season. They further tested their findings by using WRF-Chem to compare against ambient NO_x measurements from the air quality network. The default soil emissions in the model needed to be enhanced by an order of magnitude to match their chamber measurements more closely, and the enhancement was found to minimize the model's root-mean-square error relative to ambient measurements for one week in September 2012. However, this enhancement still underpredicted tropospheric column densities of NO_2, indicating that there is no single emission factor that can be used to accurately simulate both tropospheric NO_2 columns and surface NO_2 concentrations in the MEGAN parameterization they used.

To compare our integrated valley emissions to the modeled surface fluxes, we used the area of agricultural land in the Imperial Valley to be 270,500 ha based on MODIS satellite land surface characterization (Wang et al., 2023). The integrated emissions for their one week in September (the month of our highest estimate of 10.1 ± 4 tons/d) amounts to 17.2 tons/d (Table 2.4). That study also attempted to match agreement with satellite NO_2 measurements and found that the emission rate that corresponded best was more like 111.2 tons/day. Their study also

found that such soil NO_x emission increases led to concurrent rises in surface level ozone of 2-9 ppb, highlighting the importance of this source to air quality and the observed disappearance of ozone reduction in the region (Parrish et al., 2017).

We further compiled annual average modeled soil NO_x for the Imperial Valley from several other published studies that use some version of the common Berkeley Dalhousie Soil NO_x Parameterization (BDSNP) and report them in Table 2.4 (Geddes et al., 2022; Hudman et al., 2012; Jaeglé et al., 2005; Vinken et al., 2014; Wang, Ge, et al., 2021). When reading these numbers from large maps of overall emissions, we corrected the fluxes by the factor of 3.9 representing the ratio of the total county area (~1 million ha) to the arable land assuming that the majority of emissions originate from agricultural soils in the region. The study by Wang et al. (2021) proposed a higher emissions parameterization with a temperature plateau that is not reached until 40°C and compared this to the default parameterization, finding that the new one approximately doubled the emissions for the summer months. Our estimate, 2.5 kg N h^{-1} y^{-1}, falls in between their two results of 1.9 – 3.8 kg N ha^{-1} y^{-1}. Because the climate in the Imperial Valley is so different from other agricultural regions, comparisons must consider that the bulk of the planting occurs between September to April (UC Davis Agricultural and Resource Economics, 2004). Given that our observed estimates for June, July, and August closely match our annual averages, it seems reasonable to compare summer emissions to annual averages. This is because nitrogen applications might be at their lowest while soil temperatures are at their highest during these months, with these factors largely balancing each other out.

Almaraz et al. (2018) observed the highest modeled soil NO_x emissions published to date for Imperial Valley. Their method modeled the spatial distribution of soil NO_x emissions using an

N isotope model in natural areas and an Integrated Model for the Assessment of the Global Environment (IMAGE) in cropland areas to estimate N losses from soils based on surplus N. Their average NO_x flux estimated for agricultural lands in Imperial County was ~140 tons/day (51.2 kg N ha^{-1} yr^{-1}). Although this measurement is much higher than the many other studies, due to the complexity of soil NO production we believe more work should be done to evaluate whether this value represents an upper limit. Our results were also compared to a modeling study performed using an enhanced version of Fertilizer Emission Scenario Tool for the CMAQ (FEST-C) agroecosystem model paired with the Air Pollution Emission Experiments and Policy Analysis (APEEP), further abbreviated as FEST-C*(Luo et al., 2022). Data from their 2017 model for Imperial County indicates an annual average soil emission rate of 13.5 tons/day. Finally, Guo et al. (2020) modeled soil NO_x emissions using the DeNitrification-DeComposition (DNDC) model finding the total contribution to the state NO_x inventory was 1.1% (Guo et al., 2020). However, they did point out a region of anomalously high emissions in the Imperial Valley, with an annual flux of 0.58 kg N ha^{-1} yr^{-1}.

While there is considerable variability between the various estimates presented (Table 2.4), due to the highly episodic and transient nature of soil NO_x emissions, the CEPAM inventory estimate is consistently much lower than the other models and observations. We expect that the dominant control of the instantaneous emission rates is the N amendments made to the agricultural soils, so the wide range presented above is likely consistent with this variability. Therefore, to obtain an accurate annual average emission rate from soils will take much more comprehensive understanding of N availability in the soil across these highly variable croplands. More work is needed to better constrain the impact of N availability on soil NO_x emissions, as

well as the precise soil conditions that control microbial activity and gas-exchange. As of 2022, the Sustainable Groundwater Management Act was modified to require farmers in California to report their daily N inputs for consequences of excess N leaching into groundwater. This emerging data set will be crucial for future studies to investigate soil NO_x emissions in arid agricultural environments and accurately assess its impacts on air quality in rural communities.

Table 2.4. Comparing our average soil NO_x flux estimate for Imperial County to CARB and other studies.

NO_x flux	This study	CARB CEPAM	Jaeglé et al. (2005)	Human et al. (2012)	Vinken et al. (2014)	Oikawa et al. (2015)*	Almaraz et al. (2018)	Guo et al. (2020)	Wang et al. (2021)	Luo et al. (2022)
tons NO_x day^{-1}	6.7	0.9	4.3	8.5	8.5	17.2 – 111.2	140.0	1.6	5.2 – 10.4	13.5
kg N ha^{-1} yr^{-1}	2.5	0.3	6.2	3.1	3.1	6.3 – 40.6	51.2	0.6	1.9 – 3.8	4.9

*Note that Oikawa et al., 2015 estimates were for September of 2012 only.

2.4 Suggestions for Future Scientific Work

While our study does indicate the need to reassess agricultural soil influences on NO_x inventories, especially in high-temperature agroecosystems, there are some aspects of future research that we believe should be prioritized. To better understand the nonlinear relationship between nutrient availability and soil moisture for our higher-than-average NO_x fluxes, having access to publicly available databases that contain spatially and temporally relevant fertilization and irrigation information is crucial. The Irrigated Lands Regulatory Program, part of the California Water Resources Control Board, requires farmers to report their N fertilizer usage per crop type and acreage. However, this information is not currently available to the public. In addition, while fertilizer usage and irrigation data are reported annually, it is hard to describe the seasonal variability of these factors. We suggest that the state mandate reporting a shorter time

interval (weekly to monthly) and make it publicly accessible to support the ongoing study of air pollution from agricultural practices. Understanding the biogeochemical processes that contribute to the production of NO_x (and other nitrogen gases like N_2O and HONO) will allow for a better assessment for long-term air quality and climate change, as well as provide insights on agricultural best practices that could be promulgated to improve regional air quality.

It is evident by previous modeling studies that the lack of observational data is hindering the effectiveness of models to produce accurate soil NO_x emissions. Moving forward, there should be more seasonal field analysis of NO_x, HONO, and N_2O emissions from different land/crop types, especially in agricultural systems, since the environmental factors that contribute to N emissions and diffusivity change seasonally. These biogeochemical processes are highly complex and influenced by various factors, including fertilizer type, which models often oversimplify or inaccurately detail. More research needs to be supported in understanding all components of this mechanism, especially fertilizer type, amount, and application frequency, irrigation frequency, organic carbon availability, soil composition, and pH. These studies will improve modeling efforts, hopefully increasing the urgency in addressing these air quality issues that can be improved with proper management and regulatory efforts.

Moreover, Oikawa et al. (2015) showed that utilizing more complex forms of nitrogen like urea-based fertilizer have been shown to reduce the rate of N diffusivity as NO (Oikawa et al., 2015). Urea-based fertilizer has a higher nitrogen content (requiring less input), and is typically cheaper and less hazardous, but inefficient application may result in higher N_2O emissions, volatilization of ammonia, and increased soil acidity (Oikawa et al., 2015; Thornton et al., 1996). Moreover, Slemr and Seiler (1984) showed that five times the amount of NO was emitted from

soil fertilized with urea compared to ammonium nitrate, however this study was performed on bare soil, a condition which largely variable and depends on crop type and cycle (Slemr & Seiler, 1984). A comprehensive investigation on fertilizer type, application methods, cover crop effectiveness, and their environmental implications for various crop types is crucial to avoid trading NO_x emissions for other, potentially more hazardous environmental issues.

Furthermore, the impact of soil NO_x on the production of fine particulate nitrate, is uncertain and is dependent also on ammonia fluxes. To better understand the contribution of agricultural nitrate sources, there must be more research on the impacts of agriculture and controlled animal feeding operations (CAFOs) on the production of both NO_x and NH_3, specifically focused on the impacts of fertilizer usage and waste management. This information is crucial, as most agricultural regions in the state are nonattainment for the $PM_{2.5}$ NAAQS due to the recent lowering of the standard from 12 to 9 $\mu g/m^3$ (US EPA, 2024).

2.5 Policy Implications

2.5.1 Environmental Injustice in Agricultural Regions

The San Joaquin Valley (SJVAB) and Salton Sea Air Basins (SSAB) are two of the most polluted air basins in the country, renowned for their immense agricultural productivity as well as their disadvantaged human populations. These regions are nonattainment for O_3, $PM_{2.5}$, and PM_{10}. Both have failed to meet O_3 NAAQS throughout the history of regulation (US EPA, 2016a). Additionally, $PM_{2.5}$ concentrations in the SJVAB are so severe that the EPA has rejected the State Implementation Plans for attainment of the 2006 and 2012 $PM_{2.5}$ NAAQS. In fact, the 1997 $PM_{2.5}$ standard was only attained in the SJVAB in 2022 (San Joaquin Valley Air Pollution Control District, 2024). Figure 2.12 shows the plateau behavior of O_3 and $PM_{2.5}$ design values in the San Joaquin

Valley and the Salton Sea air basins. Design value is an extreme value statistic that is comparable to the values defined by the NAAQS. For ozone, it is the three-year running average of the 4th highest maximum 8-hr (MDA8) ozone observed in each year. For annual $PM_{2.5}$, it is the average of 3 consecutive years of annual averages. The absence of a decreasing trend in the last 6 years for both strongly indicates a potential missing source, i.e., one that is unregulated.

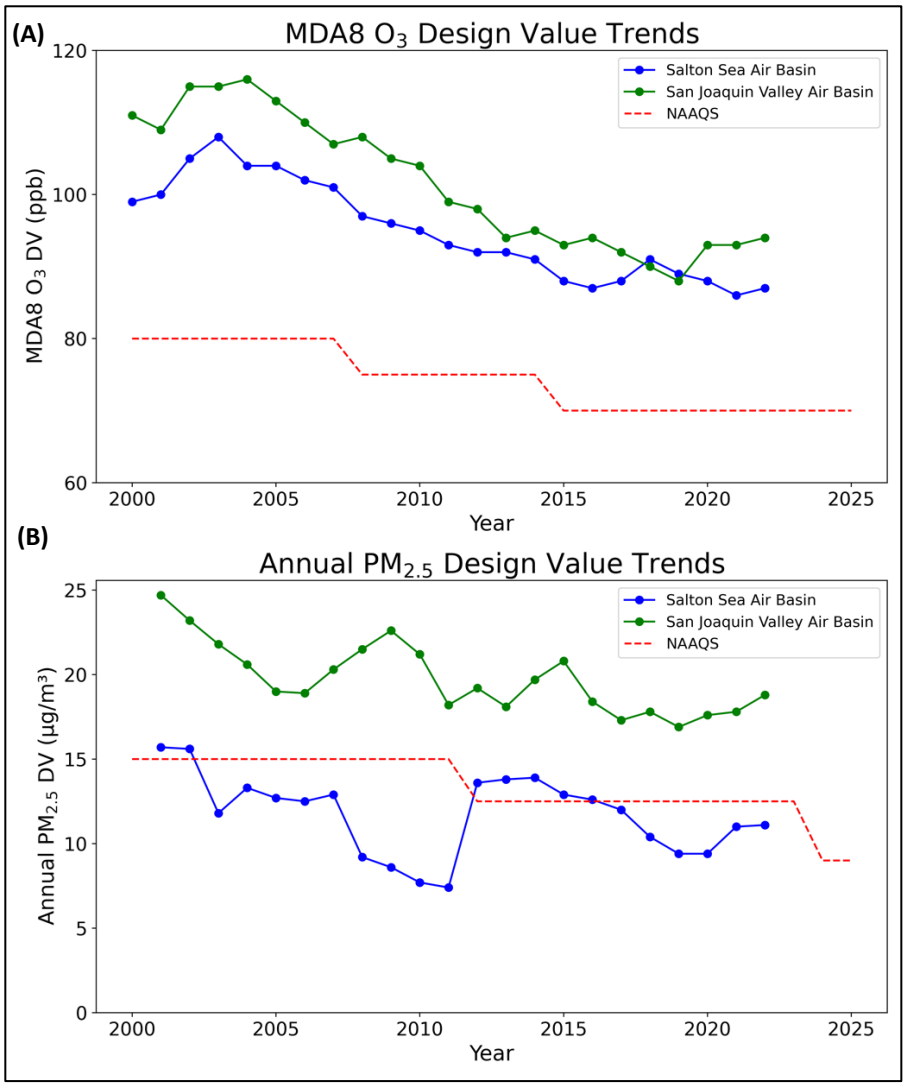

Figure 2.12. Trends in maximum daily 8-hr (MDA8) ozone (A) and annual PM2.5 design value (B) concentrations in the San Joaquin Valley and Salton Sea Air Basins over the 21st century. Data from CARB's Air Quality Data Statistics Trends Summary web site: https://www.arb.ca.gov/adam/trends/trends1.php.

Persistent exposure to air pollutants can lead to reductions in crop yield (Sampedro et al., 2020), in addition to a wide array of impacts on human mortality and morbidity involving cardiovascular and lung disease as well as adverse birth outcomes, neurodevelopment and cognitive function, and even diabetes (World Health Organization (WHO), 2013). Exposure to air pollutants like O_3 and $PM_{2.5}$ inflicts significant and irreparable harm to people, especially to those with pre-existing respiratory and cardiovascular diseases, the elderly, and children (Caiazzo et al., 2013). In fact, Imperial County (in SSAB) held both the highest infection and mortality rates per capita in the state from COVID-19 throughout the height of the pandemic, believed to be partially influenced by these poor air quality issues (The New York Times, 2023). In addition to air quality, these communities face a number of other injustices that affect their overall well-being such as exposure to water pollution, pesticides, toxic substances, and climate change related hazards (G. Huang & London, 2012; Miao et al., 2022). Residents of the SJVAB and SSAB are disproportionately people of color (>70%), and 40% of residents live below the poverty line (Environmental Protection Agency, 2024). Moreover, these communities face insufficient housing availability, poor infrastructure, language barriers, high rates of asthma, and impaired water quality (Anderson et al., 2012; OEHHA, 2023). Figure 2.13 is from CalEnviroScreen (OEHHA, 2023), an environmental justice tracker that ranks census tracts in California based on potential exposures to pollutants, adverse environmental conditions, socioeconomic factors, and prevalence of certain health conditions. It is apparent that communities in these regions rank much higher on these common environmental injustice metrics in comparison to most of the rest of the state. Environmental health and justice organizations contend with entrenched economic

power of the agricultural industry, oil and gas, transportation and land development industries in the state. In many cases, industry power takes precedence over community health.

Nitrogen oxides (NO_x = NO + NO_2) serve as important precursors to O_3 and $PM_{2.5}$, and primary NO_x sources are generated by high-temperature combustion in air from vehicles, power plants, lightning, and biomass burning (Tan et al., 2019). As traditional anthropogenic emissions from fossil fuel combustion continue to decline due to air quality (AQ) and climate regulatory efforts, the proportional impact of soil emissions is rising. Despite the long-term progress in NO_x reductions, non-attainment of national AQ standards for O_3 and $PM_{2.5}$ persists throughout intensive agricultural areas in California, like the SJVAB and SSAB (Parrish et al., 2017). This issue is a matter of environmental injustice because the impacts are felt most acutely in areas of high social vulnerability (G. Huang & London, 2012) and these conditions may be avoidable with scientifically informed political action.

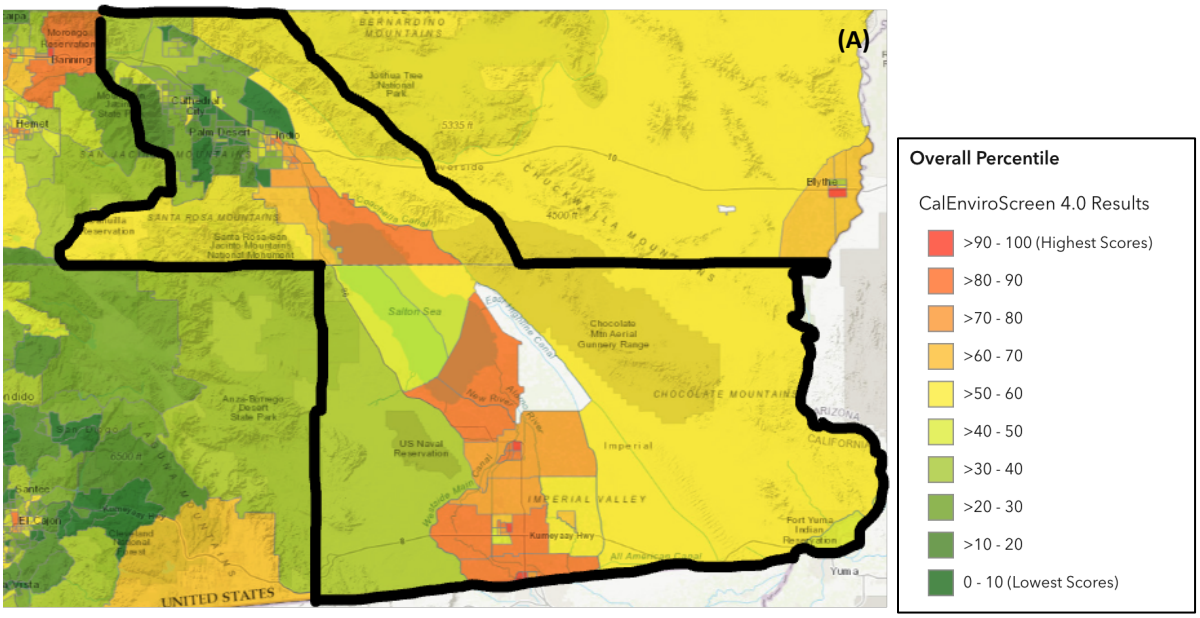

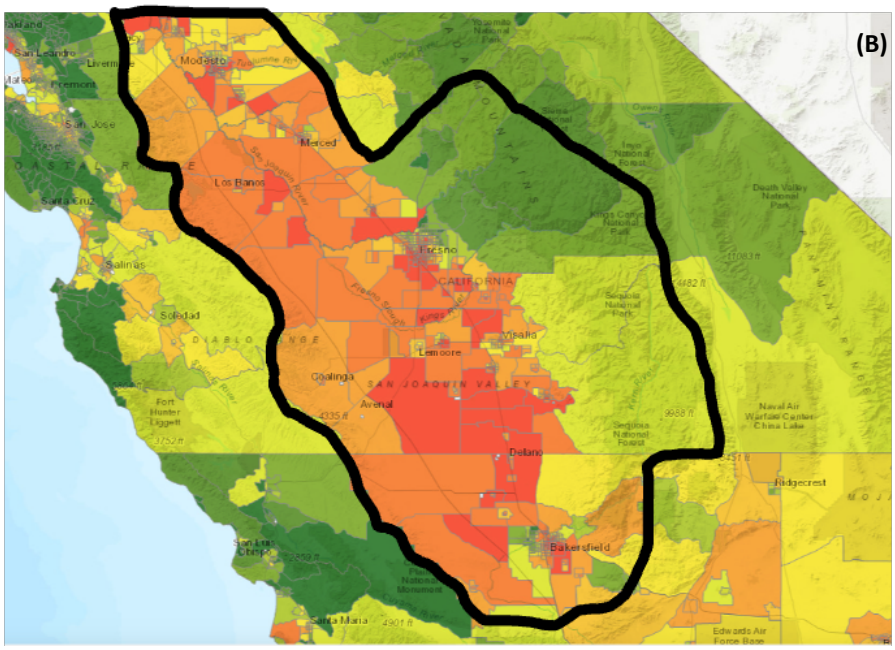

Figure 2.13. The environmental justice tracker (CalEnviroScreen) for the (A) Salton Sea Air Basin and (B) San Joaquin Valley Air Basin are shown.

2.5.2 Scientific Evidence

Several independent studies support the hypothesis that soil NO_x emissions are underestimated by regulatory AQ models (Guo et al., 2020; Kleeman et al., 2019; Luo et al., 2022; Oikawa et al., 2015; Parrish et al., 2017; Sha et al., 2021; Trousdell et al., 2019; Wang et al., 2023; Wang, Ge, et al., 2021). These studies are summarized in Table S2.6, outlining key findings, including emphasis on the continual nonattainment of AQ standards in the SJVAB and SSAB, the impact of soil NO_x on AQ nonattainment, and various environmental factors and agricultural practices that may influence soil NO_x production. Overall, one study by CARB researchers, using a soil biogeochemical model (DNDC) that has not been extensively tested in air quality studies (that is, validated by observations of NO_2 by satellite or surface network NO_x/O_3), found soil NO_x emissions from agricultural systems across California to be negligible (Guo et al., 2020). We

believe this underestimate to be partially due to their use of a default temperature coefficient for nitrification based on temperate meteorological conditions that may not accurately reflect the influence of extreme temperatures, like those observed in the SJVAB and SSAB. This negligible (~1%) contribution from agricultural soils in California is conceptually hard to justify given that the global average of soil sources of NO_x is on average ~20% (Jaeglé et al., 2005), and the contribution from the continental US is ~17% (Silvern et al., 2019). On the other hand, ten other studies, based on thoroughly tested models and observations, found emissions 2-50 times larger across California agricultural landscapes. The collective evidence strongly suggests that agricultural soil NO_x significantly aggravates AQ problems in rural California communities (and inland cities), urging policymakers and regulatory bodies to consider these insights for effective AQ management strategies. There is a pressing need for continued research to refine soil NO_x parameterizations and improve our understanding of the exact physio-chemical controls, emphasizing collaborations between researchers, regulatory agencies, and local communities for comprehensive and sustainable solutions

2.5.3 Interested Groups of Concern

The following recommendations for engagement are suggested to improve the well-being of communities and improve air quality and environmental concerns. Key stakeholders include community organizations in the SSAB and SJVAB, farmers, and various AQ management bodies. Many community organizations serve as stewards for community needs, while farmers and regulatory management bodies should work to ensure safe, sustainable, and efficient agricultural practices. Ensuring awareness among community members and organizations in agriculturally productive regions about the health impacts of current practices is crucial. Farmers should be

provided alternative strategies to improve fertilizer use efficiency, ultimately reducing expenses and minimizing environmental consequences.

The responsibility lies with local, state, and federal environmental protection agencies (i.e., Imperial County Air Pollution Control District, South Coast Air Quality Management District, SJV Air Pollution Control District, CARB, State Water Resources Control Board, California Department of Food and Agriculture (CDFA), US Department of Agriculture, and the US EPA) to support comprehensive research and disseminate vital information to communities and farmers. Specifically, environmental management bodies like CARB, CDFA, USDA, and the US EPA should be responsible for reviewing existing research and planning new projects to better understand the formation of NO_x from agricultural soils, and how fertilizer, temperature, and soil moisture influence their production. These bodies are also responsible for enforcing new agricultural practices that result from research projects. Regional air quality management districts should work with state and federal agencies to ensure their air quality complies with standards. Further, the State Water Resources Control Board passed the Sustainable Ground Water Management plan, which now requires farms to report their fertilizer usage. This information should be shared with researchers to better understand the influence of N fertilizer usage—especially when used in excess—on the production of soil NO_x.

2.5.4 Policy Recommendations

Policy makers have an important role in the reduction of soil NO_x production in agricultural communities. It is important that communities are educated about the air quality issues and concerns. Specifically, community awareness about seasonal trends influencing pollution extremes and interpreting air monitoring data for O_3 and $PM_{2.5}$ is vital for mitigating

health implications. Discussing this information in public engagement forums like AB-617 Community Air Protection Program ((California Air Resources Board, 2017). Imperial Valley Environmental Justice Task Force meetings, CARB's Subject Matter Expert Review Panel (SMERP), and other local AQ or agriculture-related meetings is imperative. Specifically, educating community members on conditions that lead to elevated O_3 and $PM_{2.5}$ concentrations should be reiterated seasonally.

To enhance AQ management, local, state, and federal organizations should collaborate with scientists to comprehend the agricultural impact of soil NO_x in rural areas, as well as research potential control measures that can be adopted into state Clean Air Act implementation plans. This is only going to become more imperative as the US EPA implements its most recent health-based refinement of the NAAQS for annual $PM_{2.5}$ from 12 to 9 $\mu g/m^3$ (US EPA, 2024). The new standard is going to push most of rural California out of attainment and will require additional resources to achieve compliance, specifically addressing this agricultural source of NO_x. Strengthening relationships with community organizations is key and leveraging resources like the EPA's Environmental and Climate Justice Community Change Grants program could aid in addressing the soil NO_x issue. These collaborations should aim to reduce pollution, enhance climate resilience, and build community capacity to address environmental and climate justice challenges. In addition, a deeper understanding of the primary components that produce soil NO_x is crucial for assessing the manageability of soil NO_x emissions. We strongly encourage regulatory agencies and state/federal funding to allocate more resources towards research projects focused on these topics for more informed policy recommendations.

We provide here scientific evidence supporting calls for investigating the impact of agricultural soil NO_x emissions in state and federal models, along with suggesting practices to minimize emissions, while benefiting farmers, community members, and the environment. Various farming methods can be employed to reduce NO_x emissions, which most often correspondingly reduce N_2O emissions. Modern agriculture is driven by the maximization of output, which is often short-term focused, results in excessive amounts of food waste, and lacks regard for input efficiency (Odum, 1989). Utilization of synthetic fertilizer maximizes output; however, input efficiency of N fertilizer is one of the lowest among the plant nutrients, contributing substantially to environmental degradation (Bohlool et al., 1992).

*Management Suggestions**.***

1. Promote precision techniques for agriculture sustainability.

   Nutrient uptake efficiency can be improved by using precision fertilization, applying fertilizer below the surface closer to the site of root uptake, as well as timing the applications to coincide with crop developmental stages (Harrison & Webb, 2001; Skiba et al., 1997; Smith et al., 2000). Farmers should be encouraged to avoid applications of N when soil is bare and on especially hot summer days (Hall et al., 1996).

2. Alternative fertigation practices may reduce NO emissions.

   Practices like Pump and Fertilize (P&F) and High Frequency Low Concentration (HFLC) have been shown to reduce N_2O emissions by 52-72% and 48-58%, respectively, although their impacts on NO emissions needs further investigation (Nichols et al., 2024). To summarize, P&F reduces the applied N rate in response to measured concentrations of N

in the groundwater so that added N and groundwater N reach the same total N applied, while HFLC applies smaller N rates per fertilization event.

3. Biogenic methods like nitrogen-fixing plants, biological nitrogen inhibitors, and cover crops reduce N outputs in soils.

   Biological nitrogen-fixing plants like legumes efficiently fix N_2 from the atmosphere, making N readily available in the soil (Bohlool et al., 1992). These plants can act as a supplement to synthetic fertilizer, offering an economically attractive and environmentally friendly means of reducing overapplication of nutrient inputs, however, further study on their reliability is necessary. In addition, biological nitrification inhibitors (BNIs) are compounds released by plant roots of certain species (e.g., Brachiaria humidicola, sorghum) that suppress the activity of soil microorganisms responsible for nitrification (Coskun et al., 2017). BNIs slow the conversion of ammonium to nitrate, decreasing the availability of N for processes that lead to the production of NO_x and N_2O, while increasing the availability for N uptake by plants. Moreover, planting cover crops improves soil structure and health while reducing N loss from soils without reducing crop yield; however, the specific impact that cover crops have on reduction of NO emissions has not been extensively studied (Skiba et al., 1997).

4. Soil remediation practices can reduce soil NO production.

   Promoting the reduction of NO_x to environmentally benign gases like N_2 can be achieved through remediation of riparian zones which collect runoff (Davidson et al., 2012). In addition, soil carbon and reduction of N and P leaching can be improved using biochar inputs (Dai et al., 2020). The large-scale dissemination of such farming practices could

ultimately reduce environmental hazards in water and air and lower farming costs. It is important to note that the amount these practices will reduce soil NO_x production is highly understudied, therefore, more research is necessary to determine which procedures should be implemented through policy.

5. Reported N inputs should be publicly available.

   The Irrigated Lands Regulatory Program (ILRP), part of the California Water Resources Control Board, regulates the use of nitrogen on irrigated lands through a Total Nitrogen Applied (TNA) report to protect ground and surface waters (California Water Boards, 2024). This information is currently not publicly available to protect farmers, however, it should be accessible upon request for researchers aiming to better understand the influence of excess N fertilizer inputs on the production of soil NO_x emissions.

2.6 Supplementary Tables

Table S2.1. Sampling durations at each site during the field study.

Calipatria			Thermal		
Start time	Stop time	Duration	Start time	Stop time	Duration
06/16/22 1400 PST	06/18/22 1900 PST	53 h			
07/20/22 1500 PST	07/23/22 1000 PST	67 h	07/22/22 1400 PST	07/27/22 1200 PST	118 h
08/24/22 1400 PST	08/27/22 0900 PST	67 h	08/24/22 1000 PST	08/30/22 0900 PST	143 h
09/14/22 1200 PST	09/19/22 0900 PST	117 h	09/19/22 1200 PST	09/26/22 1000 PST	166 h
10/14/22 1100 PST	10/18/22 1100 PST	96 h	10/20/22 1000 PST	10/25/22 0900 PST	119 h
11/18/22 1300 PST	11/22/22 1200 PST	95 h	11/17/22 1200 PST	11/21/22 1100 PST	95 h
12/16/22 1300 PST	12/21/22 1100 PST	118 h	12/15/22 1100 PST	12/19/22 1200 PST	97 h
01/20/23 1200 PST	01/25/23 1100 PST	119 h	01/12/23 1100 PST	01/17/23 0800 PST	117 h
02/24/23 1100 PST	02/28/23 1300 PST	98 h	02/27/23 0900 PST	03/01/23 0900 PST	48 h
04/19/23 1100 PST	04/23/23 1300 PST	98 h	04/12/23 0800 PST	04/17/23 0900 PST	121 h
Total time sampled		928 h (~39 d)	Total time sampled		1024 h (~43 d)

Table S2.2. Average meteorology and pollutant concentrations during field sampling in Calipatria (June 2022 – April 2023). Volumetric soil moisture (VSM) was reported from SMAP satellite data). NO_x, O_3, and $PM_{2.5}$ data were obtained from the nearest meteorological sites (El Centro, Niland, and Brawley, respectively). See Table S2 for sampling durations. Shaded rows indicate negligible soil NO_2 observed.

Month	T_{max} (°C)	O_3 (ppb)	NO_x (ppb)	$PM_{2.5}$ (μg/m^3)	PM_{10} (μg/m^3)	Scalar ws (m/s)	wd	RH (%)	Specific humidity	Precipitation (cm)	VSM (m^3/m^3)
Jun	41.2	40.4	3.6	34.6	82.9	3.9	220°	16.5	0.004	0	0.084
Jul	44.2	28.0	5.7	6.5	56.3	2.7	132°	30.5	0.011	0	0.088
Aug	43.8	28.5	5.6	5.6	35.9	2.7	135°	36.5	0.013	0.02	0.103
Sep	38.2	28.1	8.4	4.3	40.1	2.0	155°	37.0	0.008	0	0.116
Oct	32.9	21.7	6.7	3.7	21.2	1.8	140°	59.2	0.011	3.39	0.154
Nov	23.3	28.7	8.3	3.9	23.6	2.3	0°	32.3	0.003	0	0.116
Dec	18.9	23.1	13.0	6.4	21.8	1.8	109°	42.5	0.003	1.47	0.117
Jan	19.2	20.1	9.8	5.5	19.0	2.7	337°	31.8	0.002	0.25	0.151
Feb	18.8	39.0	3.6	1.0	9.8	4.5	233°	51.8	0.005	0.11	0.152
Apr	35.1	38.1	4.2	8.2	32.4	2.5	205°	27.7	0.004	0.05	0.108
Avg	31.5	29.7	6.9	8.0	34.2	2.7	163°	36.7	0.007	(sum) 5.29	0.119

Table S2.3. Average meteorology and pollutant concentrations during field sampling in Thermal (July 2022 – April 2023). O_3, NO_x, and $PM_{2.5}$ were obtained from the nearest monitoring locations (Palm Springs and Brawley). ND

denotes no data. Volumetric soil moisture (VSM) was reported from SMAP satellite data). See Table S2 for sampling durations. Shaded rows indicate negligible soil NO_x observed.

Month	T_{max} (°C)	O_3 (ppb)	NO_x (ppb)	$PM_{2.5}$ (μg/m^3)	PM_{10} (μg/m^3)	Scalar ws (m/s)	wd	RH (%)	Specific humidity	Precipitation (cm)	VSM (m^3/m^3)
Jul	40.2	54.7	5.5	9.5	ND	2.7	139°	32.6	0.011	0	0.035
Aug	40.5	50.4	4.3	2.7	31.9	3.1	347°	27.4	0.009	0.01	0.043
Sep	38.9	43.5	4.9	5.2	20.1	2.7	326°	24.3	0.007	0.01	0.051
Oct	29.0	41.2	5.6	6.9	ND	2.9	303°	28.4	0.005	0.24	0.063
Nov	23.4	34.7	10.6	3.4	15.8	2.3	310°	29.6	0.002	0.62	0.061
Dec	18.1	24.3	14.6	5.6	15.0	1.3	307°	47.3	0.003	0.30	0.063
Jan	19.2	28.2	10.2	6.4	11.6	2.5	328°	60.4	0.005	0.05	0.105
Feb	17.4	36.9	6.5	ND	4.7	3.1	297°	51.6	0.005	0	0.122
Apr	29.9	51.3	3.9	14.7	69.5	4.9	328°	37.7	0.006	0	0.082
Avg	28.5	38.4	7.3	6.04	18.7	2.8	317°	37.7	0.006	(sum) 1.23	0.069

Table S2.4. Climatology data for Calipatria, or nearest Imperial County met site* (Niland, Brawley, El Centro).

Month	T_{max} (°C)	O_3 (ppb)*	NO_x (ppb)*	$PM_{2.5}$ (μg/m^3)*	PM_{10} (μg/m^3)	Scalar ws (m/s)	wd	RH (%)	Specific Humidity	Precipitation (cm)
Jan	21.3	27.7	17.6	4.0	25.1	1.5	292°	51.6	0.004	0.69
Feb	23.0	35.0	13.5	4.4	30.5	1.6	269°	43.5	0.004	0.68
Mar	26.4	41.2	9.1	4.6	36.4	1.8	277°	40.5	0.005	0.58
Apr	29.6	46.3	6.1	7.1	50.3	2.0	269°	33.8	0.005	0.19
May	33.3	49.1	4.3	8.3	55.2	2.1	247°	31.5	0.006	0.18
Jun	38.9	47.4	5.1	8.9	56.6	2.0	191°	27.5	0.007	0.02
Jul	41.0	39.2	4.8	8.6	55.7	2.3	159°	31.7	0.010	0.14
Aug	41.0	39.6	5.1	7.5	52.3	2.1	166°	34.4	0.011	1.27
Sep	38.3	36.8	6.7	7.5	49.6	1.8	178°	36.3	0.010	0.61
Oct	32.1	34.6	9.4	6.8	46.5	1.7	268°	33.9	0.006	0.56
Nov	25.7	29.8	14.9	5.0	39.5	1.5	283°	42.5	0.005	0.33
Dec	20.0	25.6	17.7	4.0	26.8	1.5	315°	48.4	0.004	0.86
Avg	29.3	38.5	9.5	6.6	44.5	1.8	244	38.4	0.007	(sum) 6.11

Table S2.5. Climatology data for Thermal, or nearest air quality site (Palm Springs*). RH data was not available for Thermal, so the nearby Torres-Martinez$^{\oplus}$ site was substituted.

Month	T_{max} (°C)	O_3 (ppb)*	NO_x (ppb)*	$PM_{2.5}$ (μg/m^3)	PM_{10} (μg/m^3)	Scalar ws (m/s)	wd	RH (%)$^{\oplus}$	Specific Humidity	Precipitation (cm)
Jan	22.0	37.8	15.7	4.3	15.5	1.9	327°	56.3	0.004	1.89
Feb	23.7	46.2	11.5	4.4	21.4	2.4	327°	50.5	0.004	0.91

Mar	27.6	53.4	8.0	4.4	25.4	3.3	325°	40.0	0.005	0.69
Apr	31.3	61.5	5.6	6.7	42.3	4.1	327°	35.4	0.005	0.22
May	34.7	65.8	4.3	7.2	42.1	4.4	329°	34.9	0.006	0.02
Jun	40.0	71.9	4.6	8.6	46.6	3.8	331°	33.7	0.007	0
Jul	41.9	68.6	4.6	8.1	43.6	3.3	342°	37.9	0.010	0.34
Aug	41.8	67.8	5.2	9.0	36.3	3.1	342°	37.2	0.010	0.18
Sep	38.7	58.6	6.1	8.4	36.1	2.8	339°	41.2	0.008	0.76
Oct	32.6	52.0	8.4	6.7	31.8	2.7	331°	41.0	0.006	0.54
Nov	26.3	42.4	12.8	5.5	29.9	2.1	327°	50.5	0.005	0.19
Dec	20.7	35.8	15.6	5.3	24.8	1.9	326°	55.1	0.004	1.08
Avg	30.1	54.5	8.5	6.9	31.3	3.2	332	40.3	0.006	(sum) 6.82

Table S2.6. A summary of recent literature that addresses agricultural soil NO_x and its impact on air quality in California, especially in the San Joaquin Valley and Salton Sea air basins.

Study	Key Findings
Oikawa et al. (2015)	- Reported record soil NO_x emissions (up to 280 kg N ha^{-1} yr^{-1}) in Holtville, CA (Imperial Valley). - Default soil NO_x parameterization in WRF-Chem model underestimates emissions by at least one order of magnitude. - Augmenting the default soil NO_x emissions (by factors of 10-64 to improve agreements with observations) increases modeled O_3 concentrations by 2-8.5 ppb throughout Imperial Valley in the SSAB.
Parrish et al. (2017)	- Observed dramatically curtailed O_3 improvements in the San Joaquin Valley and Salton Sea air basins, despite improvements in surrounding Southern California air basins. - Suggested that recalcitrant O_3 levels are linked to sources evading regulatory efforts most probably related to the intensive agriculture that characterizes these basins.
Almaraz et al. (2018)	- Suggested in 2018 that agricultural soils emit 20-32% on average of the state's total NO_x, with the average cropland NO_x flux around 20 kg N ha^{-1} yr^{-1}.
Trousdell et al. (2019)	- Top-down aircraft measurements of NO_x and O_3, estimated a total emission rate of 215 ± 33 tons/day around Fresno in the SJVAB, a factor of 2 larger than the CARB's CEPAM inventory - Rural SJV counties exhibited no observed O_3 decreases from 2006-2016.
Kleeman et al. (2019)	- Modified soil emissions in their model using soil NO_x emissions from Almaraz et al. [2018]. - These modifications increased predicted $PM_{2.5}$ nitrate concentrations in January of three different years in the SJV, helping to correct a consistent underprediction by the model.
Guo et al. (2020)	- California Air Resources Board study using a soil biogeochemical model (DeNitrification-DeComposition, DNDC) that is mostly untested against agricultural soil NO_x emissions. - Concluded that soil emissions contribute only 1.1% of total anthropogenic NO_x in CA, although larger than normal emissions were estimated for the Imperial Valley. - Suggested default temperature coefficient for nitrification may need revision to account for hot agroecosystems like SJVAB and SSAB.
Sha et al. (2021)	- University of Iowa modified soil NO_x parameterization in WRF-Chem (Berkeley Dalhousie Iowa Soil NO Parameterization, BDISNP), e.g., enhanced land cover, soil temperature, emission pulses, and N fertilizer influences. - In July 2018, estimated soil emissions contributed ~40% of California's total NO_x, increasing rural O_3 concentrations by +23%.
Wang et al. (2021)	- Used a stronger, observation-based temperature response for soil NO_x. - Improved correlation between satellite NO_2 and modeled column NO_2 over the central US in the summer, suggesting soil emissions may be larger than expected at temps >30°C. - Emphasized hotspots in the SJVAB and SSAB due to N fertilization and warm climates.

Luo et al. (2022)	- Simulated reactive N emissions across the contiguous US by county, estimating annual emissions from the 8 counties of the SJVAB to total about 100 tons/day, compared to CARB's CEPAM inventory of ~230 tons/day anthropogenic NO_x estimate (comparable deviation to that reported in Trousdell et al. [2019]). - Incorporated daily fertilizer application estimates from the Environmental Policy Integrated Climate (EPIC) agricultural model, based entirely on simulated idealized plant demands
Wang et al. (2023)	- OMI satellite NO_2 data over croplands revealed a soil-like temperature and soil moisture dependence, with no long-term trend over croplands as opposed to continued decreases (-3.7 ± 0.3 %yr^{-1}) over urban areas. - Illustrates similar dependence of observed NO_2 columns over a variety of non-urban land types across California, implying that soil NO_x is a significant source.
Lieb et al. (2024) *in review*	- A mixing model using CARB's CEPAM NO_x inventory and source-dependent $\delta^{15}N$-NO_x isotopic measurements revealed an underestimated soil contribution. - Our adjustments showed soil NO_x to be 30% of total NO_x in the SSAB, an order of magnitude larger than CEPAM's 3%.

Table S2.7. Average meteorological and pollutant parameters and standard deviation reported for our sampling periods and for the sampling year (June 2022-May 2023). Note that the reported VSM values are for 16:30 to correspond with the time in which temperature is at its maximum.

	Average	T_{max}	O_3 (ppb)	NO_x (ppb)	$PM_{2.5}$ (μg/m^3)	PM_{10} (μg/m^3)	Scalar ws (m/s)	RH (%)	VSM (m^3/m^3)
Calipatria/ Imperial Valley	**Sampling Interval**	31.6 ± 10	38.1 ± 8	4.2 ± 3	8.2 ± 12	32.4 ± 22	2.5 ± 0.9	36.7 ± 12	0.12 ± 0.03
	Annual	30.0 ± 9	30.7 ± 12	7.8 ± 5	7.8 ± 7	41.8 ± 41	2.1 ± 1	49.1 ± 12	0.11 ± 0.03
Thermal/ Coachella Valley	**Sampling Interval**	28.5 ± 10	38.4 ± 11	7.3 ± 4	6.1 ± 4	18.7 ± 22	2.8 ± 1	37.7 ± 13	0.07 ± 0.03
	Annual	30.4 ± 9	43.0 ± 14	6.9 ± 4	7.8 ± 7	29.3 ± 39	3.0 ± 2	40.5 ± 14	0.07 ± 0.03

Chapter 3: Community-Based Participatory Research Case Studies

Abstract

Community-based participatory research (CBPR) supports the self-empowerment of those most affected by environmental injustices. Community-engagement is also useful for personal development of researchers, allowing them to connect their work to meaningful causes, such as research that is relevant to community needs and health. CBPR has made its way into the physical sciences and in the coming years there will likely be a spike in community engaged environmental research, where scientific proposals will be focused on improving the health and well-being of disadvantaged communities. Furthermore, building a sense of community allows for interconnectedness, support, and sharing of ideas. This chapter will focus on two case studies involving my engagement with community groups throughout the tenure of my PhD, which both positivity shaped the scope and broader impacts of my research projects. I hope that these anecdotes inspire and help future scientists in navigating CBPR work.

3.1 Importance of Civic Engagement in Environmental Research

Civic engagement is a primary tool for obtaining environmental justice. Communities with actively engaged citizens are stronger, more resilient, more connected, and more equitable (Irani & Rahnamayiezekavat, 2021). This engagement empowers communities by providing them with the knowledge and tools to address environmental challenges. When citizens are actively involved in research, they gain a deeper understanding of their local environment and the factors affecting it (Balazs & Morello-Frosch, 2013). Engagement in environmental science is becoming

more common, as the challenges of environmental degradation, natural disasters, and climate change loom in our communities.

Active civic participation fosters inclusivity by valuing and resourcing the voices of marginalized and underrepresented groups in the research process. This is crucial in environmental justice, as these communities often bear the brunt of environmental degradation and are typically excluded from decision-making processes. Engaging these groups helps to ensure that research outcomes are equitable and that the benefits of environmental policies and interventions are distributed fairly (Kimura & Kinchy, 2016). In addition, when communities are involved in environmental research, it builds trust between researchers and the public. Transparency in the research process, facilitated by civic engagement, helps to demystify scientific practices and promotes public understanding of environmental issues. This trust is essential for the successful adoption of research recommendations and for fostering long-term collaboration between scientists and communities.

Moreover, civic engagement in environmental research ensures that the studies conducted are directly relevant to the communities they aim to benefit. By involving local key players, researchers can identify the most pressing environmental issues and tailor their methodologies to address these concerns effectively (Balazs & Morello-Frosch, 2013; Kimura & Kinchy, 2016). This leads to more accurate data collection and a higher likelihood of successful implementation of research findings. Research that involves civic engagement is more likely to influence policy effectively. Community engaged research can bring in policy makers who can help advocate for causes that reflect the needs and priorities of their constituents. Civic

engagement thus bridges the gap between scientific research and policy, ensuring that environmental policies are practical, acceptable, and sustainable.

3.2 Case Study 1: Western Service Workers Association

Entering my graduate program without prior experience in community engagement, I quickly recognized the importance of building meaningful relationships and acquiring community engagement skills to effectively conduct CBPR. In 2020, I began volunteering with the Western Service Workers Association (WSWA), a Sacramento-based community organization committed to eradicating poverty among low-income service, in-home care, part-time, and temporary workers. WSWA aligns its mission with the United Nations' 2030 Sustainable Development Goals (SDGs) (United Nations, 2012), and its resilience lies in its ability to adapt to evolving community needs while minimizing reliance on short-term government funding. This context-aware approach, which tailors outreach to relevant circumstances, showcases WSWA's nuanced understanding of community dynamics.

Recognizing the significance of volunteer work is crucial when approaching CBPR in scientific research as it lays the foundation for meaningful relationships, cultivates essential organizational skills, builds trust, and offers insights into navigating connections within often underserved communities. These foundational steps are instrumental in the success of CBPR and in addressing environmental injustice, allowing for collaborative relationships rooted in an understanding of individual positionalities. As an environmental chemist, my commitment to addressing environmental degradation and climate change—especially those stemming from unsustainable agricultural practices—drove my engagement with CBPR. Despite the critical role agriculture plays in sustaining our food system, current profit-driven approaches often result in

environmental harm and exacerbate food scarcity in vulnerable communities (Reyers et al., 2022). Moreover, there remains a significant gap between the physical and social sciences, often leading to a lack of intersectionality in research approaches.

Through my participatory research with WSWA, I sought to enhance my community engagement skills, communicate scientific knowledge to communities in ways that foster meaningful change, and implement CBPR in my dissertation. This case study reflects an empowering action approach (Meyer, 2000), aiming to prioritize practical relevance over theoretical abstraction in the methodology and scientific proposals, thereby ensuring that scientific research contributes meaningfully to community needs beyond academic publication.

In this community partnership, I used my organizational and leadership skills to transition to a sustainable, community-centric model for addressing food insecurity, understanding that food insecurity often results from an uneven distribution of nutrient-rich foods. WSWA runs a weekly food distribution with organic produce donated from the local farmer's market. However, these food donations often result in 5-10% of food waste. Additionally, as food stamp cuts continue post-pandemic and wages stagnate, the demand for nutritious food is rising. In response to this transition, we focused on repurposing food waste for composting to replenish nutrients in degraded soil on WSWA's property, with the long-term goal of creating a volunteer-managed community garden.

To support this initiative, we worked with Jorge Espinosa, a sustainable landscape designer with a strong understanding of waste reduction. He discussed how compost tumblers may be the best option to repurpose food waste at WSWA, with the intention of using fertile compost to replenish nutrients in the soils of WSWA's land. Per his suggestion, I procured three

composting tumblers for WSWA, funded through leftover funds from small university grants that did not require a strict budget report, and developed a maintenance strategy to be sustained by the organization and its volunteers. The framework for this tactic revolves around five key components: expected results, primary and secondary purposes, tools, and maintenance mechanics. Expected results included establishing a sustainable volunteer team for the monthly composting and replenishing the soil on the property for future gardening projects. The primary purpose involved integrating new volunteers, such as environmentalists and local farmers and community gardens, into the organization. The intention was to foster discussions about the interconnectedness between humans and the environment and address the disconnection caused by factory farming. The secondary purpose aimed to offer classes to community members on sustainable practices for utilizing compost and reducing food waste. Tools employed in the project include a food scrap shredder, shovels, wheelbarrows, and compost tumblers. Maintenance mechanics involved organizing skills such as recruitment, training, briefings, and debriefings, and plans for retaining recurring volunteers. Each new volunteer will be trained by existing volunteers based on the details outlined in the tactic sheet.

While securing the supplies and materials for this project was straightforward, integrating and executing this project proved challenging. Since this project was not the primary focus of my dissertation, I had to dedicate personal time to its progress. Nevertheless, I ensured the project's continuity by training volunteers to operate the compost tumblers. Additionally, since these tumblers require a few weeks to break down the compost into soil, we had excess food waste. Jorge suggested that we try to minimize the amount of food waste going to compost and instead redistribute it to local farms to feed their livestock. I addressed this issue by connecting WSWA

with Yisreal Family Farms, a local community farm who now collects the surplus food waste weekly to feed their livestock.

By leveraging UC Davis's academic resources, I was able to bring tangible support to the community, illustrating how strong and sustainable relationships between community organizations, academia, and local stakeholders can create resilient systems capable of addressing injustices and environmental threats. Additionally, this project taught me that when possible, taking action-based approaches to address community problems without getting pulled into rigid academic research structures can prove to be more effective. Furthermore, I was able to develop more organizational and leadership skills in this role, which will serve me well as a research scientist and project manager in future positions.

Moreover, this project equipped me with valuable skills in collaborating with community organizations and led to the co-creation of an atmospheric science research project in the Imperial Valley. While volunteering with WSWA, I was introduced to Herman Barahona, a local organizer and air quality advocate in Sacramento, whom I discussed my proposed research project in the Salton Sea Air Basin down in Southern California. I had expressed interest in understanding the mechanisms of poor air quality in this region, since it has not attained air quality standards for ozone and particulate matter in over a decade. Herman mentioned Luis Olmedo, the CEO of Comité Cívico del Valle (CCV), a community organization in Imperial Valley known for their advocacy work related to the poor air quality. CCV is also known for their community-managed particulate matter monitoring network called Investigating Violations Against Neighborhoods (IVAN). I had tried to contact Luis numerous times to discuss collaboration with no avail. However, after working with Herman and expressing my interests in

community engaged research, he contacted Luis and suggested he meet with me. Within the same week, Luis had set up a zoom call with me, which resulted in him agreeing to partner with us. Through this partnership, we were able to develop a field sampling campaign to address the impact of agricultural soil NO_x in the region, a precursor emission to ozone and particulate matter.

3.3 Case Study 2: Comité Cívico del Valle

When formulating a community partnership, it is important to have alignment in research interests. Comité Cívico del Valle (CCV) believe that informed people build healthy communities, and because of this, they are community partners with three air-quality-focused programs—IVAN Community Air Monitoring Network, AIRE Collaboration, and AB617 Community Steering Committee. Each of these groups are dedicated to improving the quality of life and health of communities at local and/or statewide levels. Our intention for collaborating with CCV was to provide more information on the meteorological influences of poor air quality, as well as reassess standing theories on the persistence of poor air quality in the Salton Sea Air Basin (SSAB). We attended public AQ meetings to understand local air quality concerns, then discussed our research interests with CCV, informing them of our dedication to help improve air quality conditions in the region. We explained that we would be assessing climate trends and described our hypothesis that unregulated soil NO_x emissions were contributing to the persistent poor air quality. In addition, we described our proposal for a field sampling campaign and asked if CCV would be willing to participate, to which they agreed. In 2022, we were awarded the Environmental Health Sciences Core Center Pilot Project grant, funded by the National Institutes of Health, which funded our community partnership for our soil NO_x field sampling campaign.

In preparation for this partnership and the campaign, I practiced setting up our sampler in Davis, ensuring I understood any potential issue that could arise. I then drafted a ***detailed*** standard operating procedure (SOP) with pictures and diagrams for assembling and disassembling our sampling instrument, the ChemComb Speciation Cartridge (CCSC, discussed in more detail in Section 2.2.1). As we launched our field sampling campaign, we coordinated a day to demonstrate the set-up and break-down of our sampling device with two technicians from CCV, Matthew Maldonado and Edgar Ruiz. I set up the sampler and disassembled it with them, following the SOP I outlined. Then, I allowed both of them to set up and break down the instrument themselves, giving feedback when needed. For our second sampling the following month, I allowed both of them to lead the set up and break down, following only the guidance of the SOP. I answered questions and corrected them when needed. After this event, Matthew and Edgar were responsible for the assembly and disassembly for the remainder of our study. The sampling was performed monthly, and the denuders and filters were mailed to me for extraction in the lab.

To ensure alignment with CCV's mission statement, "informed people build healthy communities," we participated in public workshops and included CCV in the publication process of our scientific reports. Throughout the duration of my Ph.D., I participated in the Imperial Valley Environmental Justice Task Force and AB-617 meetings, both attending to better understand local concerns and presenting scientific presentations. This work gave me more experience in communicating scientific information to individuals without strong formal scientific literacy. Notably, there was one instance where the information I was presenting at an AB 617 meeting on meteorological dynamics that influence poor air quality was not communicated well. I

received feedback directly from community members expressing how the PowerPoint presentation and the scientific information was hard for them to follow. Christian Torres, the special projects manager, and I assessed new ways to communicate this information. In response to this event, I provided detailed annotations to my slides with links to references that would provide more information. In addition, Christian and I agreed to meet prior to my next presentation so that he could give me feedback on topics that may be confusing for community members. I have yet to give another presentation with this group but plan to implement these techniques in future presentations. Furthermore, all manuscripts were shared with Christian and Luis for feedback to ensure that the information published with their names was in alignment with the values of their organization.

Aside from the misunderstanding in one of our community participation meetings, the collaboration with CCV went rather smoothly. Matthew and Edgar did an awesome job with field sampling and Christian was incredible at maintaining engagement when needed. There were no issues or errors during the campaign, and I received feedback from Matthew that he appreciated my organizational skills and attention to detail and felt that I had been the easiest academic to work with. The biggest challenge was the distance, which limited the face-to-face interactions we could have with each other, ultimately limiting the impact we could have on the community members. However, we believe that our work will have significant regulatory impact soon, as the degraded air quality of agricultural communities like the Salton Sea Air Basin and the San Joaquin Valley Air Basin are of importance at the state and federal levels. Furthermore, this pilot project showed our abilities to collaborate with CCV and have formulated a strong partnership of which Ian hopes to continue in his future research.

3.4 Conclusion

Through my community-engaged research projects, I've learned that I am a scientist with a diverse range of interdisciplinary skills. My scientific background allows me to analyze community problems through a research-oriented lens, with a focus on raising public awareness about critical issues. Throughout these projects, I've also leveraged my organizational abilities to find solutions, whether by overcoming obstacles or transforming ideas into reality. My deep determination for meaningful change drives me to tackle challenges without hesitation, while resourcefulness has proven essential in addressing the complex nature of environmental injustices, which demand extensive collaboration. These experiences have reshaped how I approach research, shifting my focus toward broader impacts. Now, my research questions are centered around improving the well-being of all sentient beings.

Chapter 4: Art as a method of scientific communication: broadening the scope of science

Abstract

Environmental science is often studied with the intent of clarifying anthropogenic impacts on the natural world, including the societal and ecological implications of land mismanagement and climate change. However, peer-reviewed literature, while the cornerstone of scholarly communication, has severe limitations in impact, often resulting in a lack of public understanding of current environmental concerns. This lack of understanding originates from specialized language and statistical evaluations of methods and results. Additionally, this logos (appeal to logic) approach using statistics and figures does not always stimulate interest in the layperson. In fact, some of the most meaningful changes are seen because of ethos, which can be stimulated through artistic expression. When discussing subjects like climate change and land mismanagement, there is often an emotional response, which if used appropriately, can formulate meaningful change.

4.1 Art as a form of activism

Art has long been a powerful vehicle for social and political change, capable of transcending the limitations of traditional scholarly communication (Thompson et al., 2023). Murals have been instrumental in conveying powerful messages about social justice, identity, and environmental concerns (Greaney, 2002; Gunther, 2022; Thompson et al., 2023). Throughout history, various art movements have played significant roles in raising awareness and inspiring activism.

One prominent example is the Mexican Muralism Movement of the 1920s-1950s, led by artists such as Diego Rivera, David Alfaro Siqueiros, and José Clemente Orozco. These artists used their murals to convey social and political messages, often highlighting the plight of the working class, including agricultural laborers (Museum of Modern Art, 2022). Diego Rivera's work was especially inspiring during the culmination of this project. Rivera frequently depicted scenes of rural and agricultural life, celebrating the contributions of peasant farmers and addressing issues of land reform and social justice (Museum of Modern Art, 2022). His murals often portrayed the interdependence of humans and the land, emphasizing the dignity of agricultural labor and the need for agrarian reform.

Similarly, the Chicano Movement of the 1960s-1980s saw the creation of numerous murals that highlighted the civil rights struggles of Mexican Americans. These murals became part of the effort to reinvigorate cultural heritage and challenge racism (Palomo Acosta, 2018). This period was significant as the United Farm Workers Union was formed, allowing for farmworkers to gain fair working conditions and compensation, as they are responsible for feeding our country and some of the world. More recently, the Black Lives Matter Movement have used street art and murals to emphasize the impacts of systemic racism and police violence against black people.

The Environmental Justice movement has slowly taken form over the past several decades. The first major milestone in the national movement began in Warren County, North Carolina, where in the late 1970s, the state's government decided to store 6,000 truckloads of PCB-laced soil in a rural, poor, and primarily black county (Skelton et al., 2023). With concerns over drinking water contamination, this incidence brought in veterans of the Civil Rights

Movement; there were peaceful protests and marches to advocate for the health of their community, and some members even stopped trucks driving to dump the soil by lying down in the roads leading to the landfills (Skelton et al., 2023). Environmental injustice is described by corporations, regulatory agencies, and local planning and zoning boards intentionally targeting low-income communities and communities of color when choosing landfills, incinerators, nuclear waste storage, hog and chicken processors, oil refineries, and chemical manufacturing, or refuse to address the impacts of these living conditions (Cole & Foster, 2001; Pellow, 2018; Pulido, 1996; Sze & London, 2008).

In the wake of climate change, these low-income and minority communities are the first to receive the bulk of the burden, even though they have a much smaller carbon footprint than wealthier communities (Cole & Foster, 2001; Sze, 2022). As natural disasters become more frequent and extreme, temperatures rise, and our society aims to shift to cleaner energy, these disadvantaged communities will suffer most if environmental injustices are not brought to light and addressed. Of specific importance is addressing food insecurity. We live in a society that commodifies food production, which has resulted in heavy agricultural activity and overproduction. In fact, while 40% of our food goes to waste, 100% of US counties have food insecurity (Feeding America, 2024).

These movements, along with my volunteer experience in Sacramento, inspired me to create a mural project that encompassed environmental justice and community engagement in Southside Park Community Garden (Sacramento, CA). Mural art can be used as a tool to ignite community engagement and reduce social disconnection, therefore contributing to the development of a sustainable urban environment (Petronienė & Juzelėnienė, 2022). While the

location and theme of this project transformed just as an art piece would, the intention behind it remained the same. Through my advocacy work with Western Service Workers Association and this community workshop, I hope that our conversations on sustainable development as we painted this mural lead to more informed and engaged communities.

4.2 The necessities of failure

As an attempt to further engage communities in the Salton Sea region, the hub of my scientific research, I aimed to organize a mural with Líderes Campesinas, a Coachella-based community organization. Their mission is "to strengthen the leadership of farmworker women and youth so that they can be agents of economic, societal, and political change and ensure their human rights." Our goal was to create a youth-led mural that encapsulated the transformation of the Salton Sea because of consistent activism and demand for environmental justice. I planned to assist the youth in executing the design and implementation of this mural through a series of workshops, teaching them different methods of symbolism and artistic styles while engaging them in creative projects for inspiration. Despite continuous efforts, this project did not have consistent support from the partnering community organization, and we had to admit defeat. Yet, it is crucial to discuss the pitfalls of this process because the lessons learned promoted success in a future project.

Upon initiating this project, I had no experience in painting or organizing murals, building a strong connection with a community organization, or leading a project, but I was confident in my painting skills and was eager to learn. Líderes Campesinas in Coachella Valley is a small nonprofit organization primarily led by volunteers aside from a few paid organizers. Karina A. was a part-time volunteer interested in supporting the project and engaging the local youth.

However, her ability to commit was limited since she was a full-time undergraduate student. This evoked an internal dilemma because I had been taught that community-engaged projects should be led by the community, however, that narrow perspective does not consider the capacity of an organization to participate. It was difficult for us to move things forward because there were several hoops that we needed to jump through to gain the approval of the city to execute the mural painting. While we were successful in gaining support from both the mayor and the county supervisor, Líderes Campesinas was hesitant to advertise the project to the public in fear of disappointing the youth if the project did not come to fruition. Because of this, and because I was not an active member of their community, we were unable to organize a committee to aid in the project's organization swiftly. Karina eventually graduated and began a full-time job at Alianza as their youth coordinator and expressed her need to part ways with this project.

In attempts to maintain traction, I was informed about a similar climate activism mural project at UC Davis led by Emily Schlickman, a professor in the Department of Human Ecology. Through this connection, I was able to learn more about budgeting for these events and worked directly with Leon Willis, the muralist, to serve as his intern. My duties included transposing the design on the shed and, since this was a paint-by-numbers community engagement event, I helped outline the different color segments, label them, and execute the paint-by-numbers event. As a result, I was introduced to the Institute of the Environment at UC Davis and was invited to collaborate on their new climate activism initiative, the Climate Art Trail. Additionally, I had a new team of resources to bring the Coachella mural into fruition. Jullianne Ballou, the Institute's former strategic initiatives director, was instrumental in this forward movement. Through my independent efforts and with the help of Jullianne, we were able to raise nearly

$19,000 to pay for supplies, travel, and event logistics for the project. After I created a new team of support, I requested that Karina bring herself back on the project since there was no new appointed member of Líderes Campesinas to do the job. We were able to make progress for a while, but Karina did not have the capacity to take on another project in addition to her work. It was apparent that without securing funds to pay a member of the organization to participate, there was not going to be any progress. I tried to apply for a community engagement grant and was rejected. Consequently, I decided to cease the project and communicated this with Karina and Líderes Campesinas, who agreed that they did not have the capacity to support this mural.

Although the project with Líderes Campesinas did not come to fruition, I was able to formulate strong connections with the Institute of the Environment. Through my community work in Sacramento, we were able to create a new mural project with the Sacramento Community Gardens. Bill Maynard, the community gardens coordinator, was excited to collaborate with us on this project.

4.3 The Urban Oasis: Community Gardening Strengthens our Connection to the Land

Organizing a community-engaged mural project requires a team of well-resourced people. I painted this mural on a shed at Southside Community Garden in Sacramento, which required legal contracts to allow for the execution of this mural. I needed funding to support the painting of this mural, and a team of volunteers willing and excited to help execute the mural paint-by-numbers event.

Deeper intentions

The Institute of the Environment's Climate Art Trail is a series of murals that portray a common theme centered around the question: How can agriculture be part of the solution to

climate change? To address this, we must first acknowledge the decisions that led to environmental degradation and climate issues. As I have outlined in this dissertation, many agricultural practices are focused on mass production and efficiency, which have stimulated a decline in pollinator populations and soil health, air and water quality implications, overproduction and inefficient distribution of product, and an overall disconnection to the land. The latter point is key to addressing climate related issues—for society to develop new management practices relating to agriculture, it must first rebuild its connection to the land of which has been harmed.

Community gardens provide a space for community members to nurture a deeper connection with nature while in an urban environment. In fact, many of the community members I interviewed spoke of their countless interactions with wildlife and the abundance of joy these interactions fostered. Growing one's own food is a direct energetic transfer, meaning the energy one puts into the food that they grow will be given back to them once consumed.

In addition to foraging a stronger connection to the land, public gardening initiatives can teach residents how to grow their own food. While community gardening may never be able to sustain food for an entire community, let alone the whole world, informing communities how to grow food and sustain themselves, as well as the benefits of community sustained agriculture (CSA), can allow less reliance on industrial agricultural practices. These industrial practices are profit motivated and productivity centered, resulting in 40% of food produced being wasted, serious air and water pollution, and soil degradation, as well as an unequal distribution of food resources to vulnerable communities.

Planning

Jullianne Ballou, previous strategic initiatives director at the Institute of the Environment, handled the contract negotiation between the City of Sacramento and UC Davis. Once this process was completed, I discussed event dates with Bill Maynard from the community garden. After the date was set, I organized three volunteers to help execute the project: Laila Penny, Megan Williams, and Olmo Guerrero-Medina. Laila oversaw organizing vendors to attend the event and engage with the community, however, we were unable to secure any vendors for the event. Megan was the volunteer captain, responsible for organizing volunteers to participate with mural event preparation and day-of-event execution. Olmo was the event organizer, responsible for event logistics, setup, and breakdown; for example, we needed tables for vendors and paint stations. The space at the community garden was small, so we capped the event at 80 people.

Figure 4.1. Olmo Guerrero-Medina painting a monarch butterfly.

Leading up to the event, I was responsible for transferring the mural designs to the shed, overseeing the budget, and purchasing necessary supplies (e.g., catering, painting supplies, beverages, table and chair rentals). I designed the mural with the input of the members of the Southside Community Garden. This was the most challenging part because while I viewed this mural as an art activism project to promote awareness around climate change, it was apparent that many of the gardeners viewed this as a beautification project, ultimately limiting what I could design. One of my designs depicted night creatures playing poker and gambling with produce that they stole from the garden; this design was inspired by a whimsical story from one gardener. However, others expressed that the night creatures were not their friends and asked me to change the design with only 2 weeks until our event. Reluctantly, I quickly designed flowers and butterflies upon the gardeners' requests, pictured above. When designing a community led mural, it is important for the artist to comply with the interests of the community, which can hinder the artist's creative freedom and dilute the message behind the art. While I am grateful for this opportunity to design a mural for this garden, I was disappointed in the artwork that I produced because I did not see the connection between the images and the messages.

In preparation for the event, community gardeners volunteered to paint, which was supposed to be held on May 4th, 2024, but had to be rescheduled to May 18, 2024, due to unexpected rain. Unfortunately, the date change resulted in a small turn-out, but it worked out that there were no vendors. We were able to give away plant starters and had a local community organization, Western Service Workers Association (WSWA), attend and discuss the sustainable development goals (SDGs) (Fig 4.2).

Figure 4.2. Volunteers from Western Service Workers Association discussing the SDGs at the paint-by-numbers event.

Lessons

Overall, I was not completely satisfied with the outcomes of the project. I did not feel I was successful in conveying the message that I had intended. Although I was glad that WSWA was able to discuss the SDGs at the event, there were few outside guests present to engage with this information. Additionally, I felt increasingly disconnected from the Institute of the Environment after Jullianne left. Since the project wasn't directly related to scientific research, I believe it didn't receive the attention it deserved from the Institute. With more support from individuals experienced in organizing such initiatives, the project could have had a greater impact. Moving forward, I would like to pursue another art activism project, but I've learned that if I decide to collaborate with communities again, I need to ensure that they have the capacity to

participate meaningfully. I also need to establish clear communication about the project's theme and expectations with all participants from the beginning.

Despite these challenges, creating a community-centered mural project as part of my dissertation was an invaluable learning experience. When merging two distinct fields like art and science, it's crucial to have a strong mentorship network. These types of projects are not something that can be completed independently; they require external support, especially when venturing into unfamiliar territory. I've come to understand that challenges and unexpected obstacles are inevitable, and they may change the course of the project. However, it's important not to lose sight of the overall goals and core values, even in the face of these difficulties. While the outcome wasn't exactly what I had envisioned, I believe the project left a meaningful impact on the friends and colleagues who participated. At the very least, I was able to demonstrate that being a scientific researcher isn't limited to purely technical or statistical endeavors; we can blur the lines between science and art. I received feedback from others who were inspired by my efforts and now hope to incorporate creativity into their work as well. Ultimately, I believe this approach will foster stronger scientific researchers, as creativity is essential for navigating complex scientific questions, particularly those related to climate change and environmental degradation.

4.4 Photos

Figure 4.3. These images show the paint-by-numbers preparation. The walls were 8 ft tall so the hard-to-reach areas were painted ahead of time so that community members did not need to stand on ladders. The image on the left shows a field of wildflowers, butterflies, and a hummingbird. The image on the right shows a chinook salmon.

Figure 4.4. These are photos of the paint-by-numbers event in action. Volunteers are filling in the color blocks.

Figure 4.6. Shown here are Jean (front) and Olmo (with hat) painting at the event. Jean is a cadre at WSWA and Olmo is a graduate student in hydrology at UC Davis (credit: Elena Peters).

Figure 4.5. Shown above are more action shots from the event (credit: Elena Peters).

Figure 4.7. Two sides of the completed mural on the storage shed at Southside Park Community Garden. The image on the left are various flowers, including lupins, California poppies, tulips, and sunflowers, in addition two monarch butterflies and a hummingbird. The image on the right is a yellow-billed magpie, a bird native to the Sacramento Valley.

Figure 4.8. The interior side of the shed. This mural depicts the Sacramento Valley agricultural activity alongside the Sacramento River. Shown above are flooded rice fields, an oak tree that resembles a feminine silhouette, and the Vaca Mountain range.

References

Abman, R., Edwards, E. C., & Hernandez-Cortes, D. (2024). Water, dust, and environmental justice: The case of agricultural water diversions. *American Journal of Agricultural Economics*, ajae.12472. https://doi.org/10.1111/ajae.12472

Adams, D. K., & Comrie, A. C. (1997). The North American Monsoon. *Bulletin of the American Meteorological Society*, *78*(10), 2197–2213. https://doi.org/10.1175/1520-0477(1997)078<2197:TNAM>2.0.CO;2

Al-Hemoud, A., Al-Dousari, A., Al-Shatti, A., Al-Khayat, A., Behbehani, W., & Malak, M. (2018). Health Impact Assessment Associated with Exposure to PM10 and Dust Storms in Kuwait. *Atmosphere*, *9*(1), 6. https://doi.org/10.3390/atmos9010006

Almaraz, M., Bai, E., Wang, C., Trousdell, J., Conley, S., Faloona, I., & Houlton, B. Z. (2018). Agriculture is a major source of NOx pollution in California. *Science Advances*, *4*(1), eaao3477. https://doi.org/10.1126/sciadv.aao3477

Ammann, M., & Saurer, M. (1999). *Estimating the uptake of traf®c-derived NO2 from 15N abundance in Norway spruce needles*. *118*, 124–131.

Ammann, M., Siegwolf, R., Pichlmayer, F., Suter, M., Saurer, M., & Brunold, C. (1999). Estimating the uptake of traffic-derived NO2 from 15N abundance in Norway spruce needles. *Oecologia*, *118*, 124–131.

Anderson, J. O., Thundiyil, J. G., & Stolbach, A. (2012). Clearing the Air: A Review of the Effects of Particulate Matter Air Pollution on Human Health. *Journal of Medical Toxicology*, *8*(2), 166–175. https://doi.org/10.1007/s13181-011-0203-1

Atkinson, R. W., Butland, B. K., Dimitroulopoulou, C., Heal, M. R., Stedman, J. R., Carslaw, N., Jarvis, D., Heaviside, C., Vardoulakis, S., Walton, H., & Anderson, H. R. (2016). Long-term exposure to ambient ozone and mortality: A quantitative systematic review and meta-analysis of evidence from cohort studies. *BMJ Open*, *6*(2), e009493. https://doi.org/10.1136/bmjopen-2015-009493

Balazs, C. L., & Morello-Frosch, R. (2013). The Three Rs: How Community-Based Participatory Research Strengthens the Rigor, Relevance, and Reach of Science. *Environmental Justice*, *6*(1), 9–16. https://doi.org/10.1089/env.2012.0017

Barton, L., McLay, C. D. A., Schipper, L. A., & Smith, C. T. (1999). Annual denitrification rates in agricultural and forest soils: A review. *Soil Research*, *37*(6), 1073. https://doi.org/10.1071/SR99009

Beirle, S., Boersma, K. F., Platt, U., Lawrence, M. G., & Wagner, T. (2011). Megacity Emissions and Lifetimes of Nitrogen Oxides Probed from Space. *Science*, *333*(6050), 1737–1739. https://doi.org/10.1126/science.1207824

Bekker, C., Walters, W. W., Murray, L. T., & Hastings, M. G. (2023). Nitrate chemistry in the northeast US – Part 1: Nitrogen isotope seasonality tracks nitrate formation chemistry. *Atmospheric Chemistry and Physics*, *23*(7), 4185–4201. https://doi.org/10.5194/acp-23-4185-2023

Blum, D. E., Walters, W. W., & Hastings, M. G. (2020). Speciated Collection of Nitric Acid and Fine Particulate Nitrate for Nitrogen and Oxygen Stable Isotope Determination. *Analytical Chemistry*, *92*(24), 16079–16088. https://doi.org/10.1021/acs.analchem.0c03696

Bohlool, B. B., Ladha, J. K., Garrity, D. P., & George, T. (1992). Biological nitrogen fixation for sustainable agriculture: A perspective. *Plant and Soil*, *141*, 1–11.

Borro, M., Di Girolamo, P., Gentile, G., De Luca, O., Preissner, R., Marcolongo, A., Ferracuti, S., & Simmaco, M. (2020). Evidence-Based Considerations Exploring Relations between SARS-CoV-2 Pandemic and Air Pollution: Involvement of PM2.5-Mediated Up-Regulation of the Viral Receptor ACE-2. *International Journal of Environmental Research and Public Health*, *17*(15), 5573. https://doi.org/10.3390/ijerph17155573

Bradley, T. J., & Yanega, G. M. (2018). Salton Sea: Ecosystem in transition. *Science*, *359*(6377), 754–754. https://doi.org/10.1126/science.aar6088

Byrnes, D. K., Van Meter, K. J., & Basu, N. B. (2020). Long-Term Shifts in U.S. Nitrogen Sources and Sinks Revealed by the New TREND-Nitrogen Data Set (1930–2017). *Global Biogeochemical Cycles*, *34*(9), e2020GB006626. https://doi.org/10.1029/2020GB006626

Caiazzo, F., Ashok, A., Waitz, I. A., Yim, S. H. L., & Barrett, S. R. H. (2013). Air pollution and early deaths in the United States. Part I: Quantifying the impact of major sectors in 2005. *Atmospheric Environment*, *79*, 198–208. https://doi.org/10.1016/j.atmosenv.2013.05.081

California Air Resources Board. (2017). *Community Air Protection Program | California Air Resources Board*. https://ww2.arb.ca.gov/capp

California Air Resources Board. (2023, March 20). *Particulate Matter and Health Fact Sheet*. Particulate Matter and Health Fact Sheet. https://ww2.arb.ca.gov/resources/fact-sheets/particulate-matter-and-health-fact-sheet

California Air Resources Board. (2024a). *Air Quality Data (PST) Query Tool*. https://www.arb.ca.gov/aqmis2/aqdselect.php

California Air Resources Board. (2024b). *Meteorology Data Query Tool (PST)*. https://www.arb.ca.gov/aqmis2/metselect.php

California Air Resources Board (CARB). (2022). *Appendix C Coachella Valley Ozone Weight of Evidence Analysis*.

California Department of Food and Agriculture. (2023). *Fertilizing Materials Tonnage Report 2023*. FEED, FERTILIZER, AND LIVESTOCK DRUGS REGULATORY SERVICES DIVISION OF INSPECTION SERVICES.

California Department of Food and Agriculture (CDFA). (1991). *California Agricultural Statistics Review 1991-1992*.

California Department of Food and Agriculture (CDFA). (2022). *California Agricultural Statistics Review 2021-2022*.

California Water Boards. (2024). *Irrigated Lands Program Total Nitrogen Applied (TNA) Report Instructions*. https://www.waterboards.ca.gov/centralcoast/water_issues/programs/ilp/docs/tna/tna_instructions.pdf

Canfield, D. E., Glazer, A. N., & Falkowski, P. G. (2010). The Evolution and Future of Earth's Nitrogen Cycle. *Science*, *330*(6001), 192–196. https://doi.org/10.1126/science.1186120

Caplin, A., Ghandehari, M., Lim, C., Glimcher, P., & Thurston, G. (2019). Advancing environmental exposure assessment science to benefit society. *Nature Communications*, *10*(1), 1236. https://doi.org/10.1038/s41467-019-09155-4

Carrow, R. N. (1997). Turfgrass Response to Slow-Release Nitrogen Fertilizers. *Agronomy Journal*, *89*(3), 491–496. https://doi.org/10.2134/agronj1997.00021962008900030020x

Casciotti, K. L., Sigman, D. M., Hastings, M. G., Böhlke, J. K., & Hilkert, A. (2002). Measurement of the Oxygen Isotopic Composition of Nitrate in Seawater and Freshwater Using the Denitrifier Method. *Analytical Chemistry*, *74*(19), 4905–4912. https://doi.org/10.1021/ac020113w

Chang, Y., Zhang, Y., Tian, C., Zhang, S., Ma, X., Cao, F., Liu, X., Zhang, W., Kuhn, T., & Lehmann, M. F. (2018). Nitrogen isotope fractionation during gas-to-particle conversion of NOx to NO3- in the atmosphere – implications for isotope-based NOx source apportionment. *Atmospheric Chemistry and Physics*, *18*(16), 11647–11661. https://doi.org/10.5194/acp-18-11647-2018

Chow, J. C., Watson, J. G., C. Green, M., Lowenthal, D. H., Bates, B., Oslund, W., & Torres, G. (2000). Cross-border transport and spatial variability of suspended particles in Mexicali and California's Imperial Valley. *Atmospheric Environment*, *34*(11), 1833–1843. https://doi.org/10.1016/S1352-2310(99)00282-4

Cole, L. W., & Foster, S. R. (2001). *From the ground up: Environmental racism and the rise of the environmental justice movement*. New York University Press.

Comunian, S., Dongo, D., Milani, C., & Palestini, P. (2020). Air Pollution and COVID-19: The Role of Particulate Matter in the Spread and Increase of COVID-19's Morbidity and Mortality. *International Journal of Environmental Research and Public Health*, *17*(12), 4487. https://doi.org/10.3390/ijerph17124487

Coskun, D., Britto, D. T., Shi, W., & Kronzucker, H. J. (2017). Nitrogen transformations in modern agriculture and the role of biological nitrification inhibition. *Nature Plants*, *3*(6), 17074. https://doi.org/10.1038/nplants.2017.74

Dai, Y., Wang, W., Lu, L., Yan, L., & Yu, D. (2020). Utilization of biochar for the removal of nitrogen and phosphorus. *Journal of Cleaner Production*, *257*, 120573. https://doi.org/10.1016/j.jclepro.2020.120573

Davidson, E. A. (1992). Pulses of Nitric Oxide and Nitrous Oxide Flux following Wetting of Dry Soil: An Assessment of Probable Sources and Importance Relative to Annual Fluxes. *Ecological Bulletins*, *42*, 149–155.

Davidson, E. A., David, M. B., Galloway, J. N., Goodale, C. L., Haeuber, R., Harrison, J. A., Horwarth, R. W., Jaynes, D. B., Lowrance, R. R., Nolan, T. B., Peel, J. L., Pinder, R. W., Porter, E., Snyder, C. S., Townsend, A. R., & Ward, M. H. (2012). Excess Nitrogen in the U.S. Environment: Trends, Risks, and Solutions. *Issues in Ecology*, *15*.

de Vlaming, V., DiGiorgio, C., Fong, S., Deanovic, L. A., De La Paz Carpio-Obeso, M., Miller, J. L., Miller, M. J., & Richard, N. J. (2004). Irrigation runoff insecticide pollution of rivers in the Imperial Valley, California (USA). *Environmental Pollution*, *132*(2), 213–229. https://doi.org/10.1016/j.envpol.2004.04.025

D'Evelyn, S. M., Vogel, C. F. A., Bein, K. J., Lara, B., Laing, E. A., Abarca, R. A., Zhang, Q., Li, L., Li, J., Nguyen, T. B., & Pinkerton, K. E. (2021). Differential inflammatory potential of particulate matter (PM) size fractions from imperial valley, CA. *Atmospheric Environment*, *244*, 117992. https://doi.org/10.1016/j.atmosenv.2020.117992

Di, Q., Wang, Y., Zanobetti, A., Wang, Y., Koutrakis, P., Choirat, C., Dominici, F., & Schwartz, J. D. (2017). Air Pollution and Mortality in the Medicare Population. *New England Journal of Medicine*, *376*(26), 2513–2522. https://doi.org/10.1056/NEJMoa1702747

Doane, T. A., & Horwáth, W. R. (2003). Spectrophotometric Determination of Nitrate with a Single Reagent. *Analytical Letters*, *36*(12), 2713–2722. https://doi.org/10.1081/AL-120024647

Dominici, F., Peng, R. D., Bell, M. L., Pham, L., McDermott, A., Zeger, S. L., & Samet, J. M. (2006). Fine Particulate Air Pollution and Hospital Admission for Cardiovascular and Respiratory Diseases. *JAMA*, *295*(10), 1127. https://doi.org/10.1001/jama.295.10.1127

Environmental Protection Agency. (2024, January 23). *EJScreen*. EJScreen: Environmental Justice Screening and Mapping Tool. https://ejscreen.epa.gov/mapper/

Environmental Protection Agency (EPA). (2020a, February 27). *Clean Air Plans; 2008 8-Hour Ozone Nonattainment Area Requirements; Determination of Attainment by the Attainment Date; Imperial County, California*. Federal Register. https://www.federalregister.gov/documents/2020/02/27/2020-03152/clean-air-plans-2008-8-hour-ozone-nonattainment-area-requirements-determination-of-attainment-by-the

Environmental Protection Agency (EPA). (2020b, September 18). *PM10 Maintenance Plan and Redesignation Request; Imperial Valley Planning Area; California*. Federal Register. https://www.federalregister.gov/documents/2020/09/18/2020-18427/pm10-maintenance-plan-and-redesignation-request-imperial-valley-planning-area-california

Environmental Protection Agency (EPA). (2022, October 20). *Determination of Attainment by the Attainment Date But for International Emissions for the 2015 Ozone National Ambient Air Quality Standard; Imperial County, California*. Federal Register. https://www.federalregister.gov/documents/2022/10/20/2022-22276/determination-of-attainment-by-the-attainment-date-but-for-international-emissions-for-the-2015

Environmental Protection Agency (EPA). (2023, January 11). *Determination of Attainment by the Attainment Date, Clean Data Determination, and Approval of Base Year Emissions Inventory for the Imperial County, California Nonattainment Area for the 2012 Annual Fine Particulate Matter NAAQS*. Federal Register. https://www.federalregister.gov/documents/2023/01/11/2022-28278/determination-of-attainment-by-the-attainment-date-clean-data-determination-and-approval-of-base

EPA. (2022, October 20). *Determination of Attainment by the Attainment Date But for International Emissions for the 2015 Ozone National Ambient Air Quality Standard; Imperial County, California*. Federal Register. https://www.federalregister.gov/documents/2022/10/20/2022-22276/determination-of-attainment-by-the-attainment-date-but-for-international-emissions-for-the-2015

EPA. (2023, January 11). *Determination of Attainment by the Attainment Date, Clean Data Determination, and Approval of Base Year Emissions Inventory for the Imperial County, California Nonattainment Area for the 2012 Annual Fine Particulate Matter NAAQS*. Federal Register. https://www.federalregister.gov/documents/2023/01/11/2022-28278/determination-of-attainment-by-the-attainment-date-clean-data-determination-and-approval-of-base

EPA. (2024). *Final Rule to Strengthen the National Air Quality Health Standard for Patriculate Matter*.

Evan, A. T. (2019). Downslope Winds and Dust Storms in the Salton Basin. *Monthly Weather Review*, *147*(7), 2387–2402. https://doi.org/10.1175/MWR-D-18-0357.1

Farzan, S. F., Razafy, M., Eckel, S. P., Olmedo, L., Bejarano, E., & Johnston, J. E. (2019). Assessment of Respiratory Health Symptoms and Asthma in Children near a Drying Saline Lake. *International Journal of Environmental Research and Public Health*, *16*(20), 3828. https://doi.org/10.3390/ijerph16203828

Feeding America. (2024). *Hunger in America*. https://www.feedingamerica.org/hunger-in-america

Felix, J. D., & Elliott, E. M. (2014). Isotopic composition of passively collected nitrogen dioxide emissions: Vehicle, soil and livestock source signatures. *Atmospheric Environment*, *92*, 359–366. https://doi.org/10.1016/j.atmosenv.2014.04.005

Felix, J. D., Elliott, E. M., & Shaw, S. L. (2012). Nitrogen Isotopic Composition of Coal-Fired Power Plant NOx: Influence of Emission Controls and Implications for Global Emission Inventories. *Environmental Science & Technology*, *46*(6), 3528–3535. https://doi.org/10.1021/es203355v

Fibiger, D. L., & Hastings, M. G. (2016). First Measurements of the Nitrogen Isotopic Composition of NO_x from Biomass Burning. *Environmental Science & Technology*, *50*(21), 11569–11574. https://doi.org/10.1021/acs.est.6b03510

Fibiger, D. L., Hastings, M. G., Lew, A. F., & Peltier, R. E. (2014). Collection of NO and NO_2 for Isotopic Analysis of NO_x Emissions. *Analytical Chemistry*, *86*(24), 12115–12121. https://doi.org/10.1021/ac502968e

Firestone, M. K., & Davidson, E. A. (1989). Microbial basis of NO and N2O production and consumption in soil. *Exchange of Trace Gases Between Terrestrial Ecosystems and the Atmosphere*, 7–21.

Fowler, D., Coyle, M., Skiba, U., Sutton, M. A., Cape, J. N., Reis, S., Sheppard, L. J., Jenkins, A., Grizzetti, B., Galloway, J. N., Vitousek, P., Leach, A., Bouwman, A. F., Butterbach-Bahl, K., Dentener, F., Stevenson, D., Amann, M., & Voss, M. (2013). The global nitrogen cycle in the twenty-first century. *Philosophical Transactions of the Royal Society B: Biological Sciences*, *368*(1621), 20130164. https://doi.org/10.1098/rstb.2013.0164

Freedman, F. R., English, P., Wagner, J., Liu, Y., Venkatram, A., Tong, D. Q., Al-Hamdan, M. Z., Sorek-Hamer, M., Chatfield, R., Rivera, A., & Kinney, P. L. (2020). Spatial Particulate Fields during High Winds in the Imperial Valley, California. *Atmosphere*, *11*(1), 88. https://doi.org/10.3390/atmos11010088

Freyer, H. D. (1991). Seasonal variation of 15N/14N ratios in atmospheric nitrate species. *Tellus B*, *43*(1), 30–44. https://doi.org/10.1034/j.1600-0889.1991.00003.x

Frie, A. L., Dingle, J. H., Ying, S. C., & Bahreini, R. (2017). The Effect of a Receding Saline Lake (The Salton Sea) on Airborne Particulate Matter Composition. *Environmental Science & Technology*, *51*(15), 8283–8292. https://doi.org/10.1021/acs.est.7b01773

Frie, A. L., Garrison, A. C., Schaefer, M. V., Bates, S. M., Botthoff, J., Maltz, M., Ying, S. C., Lyons, T., Allen, M. F., Aronson, E., & Bahreini, R. (2019). Dust Sources in the Salton Sea Basin:

A Clear Case of an Anthropogenically Impacted Dust Budget. *Environmental Science & Technology*, *53*(16), 9378–9388. https://doi.org/10.1021/acs.est.9b02137

Garcia, E., Marian, B., Chen, Z., Li, K., Lurmann, F., Gilliland, F., & Eckel, S. P. (2022). Long-term air pollution and COVID-19 mortality rates in California: Findings from the Spring/Summer and Winter surges of COVID-19. *Environmental Pollution*, *292*, 118396. https://doi.org/10.1016/j.envpol.2021.118396

Geddes, J. A., Pusede, S. E., & Wong, A. Y. H. (2022). Changes in the Relative Importance of Biogenic Isoprene and Soil NOx Emissions on Ozone Concentrations in Nonattainment Areas of the United States. *Journal of Geophysical Research: Atmospheres*, *127*(13), e2021JD036361. https://doi.org/10.1029/2021JD036361

Granella, F., Renna, S., & Aleluia Reis, L. (2024). The formation of secondary inorganic aerosols: A data-driven investigation of Lombardy's secondary inorganic aerosol problem. *Atmospheric Environment*, *327*, 120480. https://doi.org/10.1016/j.atmosenv.2024.120480

Greaney, M. (2002). The Power of the Urban Canvas: Paint, Politics, and Mural Art Policy. *New England Journal of Public Policy*, *18*(1). https://scholarworks.umb.edu/nejpp/vol18/iss1/6

Gunther, A. (2022). Murals & Mother Nature: Urban environmental art in Lisbon reveals great concern and appreciation for the environment. *Independent Study Project (ISP) Collection*. https://digitalcollections.sit.edu/isp_collection/3443

Guo, L., Chen, J., Luo, D., Liu, S., Lee, H. J., Motallebi, N., Fong, A., Deng, J., Rasool, Q. Z., Avise, J. C., Kuwayama, T., Croes, B. E., & FitzGibbon, M. (2020). Assessment of Nitrogen Oxide

Emissions and San Joaquin Valley PM2.5 Impacts From Soils in California. *Journal of Geophysical Research: Atmospheres*, *125*(24), e2020JD033304. https://doi.org/10.1029/2020JD033304

Hall, S. J., Matson, P. A., & Roth, P. M. (1996). NOx EMISSIONS FROM SOIL: Implications for Air Quality Modeling in Agricultural Regions. *Annual Review of Energy and the Environment*, *21*(1), 311–346. https://doi.org/10.1146/annurev.energy.21.1.311

Hao, Y., Balluz, L., Strosnider, H., Wen, X. J., Li, C., & Qualters, J. R. (2015). Ozone, Fine Particulate Matter, and Chronic Lower Respiratory Disease Mortality in the United States. *American Journal of Respiratory and Critical Care Medicine*, *192*(3), 337–341. https://doi.org/10.1164/rccm.201410-1852OC

Harrison, R., & Webb, J. (2001). *A review of the effect of N fertilizer type on gaseous emissions*. https://www.sciencedirect.com/science/article/pii/S0065211301730052/pdf?md5=76d7e69577cfa3eafa4a8091835f76ca&pid=1-s2.0-S0065211301730052-main.pdf

Hastings, M. G., Casciotti, K. L., & Elliott, E. M. (2013). Stable Isotopes as Tracers of Anthropogenic Nitrogen Sources, Deposition, and Impacts. *Elements*, *9*(5), 339–344. https://doi.org/10.2113/gselements.9.5.339

Heaton, T. H. E. (1990). 15N/14N ratios of NOx from vehicle engines and coal-fired power stations. *Tellus*, *42*(B), 304–307.

Heuss, J. M., Kahlbaum, D. F., & Wolff, G. T. (2003). Weekday/Weekend Ozone Differences: What Can We Learn from Them? *Journal of the Air & Waste Management Association*, *53*(7), 772–788. https://doi.org/10.1080/10473289.2003.10466227

Högberg, P. (1997). Tansley Review No. 95 ^{15} N natural abundance in soil-plant systems. *New Phytologist*, *137*(2), 179–203. https://doi.org/10.1046/j.1469-8137.1997.00808.x

Hopke, P. K. (2016). Review of receptor modeling methods for source apportionment. *Journal of the Air & Waste Management Association*, *66*(3), 237–259. https://doi.org/10.1080/10962247.2016.1140693

Hu, L., Jacob, D. J., Liu, X., Zhang, Y., Zhang, L., Kim, P. S., Sulprizio, M. P., & Yantosca, R. M. (2017). Global budget of tropospheric ozone: Evaluating recent model advances with satellite (OMI), aircraft (IAGOS), and ozonesonde observations. *Atmospheric Environment*, *167*, 323–334. https://doi.org/10.1016/j.atmosenv.2017.08.036

Huang, G., & London, J. K. (2012). Cumulative Environmental Vulnerability and Environmental Justice in California's San Joaquin Valley. *International Journal of Environmental Research and Public Health*, *9*(5), 1593–1608. https://doi.org/10.3390/ijerph9051593

Huang, J., & Hartemink, A. E. (2020). Soil and environmental issues in sandy soils. *Earth-Science Reviews*, *208*, 103295. https://doi.org/10.1016/j.earscirev.2020.103295

Hudman, R. C., Moore, N. E., Mebust, A. K., Martin, R. V., Russell, A. R., Valin, L. C., & Cohen, R. C. (2012). Steps towards a mechanistic model of global soil nitric oxide emissions: Implementation and space based-constraints. *Atmospheric Chemistry and Physics*, *12*(16), 7779–7795. https://doi.org/10.5194/acp-12-7779-2012

Imperial County Air Pollution Control District. (2018). *Imperial County 2018 Redesignation Request and Maintenance Plan for Particulate Matter Less Than 10 Microns in Diameter*.

Institute for Health Metrics and Evaluation. (2021). *Air pollution*. https://www.healthdata.org/research-analysis/health-risks-issues/air-pollution

Intergovernmental Panel on Climate Change. (2022). *Climate Change and Land: IPCC Special Report on Climate Change, Desertification, Land Degradation, Sustainable Land Management, Food Security, and Greenhouse Gas Fluxes in Terrestrial Ecosystems* (1st ed.). Cambridge University Press. https://doi.org/10.1017/9781009157988

Irani, M., & Rahnamayiezekavat, P. (2021). An overview of urban resilience: Dimensions, components, and approaches. *Acta Scientiarum Polonorum Administratio Locorum*, *20*(4), 305–322. https://doi.org/10.31648/aspal.7054

Ives, R. L. (1949). Climate of the Sonoran Desert Region. *Annals of the Association of American Geographers*, *39*(3), 143–187. https://doi.org/10.1080/00045604909352003

Jaeglé, L., Steinberger, L., Martin, R. V., & Chance, K. (2005). Global partitioning of NOx sources using satellite observations: Relative roles of fossil fuel combustion, biomass burning and soil emissions. *Faraday Discussions*, *130*, 407. https://doi.org/10.1039/b502128f

Johnston, J. E., Razafy, M., Lugo, H., Olmedo, L., & Farzan, S. F. (2019). The disappearing Salton Sea: A critical reflection on the emerging environmental threat of disappearing saline lakes and potential impacts on children's health. *Science of The Total Environment*, *663*, 804–817. https://doi.org/10.1016/j.scitotenv.2019.01.365

Jones, B. A., & Fleck, J. (2020). Shrinking lakes, air pollution, and human health: Evidence from California's Salton Sea. *Science of The Total Environment*, *712*, 136490. https://doi.org/10.1016/j.scitotenv.2019.136490

Kerr, G. H., Waugh, D. W., Strode, S. A., Steenrod, S. D., Oman, L. D., & Strahan, S. E. (2019). Disentangling the Drivers of the Summertime Ozone-Temperature Relationship Over the

United States. *Journal of Geophysical Research: Atmospheres*, *124*(19), 10503–10524. https://doi.org/10.1029/2019JD030572

Kim, S.-Y., Kim, E., & Kim, W. J. (2020). Health Effects of Ozone on Respiratory Diseases. *Tuberculosis and Respiratory Diseases*, *83*(Supple 1), S6–S11. https://doi.org/10.4046/trd.2020.0154

Kimura, A. H., & Kinchy, A. (2016). Citizen Science: Probing the Virtues and Contexts of Participatory Research. *Engaging Science, Technology, and Society*, *2*, 331–361. https://doi.org/10.17351/ests2016.99

Kleeman, M. J., Kumar, A., & Dhiman, A. (2019). *Investigative Modeling of PM2.5 Episodes in the San Joaquin Valley Air Basin during Recent Years* (15–301).

Koutrakis, P., Sioutas, C., Ferguson, S. T., Wolfson, J. M., Mulik, J. D., & Burton, R. M. (1993). Development and evaluation of a glass honeycomb denuder/filter pack system to collect atmospheric gases and particles. *Environmental Science & Technology*, *27*(12), 2497–2501. https://doi.org/10.1021/es00048a029

Li, D., & Wang, X. (2008). Nitrogen isotopic signature of soil-released nitric oxide (NO) after fertilizer application. *Atmospheric Environment*, *42*(19), 4747–4754. https://doi.org/10.1016/j.atmosenv.2008.01.042

Li, H., Tatarko, J., Kucharski, M., & Dong, Z. (2015). PM2.5 and PM10 emissions from agricultural soils by wind erosion. *Aeolian Research*, *19*, 171–182. https://doi.org/10.1016/j.aeolia.2015.02.003

Li, J., Davy, P., Harvey, M., Katzman, T., Mitchell, T., & Michalski, G. (2021). Nitrogen isotopes in nitrate aerosols collected in the remote marine boundary layer: Implications for

nitrogen isotopic fractionations among atmospheric reactive nitrogen species. *Atmospheric Environment*, *245*, 118028. https://doi.org/10.1016/j.atmosenv.2020.118028

Li, J., Zhang, X., Orlando, J., Tyndall, G., & Michalsi, G. (2020). Quantifying the nitrogen isotope effects during photochemical equilibrium between NO and NO2: Implications for δ15N in tropospheric reactive nitrogen. *Atmospheric Chemistry and Physics*, *20*, 9805–9819.

Lieb, H., Walters, W., Maldonado, M., Ruiz, E., Torres, C., Olmedo, L., & Faloona, I. (2024). *Nitrogen Isotopes Reveal High NOx Emissions from Arid Agricultural Soils in the Salton Sea Air Basin*. https://doi.org/10.21203/rs.3.rs-4249148/v1

Los Angeles Times. (2023, September 26). *California coronavirus cases: Tracking the outbreak*. Los Angeles Times. https://www.latimes.com/projects/california-coronavirus-cases-tracking-outbreak/

Luo, L., Ran, L., Rasool, Q. Z., & Cohan, D. S. (2022). Integrated Modeling of U.S. Agricultural Soil Emissions of Reactive Nitrogen and Associated Impacts on Air Pollution, Health, and Climate. *Environmental Science & Technology*, *56*(13), 9265–9276. https://doi.org/10.1021/acs.est.1c08660

Madl, A. K., Carosino, C., & Pinkerton, K. E. (2010). Particle Toxicities. In *Comprehensive Toxicology* (pp. 421–451). Elsevier. https://doi.org/10.1016/B978-0-08-046884-6.00923-4

Malm, W. C., & Hand, J. L. (2007). An examination of the physical and optical properties of aerosols collected in the IMPROVE program. *Atmospheric Environment*, *41*(16), 3407–3427. https://doi.org/10.1016/j.atmosenv.2006.12.012

Marian, B., Yan, Y., Chen, Z., Lurmann, F., Li, K., Gilliland, F., Eckel, S. P., & Garcia, E. (2022). Independent associations of short- and long-term air pollution exposure with COVID-19 mortality among Californians. *Environmental Advances*, *9*, 100280. https://doi.org/10.1016/j.envadv.2022.100280

Marr, L. C., & Harley, R. A. (2002). Modeling the Effect of Weekday−Weekend Differences in Motor Vehicle Emissions on Photochemical Air Pollution in Central California. *Environmental Science & Technology*, *36*(19), 4099–4106. https://doi.org/10.1021/es020629x

Mendoza, A., Pardo, E. I., & Gutierrez, A. A. (2010). Chemical Characterization and Preliminary Source Contribution of Fine Particulate Matter in the Mexicali/Imperial Valley Border Area. *Journal of the Air & Waste Management Association*, *60*(3), 258–270. https://doi.org/10.3155/1047-3289.60.3.258

Meyer, J. (2000). *Qualitative research in health care*. *320*.

Miao, Y., Porter, W. C., Schwabe, K., & LeComte-Hinely, J. (2022). Evaluating health outcome metrics and their connections to air pollution and vulnerability in Southern California's Coachella Valley. *Science of The Total Environment*, *821*, 153255. https://doi.org/10.1016/j.scitotenv.2022.153255

Miller, D. J., Chai, J., Guo, F., Dell, C. J., Karsten, H., & Hastings, M. G. (2018). Isotopic Composition of In Situ Soil NO_x Emissions in Manure-Fertilized Cropland. *Geophysical Research Letters*, *45*(21). https://doi.org/10.1029/2018GL079619

Miller, D. J., Wojtal, P. K., Clark, S. C., & Hastings, M. G. (2017). Vehicle NOx emission plume isotopic signatures: Spatial variability across the eastern United States. *Journal of*

Geophysical Research: Atmospheres, *122*(8), 4698–4717. https://doi.org/10.1002/2016JD025877

Miyazaki, K., & Eskes, H. (2013). Constraints on surface NO $_x$ emissions by assimilating satellite observations of multiple species: MULTIPLE CONSTRAINTS ON NO $_X$ EMISSIONS. *Geophysical Research Letters*, *40*(17), 4745–4750. https://doi.org/10.1002/grl.50894

Moore, K. D., Wojcik, M. D., Martin, R. S., Marchant, C. C., Jones, D. S., Bradford, W. J., Bingham, G. E., Pfeiffer, R. L., Prueger, J. H., & Hatfield, J. L. (2015). Particulate-matter emission estimates from agricultural spring-tillage operations using LIDAR and inverse modeling. *Journal of Applied Remote Sensing*, *9*(1), 096066. https://doi.org/10.1117/1.JRS.9.096066

Museum of Modern Art. (2022). *Diego Rivera*. The Museum of Modern Art. https://www.moma.org/artists/4942

Nichols, P. K., Dabach, S., Abu-Najm, M., Brown, P., Camarillo, R., Smart, D., & Steenwerth, K. L. (2024). Alternative fertilization practices lead to improvements in yield-scaled global warming potential in almond orchards. *Agriculture, Ecosystems & Environment*, *362*, 108857. https://doi.org/10.1016/j.agee.2023.108857

Odum, E. P. (1989). Input Management of Production Systems. *Science*, *243*(4888), 177–182.

OEHHA. (2023, May 1). *CalEnviroScreen 4.0*. https://oehha.ca.gov/calenviroscreen/report/calenviroscreen-40

Oikawa, P. Y., Ge, C., Wang, J., Eberwein, J. R., Liang, L. L., Allsman, L. A., Grantz, D. A., & Jenerette, G. D. (2015). Unusually high soil nitrogen oxide emissions influence air quality

in a high-temperature agricultural region. *Nature Communications*, *6*(1), 8753. https://doi.org/10.1038/ncomms9753

Oswald, R., Behrendt, T., Ermel, M., Wu, D., Su, H., Cheng, Y., Breuninger, C., Moravek, A., Mougin, E., Delon, C., Loubet, B., Pommerening-Röser, A., Sörgel, M., Pöschl, U., Hoffmann, T., Andreae, M. O., Meixner, F. X., & Trebs, I. (2013). HONO Emissions from Soil Bacteria as a Major Source of Atmospheric Reactive Nitrogen. *Science*, *341*(6151), 1233–1235. https://doi.org/10.1126/science.1242266

Pacific Institute. (2024). Current Information on the Salton Sea. *Pacific Institute*. https://pacinst.org/current-information-salton-sea/

Palomo Acosta, T. (2018). *Chicano Mural Movement*. Texas State Historical Association. https://www.tshaonline.org/handbook/entries/chicano-mural-movement

Parrish, D. D., Faloona, I. C., & Derwent, R. G. (2024). *Maximum ozone concentrations in the southwestern US and Texas: Implications of growing predominance of background contribution*. https://doi.org/10.5194/egusphere-2024-342

Parrish, D. D., Young, L. M., Newman, M. H., Aikin, K. C., & Ryerson, T. B. (2017). Ozone Design Values in Southern California's Air Basins: Temporal Evolution and U.S. Background Contribution: Southern California Ozone Design Values. *Journal of Geophysical Research: Atmospheres*, *122*(20), 11,166-11,182. https://doi.org/10.1002/2016JD026329

Parton, W. J., Holland, E. A., Del Grosso, S. J., Hartman, M. D., Martin, R. E., Mosier, A. R., Ojima, D. S., & Schimel, D. S. (2001). Generalized model for NO_x and N_2O emissions from soils. *Journal of Geophysical Research: Atmospheres*, *106*(D15), 17403–17419. https://doi.org/10.1029/2001JD900101

Pellow, D. N. (2018). *What is critical environmental justice?* Polity Press.

Petronienė, S., & Juzelėnienė, S. (2022). Community Engagement via Mural Art to Foster a Sustainable Urban Environment. *Sustainability*, *14*(16), 10063. https://doi.org/10.3390/su141610063

Pilegaard, K. (2013). Processes regulating nitric oxide emissions from soils. *Philosophical Transactions of the Royal Society B: Biological Sciences*, *368*(1621), 20130126. https://doi.org/10.1098/rstb.2013.0126

Porter, W. C., & Heald, C. L. (2019). The mechanisms and meteorological drivers of the summertime ozone–temperature relationship. *Atmospheric Chemistry and Physics*, *19*(21), 13367–13381. https://doi.org/10.5194/acp-19-13367-2019

Prosser, J. I. (2007). The Ecology of Nitrifying Bacteria. In *Biology of the Nitrogen Cycle* (pp. 223–243). Elsevier. https://doi.org/10.1016/B978-044452857-5.50016-3

Pulido, L. (1996). A CRITICAL REVIEW OF THE METHODOLOGY OF ENVIRONMENTAL RACISM RESEARCH*. *Antipode*, *28*(2), 142–159. https://doi.org/10.1111/j.1467-8330.1996.tb00519.x

Redling, K., Elliott, E., Bain, D., & Sherwell, J. (2013). Highway contributions to reactive nitrogen deposition: Tracing the fate of vehicular NOx using stable isotopes and plant biomonitors. *Biogeochemistry*, *116*(1–3), 261–274. https://doi.org/10.1007/s10533-013-9857-x

Reyers, B., Moore, M.-L., Haider, L. J., & Schlüter, M. (2022). The contributions of resilience to reshaping sustainable development. *Nature Sustainability*, *5*(8), 657–664. https://doi.org/10.1038/s41893-022-00889-6

Ribaudo, M., Hansen, L., Livingston, M. J., Mosheim, R., Williamson, J., & Delgado, J. (2011). Nitrogen in Agricultural Systems: Implications for Conservation Policy. *SSRN Electronic Journal*. https://doi.org/10.2139/ssrn.2115532

Roelofs, G.-J., & Lelieveld, J. (1997). Model study of the influence of cross-tropopause O3 transports on tropospheric O3 levels. *Tellus B*, *49*(1), 38–55. https://doi.org/10.1034/j.1600-0889.49.issue1.3.x

Rooker, S. J. (1977). Nitrogen, Phosphorus and Sulphur—Global Cycles, SCOPE Report 7. Ecol. Bull. (Stockholm). *Journal of Aerosol Science*, *8*(5), 367. https://doi.org/10.1016/0021-8502(77)90025-8

Sampedro, J., Waldhoff, S. T., Van De Ven, D.-J., Pardo, G., Van Dingenen, R., Arto, I., Del Prado, A., & Sanz, M. J. (2020). Future impacts of ozone driven damages on agricultural systems. *Atmospheric Environment*, *231*, 117538. https://doi.org/10.1016/j.atmosenv.2020.117538

San Joaquin Valley Air Pollution Control District. (2024). *San Joaquin Valley Unified Air Pollution Control District Summary of Rules and Plans*. https://ww2.valleyair.org/media/w03p2z1i/4-2-2024-cac-plan-and-rule-update.pdf

Schroeder, R. A., Orem, W. H., & Kharaka, Y. K. (2002). Chemical evolution of the Salton Sea, California: Nutrient and selenium dynamics. In D. A. Barnum, J. F. Elder, D. Stephens, & M. Friend (Eds.), *The Salton Sea* (pp. 23–45). Springer Netherlands. https://doi.org/10.1007/978-94-017-3459-2_2

Sha, T., Ma, X., Zhang, H., Janechek, N., Wang, Y., Wang, Y., Castro García, L., Jenerette, G. D., & Wang, J. (2021). Impacts of Soil NO_x Emission on O_3 Air Quality in Rural California.

Environmental Science & Technology, *55*(10), 7113–7122. https://doi.org/10.1021/acs.est.0c06834

Shi, C., Fernando, H. J. S., & Yang, J. (2009). Contributors to ozone episodes in three U.S./Mexico border twin-cities. *Science of The Total Environment*, *407*(18), 5128–5138. https://doi.org/10.1016/j.scitotenv.2009.05.046

Sigman, D. M., Casciotti, K. L., Andreani, M., Barford, C., Galanter, M., & Böhlke, J. K. (2001). A Bacterial Method for the Nitrogen Isotopic Analysis of Nitrate in Seawater and Freshwater. *Analytical Chemistry*, *73*(17), 4145–4153. https://doi.org/10.1021/ac010088e

Silvern, R. F., Jacob, D. J., Mickley, L. J., Sulprizio, M. P., Travis, K. R., Marais, E. A., Cohen, R. C., Laughner, J. L., Choi, S., Joiner, J., & Lamsal, L. N. (2019). Using satellite observations of tropospheric NO2 columns to infer long-term trends in US NOx emissions: The importance of accounting for the free tropospheric NO2 background. *Atmospheric Chemistry and Physics*, *19*(13), 8863–8878. https://doi.org/10.5194/acp-19-8863-2019

Skelton, R., Miller, V., & Lindwall, C. (2023, August 22). *The Environmental Justice Movement*. https://www.nrdc.org/stories/environmental-justice-movement

Škerlak, B., Sprenger, M., & Wernli, H. (2014). A global climatology of stratosphere–troposphere exchange using the ERA-Interim data set from 1979 to 2011. *Atmospheric Chemistry and Physics*, *14*(2), 913–937. https://doi.org/10.5194/acp-14-913-2014

Skiba, U., Fowler, D., & Smith, K. A. (1997). Nitric oxide emissions from agricultural soils in temperate and tropical climates: Sources, controls and mitigation options. *Nutrient Cycling in Agroecosystems*, *48*(139–153).

Slemr, F., & Seiler, W. (1984). Field measurements of NO and NO2 emissions from fertilized and unfertilized soils. *Journal of Atmospheric Chemistry*, *2*(1), 1–24. https://doi.org/10.1007/BF00127260

Smith, K. A., Jackson, D. R., Misselbrook, T. H., Pain, B. F., & Johnson, R. A. (2000). PA—Precision Agriculture: Reduction of Ammonia Emission by Slurry Application Techniques. *Journal of Agricultural Engineering Research*, *77*(3), 277–287. https://doi.org/10.1006/jaer.2000.0604

Song, W., Liu, X.-Y., Houlton, B. Z., & Liu, C.-Q. (2022). Isotopic constraints confirm the significant role of microbial nitrogen oxides emissions from the land and ocean environment. *National Science Review*, *9*(9), nwac106. https://doi.org/10.1093/nsr/nwac106

Spinoni, J., Barbosa, P., Cherlet, M., Forzieri, G., McCormick, N., Naumann, G., Vogt, J. V., & Dosio, A. (2021). How will the progressive global increase of arid areas affect population and land-use in the 21st century? *Global and Planetary Change*, *205*, 103597. https://doi.org/10.1016/j.gloplacha.2021.103597

Stevenson, D. S., Dentener, F. J., Schultz, M. G., Ellingsen, K., Van Noije, T. P. C., Wild, O., Zeng, G., Amann, M., Atherton, C. S., Bell, N., Bergmann, D. J., Bey, I., Butler, T., Cofala, J., Collins, W. J., Derwent, R. G., Doherty, R. M., Drevet, J., Eskes, H. J., … Szopa, S. (2006). Multimodel ensemble simulations of present-day and near-future tropospheric ozone. *Journal of Geophysical Research*, *111*(D8), D08301. https://doi.org/10.1029/2005JD006338

Sze, J. (2022). Margins and Mainstreams: American Studies and the Environmental and Climate Justice Movements. *Transatlantica*, *2*. https://doi.org/10.4000/transatlantica.20452

Sze, J., & London, J. K. (2008). Environmental Justice at the Crossroads. *Sociology Compass*, *2*(4), 1331–1354. https://doi.org/10.1111/j.1751-9020.2008.00131.x

Tan, Y., Henderick, P., Yoon, S., Herner, J., Montes, T., Boriboonsomsin, K., Johnson, K., Scora, G., Sandez, D., & Durbin, T. D. (2019). On-Board Sensor-Based NOx Emissions from Heavy-Duty Diesel Vehicles. *Environmental Science & Technology*, *53*(9), 5504–5511. https://doi.org/10.1021/acs.est.8b07048

The New York Times. (2023, March 23). California Coronavirus Map and Case Count. *The New York Times*. https://www.nytimes.com/interactive/2023/us/california-covid-cases.html

Thermo Scientific. (2005). *Partisol Model 2300: Speciation Sampler Operation Manual*. https://assets.thermofisher.com/TFS-Assets/LSG/manuals/EPM-manual-Partisol2300.pdf

Thompson, B., Jürgens, A.-S., BOHIE, & Lamberts, R. (2023). Street art as a vehicle for environmental science communication. *Journal of Science Communication*, *22*(4), A01. https://doi.org/10.22323/2.22040201

Thornton, F. C., Bock, B. R., & Tyler, D. D. (1996). Soil Emissions of Nitric Oxide and Nitrous Oxide from Injected Anhydrous Ammonium and Urea. *Journal of Environmental Quality*, *25*(6), 1378–1384. https://doi.org/10.2134/jeq1996.00472425002500060030x

Trousdell, J. F., Caputi, D., Smoot, J., Conley, S. A., & Faloona, I. C. (2019). Photochemical production of ozone and emissions of NOx and CH4 in the San Joaquin Valley.

Atmospheric Chemistry and Physics, *19*(16), 10697–10716. https://doi.org/10.5194/acp-19-10697-2019

UC Davis Agricultural and Resource Economics. (2004). *Cost & Return Studies*. https://coststudies.ucdavis.edu/

United Nations. (2012). *Transforming our world: The 2030 Agenda for Sustainable Development | Department of Economic and Social Affairs*. https://sdgs.un.org/2030agenda

U.S. Census Bureau. (2023). *U.S. Census Bureau QuickFacts: Imperial County, California*. https://www.census.gov/quickfacts/fact/table/imperialcountycalifornia/PST045223

US EPA. (2016a, April 14). *Nonattainment Areas for Criteria Pollutants (Green Book)*. https://www.epa.gov/green-book

US EPA. (2016b, August 17). *Chemical Speciation Network* [Data and Tools]. https://www.epa.gov/outdoor-air-quality-data/interactive-map-air-quality-monitors

US EPA. (2024, January 24). *Final Reconsideration of the National Ambient Air Quality Standards for Particulate Matter (PM)* [Overviews and Factsheets]. https://www.epa.gov/pm-pollution/final-reconsideration-national-ambient-air-quality-standards-particulate-matter-pm

van Vuuren, D. P., Bouwman, L. F., Smith, S. J., & Dentener, F. (2011). Global projections for anthropogenic reactive nitrogen emissions to the atmosphere: An assessment of scenarios in the scientific literature. *Current Opinion in Environmental Sustainability*, *3*(5), 359–369. https://doi.org/10.1016/j.cosust.2011.08.014

Vinken, G. C. M., Boersma, K. F., Maasakkers, J. D., Adon, M., & Martin, R. V. (2014). Worldwide biogenic soil NO_x emissions inferred from OMI

NO₂ observations. *Atmospheric Chemistry and Physics*, *14*(18), 10363–10381. https://doi.org/10.5194/acp-14-10363-2014

Walters, W. W., Fang, H., & Michalski, G. (2018). Summertime diurnal variations in the isotopic composition of atmospheric nitrogen dioxide at a small midwestern United States city. *Atmospheric Environment*, *179*, 1–11. https://doi.org/10.1016/j.atmosenv.2018.01.047

Walters, W. W., Goodwin, S. R., & Michalski, G. (2015). Nitrogen Stable Isotope Composition (δ15N) of Vehicle-Emitted NOx. *Environmental Science & Technology*, *49*, 2278–2285. https://doi.org/10.1021/es505580v

Walters, W. W., & Michalski, G. (2015). Theoretical calculation of nitrogen isotope equilibrium exchange fractionation factors for various NO y molecules. *Geochimica et Cosmochimica Acta*, *164*, 284–297. https://doi.org/10.1016/j.gca.2015.05.029

Walters, W. W., Simonini, D. S., & Michalski, G. (2016). Nitrogen isotope exchange between NO and NO_2 and its implications for $\delta^{15}N$ variations in tropospheric NO_x and atmospheric nitrate. *Geophysical Research Letters*, *43*(1), 440–448. https://doi.org/10.1002/2015GL066438

Wang, Y., Faloona, I. C., & Houlton, B. Z. (2023). Satellite NO_2 trends reveal pervasive impacts of wildfire and soil emissions across California landscapes. *Environmental Research Letters*, *18*(9), 094032. https://doi.org/10.1088/1748-9326/acec5f

Wang, Y., Fu, X., Wu, D., Wang, M., Lu, K., Mu, Y., Liu, Z., Zhang, Y., & Wang, T. (2021). Agricultural Fertilization Aggravates Air Pollution by Stimulating Soil Nitrous Acid Emissions at High Soil Moisture. *Environmental Science & Technology*, *55*(21), 14556–14566. https://doi.org/10.1021/acs.est.1c04134

Wang, Y., Ge, C., Castro Garcia, L., Jenerette, G. D., Oikawa, P. Y., & Wang, J. (2021). Improved modelling of soil NOx emissions in a high temperature agricultural region: Role of background emissions on NO2 trend over the US. *Environmental Research Letters*, *16*(8), 084061. https://doi.org/10.1088/1748-9326/ac16a3

Ward, B. B. (2008). *Nitrification*. Encyclopedia of Ecology.

Watson, J. G., & Chow, J. C. (2001). *Source characterization of major emission sources in the Imperial and Mexicali Valleys along the USrMexico border*.

Williams, E. J., & Fehsenfeld, F. C. (1991). Measurement of soil nitrogen oxide emissions at three North American ecosystems. *Journal of Geophysical Research: Atmospheres*, *96*(D1), 1033–1042. https://doi.org/10.1029/90JD01903

Williams, E. L., & Grosjean, D. (1990). Removal of atmospheric oxidants with annular denuders. *Environmental Science & Technology*, *24*(6), 811–814. https://doi.org/10.1021/es00076a002

World Health Organization (WHO). (2013). *Review of evidence on health aspects of air pollution – REVIHAAP Project*.

Xue, C., Ye, C., Zhang, C., Catoire, V., Liu, P., Gu, R., Zhang, J., Ma, Z., Zhao, X., Zhang, W., Ren, Y., Krysztofiak, G., Tong, S., Xue, L., An, J., Ge, M., Mellouki, A., & Mu, Y. (2021). Evidence for Strong HONO Emission from Fertilized Agricultural Fields and its Remarkable Impact on Regional O3 Pollution in the Summer North China Plain. *ACS Earth and Space Chemistry*, *5*(2), 340–347. https://doi.org/10.1021/acsearthspacechem.0c00314

Yienger, J. J., & Levy, H. (1995). Empirical model of global soil-biogenic NO_χ emissions. *Journal of Geophysical Research: Atmospheres*, *100*(D6), 11447–11464. https://doi.org/10.1029/95JD00370

Yu, Z., & Elliott, E. M. (2017). Novel Method for Nitrogen Isotopic Analysis of Soil-Emitted Nitric Oxide. *Environmental Science & Technology*, *51*(11), 6268–6278. https://doi.org/10.1021/acs.est.7b00592

Zhang, L., Lin, M., Langford, A. O., Horowitz, L. W., Senff, C. J., Klovenski, E., Wang, Y., Alvarez Ii, R. J., Petropavlovskikh, I., Cullis, P., Sterling, C. W., Peischl, J., Ryerson, T. B., Brown, S. S., Decker, Z. C. J., Kirgis, G., & Conley, S. (2020). Characterizing sources of high surface ozone events in the southwestern US with intensive field measurements and two global models. *Atmospheric Chemistry and Physics*, *20*(17), 10379–10400. https://doi.org/10.5194/acp-20-10379-2020